

# **2013 Asia Pacific Microwave Conference**

**(APMC 2013)**

**Seoul, South Korea  
5-8 November 2013**

**Pages 1-626**



**IEEE Catalog Number: CFP13APM-POD  
ISBN: 978-1-4799-1473-9**

## [W1A] Sensors and Packaging

- Date: November 6, 2013 (Wednesday)
- Time: 09:00 ~ 10:40
- Room: Room A (Room 101)
- Session Chairs: Ashraf Uz Zaman (Chalmers University of Technology)  
Jinho Jeong (Sogang University)

[W1A-1]

09:00 ~ 09:20

### Fast and Highly Accurate RF Phase Detector with Analog Integrator for APAA System 1

Akihito Hirai, Koji Tsutsumi, Yoshinori Takahashi, Hideyuki Nakamizo, Kenichi Tajima, Eiji Taniguchi, Mitsuhiro Shimozawa, Morishige Hieda, Masatoshi Nakayama, Mitsubishi Electric Corporation, Japan

An RF phase detector employing an analog integrator is proposed for active phased array antenna system. The RF phase detector, consisting of an analog integrator, a mixer and a divider can realize both fast and highly accurate detection at the same time. By setting the integral time of the analog integrator as integral multiple of the half cycle of RF signal, the variation of output voltage due to second harmonic of the mixer output can be prevented. The proposed RF phase detector is fabricated in 0.18 $\mu$ m SiGe-BiCMOS process. It is achieved that the measured accuracy of phase detection is 0.52 deg.-rms in the detection time of 8ns at 1GHz.

[W1A-2]

09:20 ~ 09:40

### A Low Power Power Sensor for Optical Communication 4

Hung-Yang Shih, Hen-Wei Tsao, National Taiwan University, Taiwan

A power sensor operating at low dc power with cyclic logarithmic amplifier is proposed in this paper. The input signal passes RC low pass filter firstly, and then feeds to a cyclic logarithmic amplifier to have linear-in-dB output. DC offset and flicker noise are eliminated by using a chopper. It is fabricated by TSMC 0.18  $\mu$ m 1P6M CMOS process. For 10 Gbps pseudo random bit sequence (PRBS) input, the dynamic range is 31-dB, with  $\pm 1.1$  dB linearity. It consumes only 1.73 mW.

[W1A-3]

09:40 ~ 10:00

### Design Methodology of Tunable Impedance Matching Circuit With SOI CMOS Tunable Capacitor Array for RF FEM 7

Bum-Kyum Kim<sup>1</sup>, Taeyeop Lee<sup>1</sup>, Donggu Im<sup>1</sup>, Do-Kyung Im<sup>1</sup>, Bonkee Kim<sup>2</sup>, Kwyro Lee<sup>2</sup>, <sup>1</sup>KAIST, Korea, <sup>2</sup>HiDeep, Korea

For the tunable RF FEMs or Antennas, analysis on optimal design of tunable capacitors which consist of MIM capacitors and RF CMOS switches is performed in terms of quality factor, tuning ratio and harmonics. To handle up to +36dBm RF signal, the Stacked-FET and series Capacitor-Transistor-Capacitor (CTC) configuration applied Coupled-Bias(CB) are proposed, which in addition to being high-linearity can eliminate a negative voltage generator. Using the designed tunable capacitors, optimal tunable matching circuit is proposed.

[W1A-4]

10:00 ~ 10:20

### Packaging of MMIC by using Gap Waveguide and Design of a Microstrip to Ridge Gap waveguide Transition 10

Ashraf Uz Zaman, Per-Simon Kildal, Chalmers University of Technology, Sweden

In this work, gap waveguide based packaging technique is used to improve the isolation among critical microwave circuit components such as high gain amplifier chain. Amplifier chains at Ka-band were tested for a stable forward gain and it was found that-with gap waveguide packaging, 65 ~ 70dB of forward gain is achievable without the problem of self-resonance. Apart from the new packaging technique, a low-loss transition from microstrip to ridge-gap waveguide had been designed and tested. This transition is a key component to connect such amplifier chains to a planar slot array antenna. Experimental results for manufactured back to back transition show 14 dB return loss over 55% relative bandwidth from 23-43GHz.

[W1A-5]

10:20 ~ 10:40

### Substrate Integrated Waveguide Transmitter Design 13

Yang Fei, Yu Hong-xi, Sun Shu-feng, He Xin-yang, Liu Rui-zhu, China Academy of Space Technology, China

In this paper, two novel substrate integrated waveguide (SIW) Transmitters, in Ku band and K band respectively, based on low-temperature co-fired ceramic (LTCC) technology, are proposed. A Ku band SIW filter with elliptic response are located in the Ku band single channel transmitter, as well as SIW transmission lines embedded in LTCC substrate for good isolation with DC bias. A SIW divider is then proposed to realize a K-band four channels transmitter module to make sure the RF layer is in the bottom of LTCC substrate to get better heat dissipating performance. Both are verified by experiments. Good agreements between the simulated and measured results are observed, which have also validated the proposed concept of the transmitter design with the SIW technology in LTCC.

## [W1B] Passive Components

- Date: November 6, 2013 (Wednesday)
- Time: 09:00 ~ 10:40
- Room: Room B (Room 102)
- Session Chairs: Ke-Li Wu (The Chinese University of Hong Kong)  
Yongchae Jeong (Chonbuk National University)

[W1B-1]

09:00 ~ 09:20

### Multilayer Phase Shifter with Wide Range of Phase and Ultra-Wideband Performance 16

L. Guo, A. Abbosh, The University of Queensland, Australia

A compact planar phase shifter with ultrawideband (UWB) performance and wide range of differential phase shift is proposed. To achieve that performance, the device uses broadside electromagnetic coupling between top and bottom microstrip patches via a slot located in the middle layer that forms the ground plane. Two short-ended stubs are connected to the microstrip patches to expand the range of the phase shift up to 270°. The theory of operation for the proposed device is derived. Three designed phase shifters demonstrate a differential phase of 90°, 180°, and 270° across the band from 3.1 GHz to 10.6 GHz with less than  $\pm 8^\circ$  differential phase imbalance, and less than 0.8 dB insertion loss.

[W1B-2]

09:20 ~ 09:40

### Switchable Matched Band-Stop Filter for High Power Interference Mitigation 19

Bakhit Amine Adoum<sup>1</sup>, Wong Peng Wen<sup>1</sup>, Mohamad Sharif Osman<sup>2</sup>, <sup>1</sup>Universiti Teknologi PETRONAS, Malaysia, <sup>2</sup>PETRONAS Carigali Sdn Bhd, Malaysia

This paper describes an investigation into a novel miniaturized microwave matched band-stop filter with pseudo-infinite attenuation for the enhancement of wireless link on floating production storage and offloading (FPSO) vessels. The proposed method is capable to produce almost infinite attenuation even with very low Q resonator and is suitably used to suppress very high power interference signal. Another important feature of the filter is that it possesses matching response at all frequency. The solution can be easily integrated with the existing system with minimum cost and more importantly without interrupting the service. Furthermore, the filter can be switched to exhibit an all pass response by turning "OFF" the PIN diodes incorporated into the filter topology. An experimental prototype will be demonstrated for the proof-of-concept.

[W1B-3]

09:40 ~ 10:00

### Compact Negative Group Delay Circuit using Defected Ground Structure 22

Girdhari Chaudhary<sup>1</sup>, Junhyung Jeong<sup>1</sup>, Phirun Kim<sup>1</sup>, Yongchae Jeong<sup>1</sup>, Jongsik Lim<sup>2</sup>, <sup>1</sup>Chonbuk National University, Korea, <sup>2</sup>Soonchunhyang University, Korea

A novel design of compact negative group delay circuit (NGDC) using U-shaped defected ground structure (DGS) is presented in this paper. The required group delay (GD) time can be controlled by an external resistor connected across the DGS slot. For experimental verification, a single stage NGDC is designed, fabricated, and compared with a circuit simulation. To enhance NGD bandwidth, two stages NGDC with the different center frequencies in cascade are demonstrated and GD of -3.8 ns with maximum signal attenuation of 37.10 dB was obtained on 3.45-3.55 GHz.

[W1B-4]

10:00 ~ 10:20

### A Direct Synthesis Approach of Bandpass Filters with Extracted-poles 25

Ping Zhao, Ke-Li Wu, The Chinese University of Hong Kong, Hong Kong

A new direct coupling matrix synthesis approach for bandpass filters with extracted-poles is presented. Different from existing synthesis methods, the extracted-pole sections and the remaining cross-coupled resonators are synthesized in a unified approach. As a result, the coupling matrix synthesized contains both resonant and non-resonant nodes. Another distinct feature of the coupling matrix synthesized by the proposed approach is that its frequency response can involve certain phase offset, which can be determined from our synthesis approach.

[W1B-5]

10:20 ~ 10:40

### Improvement of Waveguide Diplexer Components 28

T. Gál<sup>1</sup>, J. Ladvánszky<sup>2</sup>, F. Lénárt<sup>1</sup>, <sup>1</sup>Budapest University of Technology, Hungary, <sup>2</sup>Ericsson Telecom Hungary Ltd., Hungary

Important parameters of waveguide diplexer components as lowpass filter and combiner, have been improved. Concave shaping of vertical walls of a corrugated filter decreases reflection coefficients by 10 dB in the 14.5-15.35 GHz band. Placement of inserts at the antenna port of a combiner increases bandwidth by more than 50%.

## [W1C] Special Session: Advanced Metamaterial Technologies

- Date: November 6, 2013 (Wednesday)
- Time: 09:00 ~ 10:40
- Room: Room C (Room 104)
- Session Chairs: Petri Piironen (European Space Agency)  
Sungtek Kahng (Incheon National University)

[W1C-1]

09:00 ~ 09:25

### [Invited] Nonreciprocal CRLH Metamaterials and Their Applications to Beam-Scanning Antennas 31

Tetsuya Ueda<sup>1</sup>, Tatsuo Itoh<sup>2</sup>, <sup>1</sup>Kyoto Institute of Technology, Japan, <sup>2</sup>University of California, USA

This paper reviews recent progress on nonreciprocal CRLH metamaterials with nonreciprocal phase constants and their applications to beam-scanning antennas. The nonreciprocal CRLH metamaterials show positive and negative refractive indices at the same frequency, selection of which depends on directions of the transmitted power. Traveling wave resonators with variable size and phase gradient of the field profile can be designed for a given frequency. In addition, beam-scanning antenna with the externally applied dc magnetic field is demonstrated based on the resonator showing high radiation efficiency and small beam squint, compared to conventional leaky wave antennas.

[W1C-2]

09:25 ~ 09:50

### [Invited] Gap Waveguides and PMC Packaging: Octave Bandwidth mm- and Submm-Wave Applications of Soft & Hard Surfaces, EBGs and AMCs 34

Per-Simon Kildal, Chalmers University of Technology, Sweden

AMCs, EBGs and other surface-based metamaterials are known to have narrow bandwidths. However, when they are used to generate stopbands for parallel-plate modes, the bandwidth can be very large. This characteristic is used in the gap waveguide technology that was invented in 2008, based on old research on soft and hard surfaces. The gap waveguide technology can be used to package microstrip and CPW circuits, but can also with advantage replace such standard technologies and in particular above 30 GHz. The gap waveguides can have similar lowloss performance as solid rectangular waveguides, but they can be realized in a much better way. Rectangular waveguides are normally realized by split blocks which are screwed tightly together to ensure good conductive contact, whereas gap waveguides can be realized between parallel plates without metal connection. This paper overviews how the gap waveguide technology has been explored during the passed five years including: demonstrations of the wideband lowloss guiding characteristics up to 260 GHz, demonstrations of packaging in different frequency ranges with different AMCs or EBGs, and demonstrations of filters, transitions, MMIC packaging, corporate distribution networks, and slot and horn array antennas. The technology demonstrators cover the three different versions of gap waveguides: groove gap waveguide, ridge gap waveguides and microstrip gap waveguides.

[W1C-3]

09:50 ~ 10:15

### [Invited] Study on a Leaky Wave Antenna for High Gain 37

Ju Jeong Ho, Eom Sung Yong, Kim Joung Myoun, Song Myung Sun, Choi Jae Ick, Electronics and Telecommunications Research Institute, Korea

A leaky wave antenna(LWA) is studied by using dispersion diagram. The advantages are a simple design, a low profile, and high boresight directivity over the frequency bands. Moreover, the radiation properties of the leaky wave are investigated by means of the theoretical analysis by using dispersion properties of a unit cell for the LWA. The measured and predicted results verify the performance of the antenna.

[W1C-4]

10:15 ~ 10:40

### [Invited] Metamaterial-Based Planar Waveguide Filters and Components for Light-Weight Multi-Channel Vehicular Transceivers 40

Sungtek Kahng<sup>1</sup>, Kyungseok Kahng<sup>1</sup>, Inkyu Yang<sup>1</sup>, Jinil Lee<sup>1</sup>, Hosub Lee<sup>2</sup>, <sup>1</sup>Incheon National University, Korea, <sup>2</sup>LIGNEX1, Korea

In this paper, it is presented that novel and compact filters and channel combiners are developed for a lighter multi-channel vehicular transceiver working at an X-band and a Ku-band as high frequencies instead of bulky metallic waveguides. The components are in the form of so-called substrate integrated waveguide(SIW) as planar layered structures. For the purpose of reducing the physical sizes of the aforementioned components further from the conventional SIWs for the frequency bands near the millimeter-wave region, the internal parts of the proposed SIWs play the components of the CRLH-line as a metamaterial structure, which turns out much smaller than the SIWs of the same frequency. This is indebted to the phase-lead effect from the LH zone. Firstly, the compact SIW filters are implemented for the channels, particularly, an X-band and a Ku-band in this case, but applicable to millimeter-wave bands, if needed. Secondly, they are combined in another SIW to keep the two channels least distorted as a compact duplexer. The frequency responses of the filters and the channel combiner are given with the photographs of the fabricated versions. The size-reduction effect by the proposed method is mentioned with the conventional waveguide counterparts. It is easy to predict that the design scheme can be adopted for light-weight and low-profile vehicular transceivers.

## [W1D] MIMO Antennas

- Date: November 6, 2013 (Wednesday)
- Time: 09:00 ~ 10:40
- Room: Room D (Room 105)
- Session Chairs: Andrey S. Andrenko (Fujitsu Laboratories LTD.)  
Wen-Shan Chen (Southern Taiwan University of Science and Technology)
- 

[W1D-1]

09:00 ~ 09:20

### Novel Antenna Arrangement for 4x4 LOS-MIMO Aystems 43

Satoshi Sasaki, Kentaro Nishimori, Ryoichi Kataoka, Hideo Makino, Niigata University, Japan

This paper proposes novel antenna arrangements which improve the channel capacity for 4x4 multiple-input multiple-output (MIMO) system in line-of-sight (LOS) environment. It is shown that the channel matrix is unitary matrix by the proposed antenna arrangement and the high channel capacity is obtained by the proposed antenna arrangement with directional antennas even if the multipath signals in indoor scenario are considered.

[W1D-2]

09:20 ~ 09:40

### MIMO Antenna with Decoupling Network for Headset Applications 46

Dongtak Kim, Kyeol Kwon, Dogu Kang, Jaehoon Choi, Hanyang University, Korea

A MIMO antenna with decoupling network for headset applications is proposed. The performance of the antenna is investigated when the antenna is placed on a head phantom. The antenna consists of two monopole type radiators and a decoupling network that improves the isolation between two radiators. The antenna on the human head phantom covers ISM band and the isolation exceeds 20 dB. Because the ECC is lower than 0.1 over the ISM band, the proposed antenna is a good candidate for diversity application.

[W1D-3]

09:40 ~ 10:00

### Multiband MIMO Antenna for 4G Mobile Terminal 49

Xing Zhao, Jaehoon Choi, Hanyang University, Korea

A multiband MIMO antenna for a 4G mobile terminal is proposed. The antenna structure consists of a multiband main antenna element, a printed inverted-L sub-antenna element operating in the higher 2.5 GHz band, and a wideband loop sub-antenna element working in lower 0.9 GHz band. In order to improve the isolation and ECC characteristics of the proposed MIMO antenna, each element is located at a different corner of the ground plane. In addition, the inductive coils are employed to reduce the antenna volume and to realize the wideband property of the loop sub-antenna element. The proposed antenna covers LTE band 7/8, PCS, WiMAX, and WLAN services, simultaneously. The MIMO antenna has ECC lower than 0.15 and isolation higher than 12 dB over the frequency bands.

[W1D-4]

10:00 ~ 10:20

### 4x4 Textile MIMO Antenna Array for Mobile Router Applications 52

Sungjin Choi, Sungjoon Lim, Chung-Ang University, Korea

In this paper, a novel foldable textile antenna array is proposed for mobile router applications. The antenna array is composed of four antenna elements on a felt textile substrate and manufactured using an adhesive electro-textile. Two antenna elements are constructed by using double feeding on a rectangular monopole, and their isolation is improved by a decoupling slit. Another two antennas are placed after rotating them by 180°. A slit on the ground plane is introduced to further improve the isolation.

[W1D-5]

10:20 ~ 10:40

### Broadband MIMO PIFA Antenna with Circular Polarization for RFID Readers 55

Yuan Yao<sup>1</sup>, Junsheng Yu<sup>1</sup>, Xiaodong Chen<sup>2</sup>, <sup>1</sup>Beijing University of Posts and Telecommunications, China, <sup>2</sup>University of London, UK

A novel broadband circular polarized two-element PIFA antenna with pattern diversity and high isolation is proposed which can be easily fabricated and embedded into RFID readers. Circular polarization characteristic of the proposed antenna is achieved by introducing a cross branch at its corner of the ground. The modified PIFA structure gives the antenna a broadband impedance bandwidth characteristic. A prototype is fabricated and measured. The results show that this circular polarized antenna with compact dimension has broadband from 840MHz-960MHz and good isolation of 15dB between the two elements over the whole band, which make the antenna suitable for terminal application of RFID readers.

## [W1E] Microwave Imaging and SAR Remote Sensing

- Date: November 6, 2013 (Wednesday)
- Time: 09:00 ~ 11:00
- Room: Room E (Room 203)
- Session Chairs: Yoshio Nikawa (Kokushikan University)  
Woo-Kyung Lee (Korea Aerospace University)

[W1E-1]

09:00 ~ 09:30

### [Invited] Interference Suppression Techniques for Remote Sensing Radar Applications 58

Lee Bo-Yun, Lee Seul-Ki, Woo-Kyung Lee, Korea Aerospace University, Korea

SAR(Synthetic Aperture Radar) is known to be vulnerable to interference signals coming from other communication devices or radar instruments and suffer from undesirable performance degradations. In this paper, a modified LMS adaptive filter is proposed that can be easily applied to the SAR images affected by the interference signals. We present a simulation results that proves to be effectiveness of the LMS algorithm for interference suppression while the SAR image quality is well preserved compared with the notch-filter case.

[W1E-2]

09:30 ~ 10:00

### [Invited] Application of Microwaves in Medical Sensing and Treatment 62

Yoshio Nikawa, Kokushikan University, Japan

RF and Microwaves are non-ionizing radiation energy. They are very safe in application of medicine, especially in diagnosis and treatment. Application of Magnetic Resonance Imaging (MRI) has greatly progress in medical diagnosis. Microwave techniques have a great potential to help to advance MRI techniques. In this paper, microwave reflection sensing and microwave irradiation for heating treatment is introduced with using MRI.

[W1E-3]

10:00 ~ 10:20

### Terahertz Tomographic Imaging with Sub-millimeter Depth Resolution 65

H. Nishii<sup>1</sup>, T. Ikeou<sup>1</sup>, K. Ajito<sup>2</sup>, N. Kukutsu<sup>2</sup>, T. Nagatsuma<sup>1</sup>, <sup>1</sup>Osaka University, Japan, <sup>2</sup>NTT Microsystem Integration Laboratories, Japan

This paper presents a terahertz (THz) tomographic imaging system using monochromatic 400~800-GHz signals, which have been generated and swept by photonic techniques. Measurable thickness of plastic plates has been experimentally verified as small as 0.37 mm, which corresponds to a depth resolution of 0.61 mm in the air.

[W1E-4]

10:20 ~ 10:40

### 3D Radar Imaging with a MIMO OFDM-based Radar 68

Yoke Leen Sit, Thuy T. Nguyen, Thomas Zwick, Karlsruhe Institute of Technology, Germany

This paper presents a 3-dimensional radar imaging concept using a MIMO OFDM-based radar. The transmit OFDM signal is designed in such a way that the multiple transmitters will only radiate at the subcarriers unique to itself while preserving the total bandwidth and the range resolution. The virtual antenna array concept is utilized to widen the basis of the antenna array with the least possible transmit-receive elements. Using beamforming techniques at the receiver together with novel radar processing techniques, the range, azimuth and elevation information for an arbitrary number of objects (relative to the number of antenna elements used in the antenna array) can be estimated through a simultaneous transmission.

[W1E-5]

10:40 ~ 11:00

### Design and Analysis of the Quasi-Optics for High Resolution Millimeter Wave Imaging System N/A

Wang Nannan, Qiu Jinghui, Zong Hua, Zhang Yang, Zhang Pengyu, Dong Jiaxin, Harbin Institute of Technology, China

High spatial resolution is one of the most important design targets in the millimeter-wave imaging system. In this paper, quasi-optics design has been performed for the high resolution. A novel dielectric rod antenna employed as the feed antenna. The proposed antenna has good performances of low return loss, low side-lobe level, symmetrical radiation patterns, and easy to form feed antenna arrays with low mutual coupling. Due to the large diameter and small F/D ratio of regular lens antenna, loss and cost could be quite high. In order to overcome these disadvantages, a new bias-placed ellipsoid antenna is used. The focusing characteristics of the bias-placed ellipsoid antenna with bias-feed have been analyzed by the MLFMM method.

## [W1F] Wireless Power Transfer and Energy Harvesting

- Date: November 6, 2013 (Wednesday)
- Time: 09:00 ~ 10:40
- Room: Room F (Room 208)
- Session Chairs: Shigeo Kawasaki (ISAS/JAXA)  
Kang-Yoon Lee (Sungkyunkwan University)

[W1F-1]

09:00 ~ 09:20

### Reversible High Efficiency Amplifier/Rectifier Circuit for Wireless Power Transmission System 74

Ryo Ishikawa, Kazuhiko Honjo, The University of Electro-Communications, Japan

A reversible high efficiency amplifier/rectifier circuit using one transistor has been proposed. For a gate side of the transistor, an input circuit for the amplifier and a gate adjusting circuit for the rectifier are prepared. By switching the circuits, the operation mode is changed. For a drain side of the transistor, a harmonic treatment circuit can be shared for both the operations. The harmonic treatment induces a high efficiency operation not only for the amplifier, but also for the rectifier. To verify both the operations, a GaAs pHEMT amplifier and rectifier which varied only the gate side circuit were designed and fabricated at 5.8 GHz. The fabricated amplifier exhibited a maximum drain efficiency of 71%, and the fabricated rectifier exhibited an RF to DC conversion efficiency of 68%.

[W1F-2]

09:20 ~ 09:40

### Wireless Power Transfer Guides 77

Ikuo Awai<sup>1</sup>, Yuichi Sawahara<sup>2</sup>, Toshio Ishizaki<sup>2</sup>, <sup>1</sup>Ryutech Corporation, Japan, <sup>2</sup>Ryukoku University, Japan

It is experimentally studied that the power transfer efficiency is improved by inserting a proper structure made of dielectrics, magnetic materials or metals between two spiral coils constituting a coupled-resonator WPT (Wireless power transfer) system. The structures can be hollow/solid circular cylinder, plate or rectangular parallelepiped. The power transfer is based on the interaction of evanescent fields, not propagating fields. The principle of power guide is considered originating from the refraction rules of the electric and magnetic fields at the boundary of 2 different materials. But it is still not clear.

[W1F-3]

09:40 ~ 10:00

### An Investigation of Cross-Coupling for Magnetically Coupled Wireless Power Transfer 80

Gunbok Lee<sup>1</sup>, Benjamin H. Waters<sup>2</sup>, Brody J. Mahoney<sup>2</sup>, Joshua R. Smith<sup>2</sup>, Wee Sang Park<sup>1</sup>, <sup>1</sup>Pohang University of Science and Technology, Korea, <sup>2</sup>University of Washington, USA

The effects of parasitic couplings in 4-coil wireless power transfer (WPT) systems are investigated. In WPT applications, the available space for the receive coil is limited in comparison to that of the transmit coil. This physical limitation, therefore, results in different sizes for transmit and receive coils. However, asymmetry in the dimensions of the coupled coils can result in significant parasitic effects. Coupling between coil<sub>1</sub> and coil<sub>3</sub> ( $k_{13}$ ), and coupling between coil<sub>2</sub> and coil<sub>4</sub> ( $k_{24}$ ) cause deviation of optimal frequency and degradation of efficiency. Coupling between coil<sub>1</sub> and coil<sub>4</sub> affects only the efficiency degradation, with independence of  $k_{13}$  and  $k_{24}$ . To reduce parasitic effects, a capacitive compensation method is proposed. This method can compensate for the unwanted shift in peak efficiency due to parasitic effects by adding capacitance to coil<sub>1</sub>. In our work, the proposed method increased the efficiency from 69.5% to 85.3% at the desired operating frequency.

[W1F-4]

10:00 ~ 10:20

### A Study on Low Power Rectenna using DC-DC Converter to Track Maximum Power Point 83

Yong Huang, Naoki Shinohara, Tomohiko Mitani, Kyoto University, Japan

This study proposed a maximum power point tracking (MPPT) method for an mW low power RF-DC rectenna by using a DC-DC converter. The conversion efficiency of RF-DC rectifier circuit is affected by the load and the input power. In order to solve this problem, an RF-DC-DC circuit is proposed which consists of a RF-DC rectifier circuit and a DC-DC converter in this study. We designed a Buck-Boost converter with stable input impedance to match the optimal load of rectenna. The measured RF to DC efficiency of rectifier is almost steady at 75% in spite of the load resistance changed from 100  $\Omega$  to 5000  $\Omega$  when we connected the proposed Buck-Boost converter to the rectenna. The total efficiency of RF-DC-DC circuit is almost still over 60% even though the load resistance changed from 100  $\Omega$  to 5000  $\Omega$  with the input power of 82 mW.

[W1F-5]

10:20 ~ 10:40

### Small Loop Rectenna for RF Energy Harvesting 86

Akira Noguchi, Hiroyuki Arai, Yokohama National University, Japan

This paper presents a small loop antenna and high output voltage rectifier in wide frequency band for RF (radio frequency) energy harvesting of FM broadcasting signals. Target input power level of -20dBm is used to design a loop antenna for DC output voltage-boosting. The RF energy harvesting on suburb area provides 924mV DC output for a single rectenna and 1.72V DC output for twin rectennas by receiving several FM broadcasting signals simultaneously.

## Poster Session I : Active Components & EM Field and Techniques

- Date: November 6, 2013 (Wednesday)
- Time: 14:20 ~ 16:00
- Room: Room 103

[P1-1] 14:20 ~ 16:00

### X-band Low Noise Amplifier MMIC using AlGaIn/GaN HEMT Technology on SiC Substrate 681

Woojin Chang<sup>1</sup>, Gye-ik Jeon<sup>2</sup>, Young-Rak Park<sup>1</sup>, Sangheung Lee<sup>1</sup>, Jae-Kyoung Mun<sup>1</sup>, <sup>1</sup>Electronics and Telecommunications Research Institute, Korea, <sup>2</sup>RF Core Co. Ltd., Korea

A 9.7-12.9 GHz monolithic microwave integrated circuit (MMIC) low-noise amplifier (LNA) is designed and fabricated using AlGaIn/GaN 0.25  $\mu\text{m}$  high electron mobility transistor (HEMT) on silicon carbide (SiC) technology. The LNA shows a noise figure of 1.7-2.1 dB with a small-signal gain of 20-26 dB across the 9.7-12.9 GHz frequency range. In continuous wave (CW) conditions, the saturated output power of 34 dBm is showed at 11.2 GHz and the output third-order intercept point (OIP3) of 42 dBm is also achieved at 11.4 GHz.

[P1-2] 14:20 ~ 16:00

### An Improved Gm-boosted Technique for a K-band Cascode Colpitts CMOS VCO 685

Tzu-Yi Lian, Kuan-Hsiu Chien, Hwann-Kaeo Chiou, National Central University, Taiwan

This paper presents an improved gm-boosted techniques for a K-band cascode Colpitts voltage controlled oscillator (VCO). This modified topology is derivative from conventional gm-boosted technique by using cascoded cross-coupled pairs. By a quantitative small signal analysis, the gm-boosted cascode Colpitts VCO increases its transconductance more than a factor of  $0.5[1 + (g_{m1}/g_{m3})(1 + C_1/C_2)]$ . A K-band VCO was designed to verify the concept. The measured central frequency of the designed VCO is 25.0 GHz with the tunable frequency range from 25.3 to 24.7 GHz. The core power consumption is 13.2 mW from a power supply of 1.5 V, and -103.1 dBc/Hz phase noise at 1 MHz offset. The maximum output power is -7.5 dBm. The calculated figure of merit (FoM) of this VCO is -180 dBc/Hz.

[P1-3] 14:20 ~ 16:00

### A 0.6-6.2 GHz Wideband LNA using Resistive Feedback and Gate Inductive Peaking Techniques for Multiple Standards Application 688

Kuan-Hsiu Chien, Hwann-Kaeo Chiou, National Central University, Taiwan

This paper presents a 0.6-6.2 GHz wideband CMOS low noise amplifier (LNA) for multi-band application. The LNA design is based on a common source (CS) cascade amplifier with resistive feedback, gate inductive peaking, and source degeneration inductive topologies to realize the matching networks for broadband operation. The authors also derived the formula of the input and output impedances those help to select proper values of biasing and matching elements. The LNA achieves a peak gain S21 of 11.61 dB, a noise figure (NF) of 5.28 to 5.82 dB at frequency from 0.6 to 6.2 GHz, and an input third-intercept point (IIP3) of -2.55 dBm at 2.5 GHz under DC power of 8.45 mW from a 1.5 V supply voltage. The figure-of-merit (FOM) for wideband LNA is up to 0.51 at 2.5 GHz. The LNA is fabricated in tsmcTM 0.18- $\mu\text{m}$  RF CMOS technology with a chip area of 0.8 mm<sup>2</sup>.

[P1-4] 14:20 ~ 16:00

### A 147 GHz Fully Differential D-Band Amplifier Design in 65 nm CMOS 691

Chun-Hsing Li, Chih-Wei Lai, Chien-Nan Kuo, National Chiao Tung University, Taiwan

This work presents a 147 GHz D-band fully differential amplifier design in 65 nm CMOS. By using a T-network, composed of three inductors, to replace an on-chip transformer, the proposed impedance transformation network can provide an impedance transformation ratio larger than one. So the passive gain can be acquired to increase the amplifier gain. The measured results show that the amplifier can provide power gain of 7.1 dB at 147 GHz. The power consumption is 104 mW from a 2 V supply voltage.

[P1-5] 14:20 ~ 16:00

### A CMOS Wideband Highly Linear Variable Gain Amplifier 694

Hoang Viet Le<sup>1</sup>, Hoa Thai Duong<sup>2</sup>, Anh Trong Huynh<sup>1</sup>, Robin John Evans<sup>1,2</sup>, Efstratios Skafidas<sup>1,2</sup>, <sup>1</sup>National ICT Australia, Australia, <sup>2</sup>The University of Melbourne, Australia

This work presents the design of a wideband highly linear variable gain amplifier (VGA). The proposed VGA consists of 3 stage digitally gain controlled amplifiers and a fixed gain amplifier. The circuit topologies of the amplifiers are pseudo differential inverter, which allows maximum headroom voltage swing. As a result, highly linear operation is achieved. A simple digitally gain controlled method is proposed, that provides 15 dB control range, with 3 control bits. Furthermore, with the proposed gain control method, linearity and gain bandwidth is maintained in low gain mode operation. The proposed VGA is implemented in a 65 nm CMOS technology. The measured VGA shows more than 1.2 GHz 3 dB gain bandwidth, 15 dB control gain range. The measured VGA consumes 7.5 mA from 1.2 V power supply.



## Poster Session I : Active Components & EM Field and Techniques

- Date: November 6, 2013 (Wednesday)
- Time: 14:20 ~ 16:00
- Room: Room 103

[P1-6] 14:20 ~ 16:00

### Low Noise and High Gain Dual-band Active Band-pass Filter with GaAs MESFET using CRLH Metamaterial 697 Ki-Cheol Yoon, Jaegook Lee, Hyunwook Lee, Jong-Chul Lee, Kwangwoon University, Korea

In this paper, a low noise and high gain dual-band active bandpass filter (BPF) with GaAs MESFET using the CRLH (Composite Right/Left-Handed) metamaterial is presented. The CRLH is applied to develop a dual-band BPF using an amplifier circuit with two arbitrary frequency bands. Then, the two center frequencies of the filter are chosen as  $f_1 = 1.23$  GHz and  $f_2 = 1.63$  GHz, where the phase slope characteristics of the response are chosen as  $f_1 = -90^\circ$  and  $f_2 = -270^\circ$ . The experimental results are gain value of 7.82 dB and 7.03 dB and the return losses of -15.1 dB and -10.1 dB with bandwidth of 55 MHz (4.4 %) and 105 MHz (6.4 %) at the center frequencies of 1.22 GHz and 1.61 GHz, respectively.

[P1-7] 14:20 ~ 16:00

### Low Power and High Linearity Millimeter Wave Differential Mixer using Passive Transformer 700 Jae-Sik Jang<sup>1,2</sup>, Laurence Moquillon<sup>1</sup>, Patrice Garcia<sup>1</sup>, Estelle Lauga-Larroze<sup>2</sup>, Jean-Michel Fournier<sup>2</sup>, <sup>1</sup>STMicroelectronics, France, <sup>2</sup>IMEP-LAHC, France

A low power and high linearity millimeter wave mixer for automotive radar application is designed using SiGe BiCMOS technology. The concept of design is based on a Gilbert type cell. The proposed topology uses separated voltage sources (1.5 V and 2 V for the transconductance and switching stage respectively) via a transformer. This mixer allows high output dynamic range with low power consumption. The chip was characterized by on-wafer measurements. At 77 GHz, the voltage conversion gain ( $G_c$ ) and double side band noise figure ( $NF_{DSB}$ ) are 13.7 dB and 11.4 dB respectively. Input referred 1-dB compression point ( $ICP_{1dB}$ ) is 2 dBm. Total power consumption is 15 mW. The size of mixer core is 550 x 410  $\mu m^2$ .

[P1-8] 14:20 ~ 16:00

### InGaP/GaAs WLAN Power Amplifier with Detector using On-chip Coupler 703 Trung-Sinh Dang, Anh-Dung Tran, Sun-Jun Ham, Hyun-Woo Park, Lai-Ngoc-Duy Hien, Sang-Woong Yoon, Kyung Hee University, Korea

This paper presents a power amplifier with an on-chip power detector for 2.4 GHz wireless local area network (WLAN) application. The power detector consists of a clamp circuit, a diode detector and a coupled line directional coupler. A series inductor for an output matching network in the power amplifier is combined with a through line of the coupler, which reduces the coupling level. Therefore, the coupler employs a metamaterial-based transformer configuration to increase coupling. The amount of coupling is increased by 2.5 dB in the 1:1 symmetric transformer structure and by 4.5 dB from 2 metamaterial units along the coupled line.

[P1-9] 14:20 ~ 16:00

### Efficiency Enhanced Class-F Doherty Power Amplifier at 3.5GHz for LTE-Advanced Application 707 Cheng-zhi Fan, Xiao-Wei Zhu, Jing Xia, Lei Zhang, Southeast University, China

This paper presents a high-efficiency broadband GaN HEMT class-F Doherty Power amplifier at 3.5GHz for LTEAdvanced applications. The carrier and peak amplifier of the Doherty amplifier both adopts class-F design strategy to obtain higher efficiency, in which the transmission-line harmonic suppression network for controlling the second and third harmonics is employed. Measurement results show that DE of the proposed PA can achieve higher than 50% at the output power range of 40-46dBm. The efficiency is improved 10% comparing to conventional class-AB Doherty amplifier at most. The linearity performance of class-F Doherty PA is demonstrated with LTEAdvanced signals by utilizing the PA linearization technique combined of DPD and PAPR reduction techniques, the ACLR can reach -47dBc and -46dBc for 40MHz and 60MHz bandwidth respectively.

[P1-10] 14:20 ~ 16:00

### A 1.9–2.6 GHz Router Switch IC for MIMO Applications in 0.18 $\mu m$ CMOS Technology 710 Feng-Hsu Chung, Chang-Ming Lai, Chun-Hsiang Chi, Chia-Hao Tu, Ping-Hsun Wu, Jian-Yu Li, ITRI, Taiwan

In MIMO applications, beam forming and spatial diversity are two possible solutions to enhance system performance. To operate in these two scenarios with a utility hardware, the function of reconfiguration is required. In beam forming, power combining and power splitting are needed in receiver and transmitter respectively. In spatial diversity, signal from each antenna are processed by RF paths and basebands separately to against the fading distortions. In this work, a router switch implemented in 0.18  $\mu m$  CMOS for 2x2 MIMO is proposed. The proposed router switch can be configured to provide three operation modes, which are power combining mode, power splitting mode, and power paralleling mode. It provides a flexible interface between RF front-end and transceiver chip in MIMO systems.

## Poster Session I : Active Components & EM Field and Techniques

- Date: November 6, 2013 (Wednesday)
- Time: 14:20 ~ 16:00
- Room: Room 103

[P1-11] 14:20 ~ 16:00

### An Ultra Low-power Q-band LNA with 50% Bandwidth in WIN GaAs 0.1- $\mu$ m pHEMT Process 713 Ping-Han Ho<sup>1</sup>, Chau-Ching Chiong<sup>2</sup>, Huei Wang<sup>1</sup>, <sup>1</sup>National Taiwan University, Taiwan, <sup>2</sup>Academia Sinica, Taiwan

A pHEMT Q-band low noise amplifier (LNA) for radio astronomy applications was designed and measured. This LNA exhibits a bandwidth from 27 to 45 GHz with the small signal gain of 25 dB, and with the noise figure below 3.1 dB. The total power consumption is only 9 mA, and the figure-of-merit (FOM) is 34.2 (GHz/mW), which is highest compared with the previously published LNAs.

[P1-12] 14:20 ~ 16:00

### A Resistive Double-Balance Mixer using Bulk-Driven Method with Low Pumping Power in 0.18 $\mu$ m CMOS Technology 716 Chien-Chang Huang, George Changlin Guu, Chia-Kai Chen, Chih-Wen Huang, Yuan Ze University, Taiwan

This paper presents a 0.18  $\mu$ m CMOS resistive double-balanced mixer using bulk-driven method with -1.3 dBm pumping power of local oscillator (LO), for 5.8 GHz dedicated short range communications (DSRC) applications. The LO signal is applied to the bulk and the source terminals differentially to reduce the required LO power without needs of impedance matching. The on-chip central-taped transformers are utilized as balance-to-unbalance (BALUN) function for RF and LO ports, while the differential output is used for intermediate-frequency (IF) port. The measured results show about -8 dB conversion gain and 8 dB noise figure in 5.8 GHz of RF frequency and 100 MHz of IF frequency. The input 1 dB compression point and the input interception point in the third order (IP3) are about -7.5 dBm and 3 dBm, respectively, to fulfill the mobile communication requirements.

[P1-13] 14:20 ~ 16:00

### Wideband Colpitts Voltage Controlled Oscillator with Nanosecond Start-up Time for Bubble-Type Motion Detector 719 Im-Hyu Shin, Dong-Wook Kim, Chungnam National University, Korea

This paper presents a wideband Colpitts voltage controlled oscillator (VCO) with a center frequency of 7.2GHz and nanosecond start-up time for a new bubble-type motion detector that has a bubble layer of detection zone at the specific distance from itself. Combined with the varactor diode, the shunt microstrip line resonating at 6.7GHz is proposed to compensate the input reactance of the transistor that changes from capacitive to inductive at 7.6GHz. The measured VCO shows the tunable bandwidth of 2.1GHz, the output power of 8~11dBm and the start-up time of less than 2nsec. It will be utilized for the novel bubble-type motion detector later.

[P1-14] 14:20 ~ 16:00

### A 1.2-2.0 GHz-band GaAs pHEMT Cascode Power Amplifier MMIC Consisting of Independently Biased Transistors 722 Satoshi Tasaki, Yoichiro Takayama, Ryo Ishikawa, Kazuhiko Honjo, The University of Electro-Communications, Japan

An L-band wideband cascode power amplifier MMIC with independently biased GaAs pHEMTs is developed. This amplifier can control distortion and power-efficiency independently, and achieved power added efficiency (PAE) over 53% from 1.2 to 2.0 GHz, and third-order intermodulation distortion (IMD3) better than -40 dBc with maximum PAE of 33.3% for a maximum output power of 17.0 dBm, and showed superior performance compared to a conventional cascode amplifier.

[P1-15] 14:20 ~ 16:00

### Analysis of Deterministic Modes of Optical Modulators Laser Diode Affected by External Harmonic Signals 725 M. Orda-Zhigulina, Yu. Alekseev, Southern Federal University, Russia

Semiconductor laser diodes are the main part of optical modulators. Semiconductor injection laser diode affected by external microwave modulating signal is a complex nonlinear oscillation system. Such non-linear systems are usually described by some systems of well-known differential equations. In the article the non-linear oscillation systems were analyzed by method of Poincare maps and different modes of semiconductor laser diodes under microwave modulating signal influence were described. Results of numerical experiments are discussed.

## Poster Session I : Active Components & EM Field and Techniques

- Date: November 6, 2013 (Wednesday)
- Time: 14:20 ~ 16:00
- Room: Room 103

[P1-16] 14:20 ~ 16:00

**Design of A DC-33 GHz Cascode Distributed Amplifier using Dualgate Device in 0.5- $\mu$ m GaAs E/D-Mode HEMT Process** 728  
Si-Hua Chen<sup>1</sup>, Chih-Chun Shen<sup>1</sup>, Shou-Hsien Weng<sup>1</sup>, Yu-Cheng Liu<sup>1</sup>, Hong-Yeh Chang<sup>1</sup>, Yu-Chi Wang<sup>2</sup>, <sup>1</sup>National Central University, Taiwan, <sup>2</sup>WIN Semiconductors Corporation, Taiwan

Design of a DC-33 GHz cascode distributed amplifier (DA) using dual-gate device in 0.5- $\mu$ m GaAs enhancement/depletion-mode (E/D-mode) high electron mobility transistor (HEMT) process is presented in this paper. A compact dual-gate HEMT is adopted in the gain cell of the DA. By using the dual-gate HEMT, the gain-bandwidth product of the DA can be further improved. The proposed DA achieves a small-signal gain of 10.6 dB, an output power 1-dB compress point (OP1dB) of 8.9 dBm, and a 3-dB bandwidth from dc to 33 GHz. The DA is also successfully evaluated using pseudorandom bit stream (PRBS) signal with a data rate up to 12-Gbps. The proposed dual-gate DA is suitable for the high-speed data rate transmission due to its superior performance.

[P1-17] 14:20 ~ 16:00

**Novel Method to Measure the Conversion-Losses (C.L.) of Microwave and mm-Wave Mixers** 731  
Alireza Kazemipour, Mohammed Salhi, Thomas Kleine-Ostmann, Thorsten Schrader, Physikalisch-Technische Bundesanstalt, Germany

Classic methods to measure the mixer conversion-losses (C.L.) usually need an absolute RF and IF power-measurement at the mixer's ports. However, absolute power-measurement cannot be achieved with a low uncertainty level for the higher frequencies and mm-waves because of non-available standards and source & load mismatch problems. A new method is proposed based on relative-power measurement at IF-port when the RF-port is fed/measured by VNA. Therefore, the C.L. can be evaluated for the mm-wave mixers by using a suitable VNA and its relevant frequency-converters up to 325GHz. The setup is described and preliminary results are presented for a microwave-mixer and a mm-wave one.

[P1-18] 14:20 ~ 16:00

**3D Digital Predistortion for Dual-Band Envelope Tracking Power Amplifiers** 734  
Pere L. Gilabert<sup>1</sup>, Gabriel Montoro<sup>1</sup>, David López<sup>1</sup>, José A. García<sup>2</sup>, <sup>1</sup>Universitat Politècnica de Catalunya, Spain, <sup>2</sup>Universidad de Cantabria, Spain

This paper proposes a novel three-dimensional digital predistorter (3D-DPD) suitable for compensating nonlinear distortion in dual-band (DB) envelope tracking (ET) power amplifiers (PAs). By taking into account the cross-band modulation effects (due to DB operation) and the slow-envelope dependent distortion effects (due to ET), the 3D-DPD is design by properly modifying the memory polynomial (MP) behavioral model. In a first approach, the accuracy and reliability of the proposed 3D-MP model are evaluated. Finally, experimental results are shown to validate the linearization performance of the proposed 3D-DPD.

[P1-19] 14:20 ~ 16:00

**Chip Design of 5.2 GHz Frequency Synthesizer with a Gate-to-Source Feedback Colpitts VCO** 737  
Wen-Cheng Lai, Jhin-Fang Huang, Shao-Yu Chen, National Taiwan University of Science and Technology, Taiwan

A 5.2 GHz phase-locked loop (PLL) frequency synthesizer is implemented in TSMC 0.18  $\mu$ m CMOS process. The main features include the uses of a gate-to-source feedback Colpitts voltage-controlled oscillator (VCO) to lower phase noise, and an off-chip tunable low-pass filter to compensate the variations of resistance R and capacitance C to speed locking time and reduce chip area. At the supply voltage of 1.8-V, measured results achieve the tunable locked output frequency from 4.97 ~ 5.32 GHz, corresponding to 6.8% and at 1 MHz offset frequency away from the center frequency of 5.2 GHz, the phase noise of -109.57 dBc/Hz and the output power of -11.35 dBm with a reference spur of -58 dBc respectively. The overall power consumption is 22.4 mW. Including pads, the chip area is 0.7654 (0.89 $\times$ 0.86) mm<sup>2</sup>.

[P1-20] 14:20 ~ 16:00

**Doherty Power Amplifier using a Compact Load Network for Bandwidth Extension** 742  
Mincheol Seo, Hwiseob Lee, Jehyeon Gu, Youngoo Yang, Sungkyunkwan University, Korea

This paper presents a Doherty power amplifier (DPA) with a compact load network for an extended bandwidth compared to the conventional DPA. The compact load network takes less area since it has just one load matching network after the quarter-wave transmission line and no offset-lines. For the verification, both conventional and compact DPA's are designed and built using GaN HEMT for the band from 650 to 800 MHz. They were evaluated using the down-link 16-QAM FDD LTE signal that has a PAPR of 9.96 dB and a signal bandwidth of 5 MHz. At an average output power of 34 dBm, which is approximately 9 dB back-off from the 1 dB compression point, the proposed compact DPA exhibited a power-added efficiency (PAE) level of more than 40% and an adjacent channel leakage power ratio (ACLR) level of lower than -25 dBc over the frequency band of from 650 to 800 MHz, while the conventional DPA showed a PAE level of more than 26.6 % and an ACLR level lower than -23 dBc. In addition, the proposed compact DPA has a reduced circuit size by 40.9 % compared to the conventional one.

## Poster Session I : Active Components & EM Field and Techniques

- Date: November 6, 2013 (Wednesday)
- Time: 14:20 ~ 16:00
- Room: Room 103

[P1-21] 14:20 ~ 16:00

### Frequency Characteristic of Power Efficiency for 10 W/30W-Class 2 GHz Band GaN HEMT Amplifiers with Harmonic Reactive Terminations 745

Tomohiro Yao<sup>1</sup>, Ryo Ishikawa<sup>1</sup>, Yoichiro Takayama<sup>1</sup>, Kazuhiko Honjo<sup>1</sup>, Hiroyoshi Kikuchi<sup>2</sup>, Takashi Okazaki<sup>2</sup>, Kazuhiro Ueda<sup>2</sup>, Eiichiro Otobe<sup>2</sup>, <sup>1</sup>The University of Electro-Communications, Japan, <sup>2</sup>Samsung R&D Institute, Japan

An increase in amplifier efficiency is generally accompanied by a narrow bandwidth characteristic, especially when used with distributed transmission lines, since higher harmonics have to be treated. The frequency dependence of harmonic reactive terminations using transmission lines has been discussed for a high-efficiency amplifier design. In simulation, the designed amplifiers showed steep efficiency degradation due to a small source-side impedance shift for the second-order harmonic frequency. Therefore, both the source- and load-side circuits have to be optimized simultaneously. Fabricated 10-W and 30-W class GaN HEMT amplifiers including DC bias circuits exhibited a maximum drain efficiency of 81% at 1.98 GHz and 77% at 1.95 GHz, respectively.

[P1-22] 14:20 ~ 16:00

### Expanding bandwidth of Class-F Power Amplifier with Harmonic Structures 748

Teaggu Kang, Youngcheol Park, Hankuk University of Foreign Studies, Korea

This paper presents a methodology for designing compact broad-band RF power amplifiers with stretched harmonic tuning output networks. Rather than adopting a conventional output matching for wideband class-F operations, which is bulky in its size, this paper suggests a simpler way to achieve small-sized but wideband class-F operation. The proposed idea is achieved by stretched harmonic tuning circuits, and is verified by implementing a power amplifier at 1.9 GHz with a 10W GaN HEMT transistor. It showed 50 % of drain efficiency over the bandwidth of 250 MHz with significantly smaller size than the conventional continuous-mode class-F designs. The maximum output power is 14.45 W and a peak gain is 12.9 dB at 1.9 GHz.

[P1-23] 14:20 ~ 16:00

### The Maintenance of HPA MMIC's Efficiency for K-band 751

Hong-gu Ji, Inkwon Ju, Donghwnag Shin, Sungmo Mun, Inbok Yom, ETRI, Korea

This paper describes methods of supporting efficiency of an HPA at K band. We designed and fabricated HPA MMIC for K band using UMS 0.25  $\mu\text{m}$  GaAs process and then added adaptive biasing circuits for preservation of HPA efficiency. The circuits for maintenance of PAE consist of a directional coupler, a RF detector, a buffer amplifier and a DCDC convertor. The 8V supplied HPA's PAE is presented 13.5 % at 32.3 dBm but adaptive bias supplied HPA's PAE is displayed 18.2 % at Pout 31.9 dBm. The PAE of adaptive biased HPA increases 4.7 % than 8 V supplied HPA. Also, the amplifier PAE is maintained at back off 3.5 dB in CW operation conditions. The MMIC power amplifier and adaptive biasing circuits for HPA MMIC's efficiency are presented in this paper.

[P1-24] 14:20 ~ 16:00

### PMOS-Switching-Biased Voltage-Control-Oscillator 754

Te-Feng Chiao, Ming-Cheng Tu, Han-Hsin Wu, Yao-Jia Gao, Peng Kao, Jheng-Wei Wu, Sing-Jhang Cai, Chih-Ho Tu, Sheng-Wen Chen, Janne-Wha Wu, Ching-Wen Tang, National Chung Cheng University, Taiwan

A PMOS switching-biased VCO is investigated and fabricated by using TSMC 0.35  $\mu\text{m}$  CMOS technology with 2.8 V power supply voltage. A switching bias is employed for the PMOS tail transistor to improve the phase noise. The measured frequency tuning range is ranged from 2.87 GHz to 3.2 GHz. At 1 MHz offset from the carrier, the measured phase noise is -118.2 dBc/Hz. The total chip area takes 0.32  $\text{mm}^2$ . Under the consideration of output power, this design shows better performance over the figure of merit.

[P1-25] 14:20 ~ 16:00

### Development of a Highly Efficient and Linear Differential CMOS Power Amplifier With Harmonic Control 757

Sangsu Jin<sup>1</sup>, Kyunghoon Moon<sup>1</sup>, Myeongju Kwon<sup>2</sup>, Byungjoon Park<sup>1</sup>, Hadong Jin<sup>1</sup>, Jongjin Park<sup>1</sup>, Bumman Kim<sup>1</sup>, <sup>1</sup>POSTECH, Korea, <sup>2</sup>LG Electronics, Korea

This paper presents a highly linear differential cascode CMOS power amplifier (PA) with a second harmonic circuit at the common-gate (CG) stage. The proposed single stage PA including the harmonic control circuit is fabricated using 0.18- $\mu\text{m}$  RF CMOS technology with a printed board circuit based output transformer. The impact on the nonlinearity of the common-gate stage is analyzed. The CMOS PA module achieves a power added efficiency (PAE) of 38.7%, an error vector magnitude (EVM) of 5.4%, and the adjacent channel leakage ratio (ACLR) of -30.4 dBc at the average output power of 27.8 dBm and the frequency of 1.85 GHz for the 20-MHz bandwidth (BW) 16-QAM 7.5-dB peak-to-average power ratio (PAPR) long-term evolution (LTE) signal.

## Poster Session I : Active Components & EM Field and Techniques

- Date: November 6, 2013 (Wednesday)
- Time: 14:20 ~ 16:00
- Room: Room 103

[P1-26] 14:20 ~ 16:00

### A Comparator with Reduced Regeneration Time for Continuous-Time Delta-Sigma Modulator 760

Hi Yuen Song<sup>1</sup>, So Young Kang<sup>2</sup>, Dongmin Kang<sup>1</sup>, Hyunseok Choi<sup>1</sup>, Inn Yeal Oh<sup>1</sup>, Chul Soon Park<sup>1</sup>, <sup>1</sup>KAIST, Korea, <sup>2</sup>Samsung Electronics, Korea

A design of the comparator with reduced regeneration time and voltage scaling down for continuous-time delta-sigma modulators (CT DSM) was proposed. It has voltage scaling down to 0.65V, and gives worst case delay under 10%Ts (i.e. 125ps for 800MHz sampling frequency) at 1.2V supply voltage. A 3<sup>rd</sup> order low pass CT DSM employing the proposed comparator achieves 50.76 dB of SNDR and 3.2 MHz bandwidth, which are 5.2 dB higher and 3.2 times wider than those of a 3<sup>rd</sup> order low pass CT DSM employing the reference comparator, respectively.

[P1-27] 14:20 ~ 16:00

### Design of VCO using Bump Structure for High-Power Harmonics 763

Yoon Jae Bae, Nam Hwi Jeong, Choon Sik Cho, Korea Aerospace University, Korea

In this paper, we propose a VCO using the negative resistance property of bump structure. The proposed VCO consists of a bump circuit and an LC resonator for obtaining high power at the harmonic frequencies. The VCO is fabricated in 0.13  $\mu\text{m}$  RF CMOS process. The VCO works at the center frequency of 3.35GHz with -2.1dBm output power while this circuit consumes 20mW with 1.2V supply. Due to the negative resistance of bump circuit, second and third harmonics with high output power are achieved as -6.42dBm and -18.39dBm respectively.

[P1-28] 14:20 ~ 16:00

### A 28 dBm Pout 5-GHz CMOS Power Amplifier using Integrated Passive Device Power Combining Transformer 766

Kuei-Cheng Lin<sup>1,2</sup>, Hwann-Kaeo Chiou<sup>1</sup>, Po-Chang Wu<sup>2</sup>, Chun-Lin Ko<sup>2</sup>, Hann-Huei Tsai<sup>2</sup>, Ying-Zong Juang<sup>2</sup>, <sup>1</sup>National Central University, Taiwan, <sup>2</sup>National Applied Research Laboratories, Taiwan

This work presents a 5 GHz power amplifier (PA) in tsmc<sup>TM</sup> 0.18- $\mu\text{m}$  CMOS process. A high quality factor (Q) transformer adopted in the PA is fabricated using wafer-level integrated passive device (IPD) technology. The IPD transformer was stacked on the top of the active region of the CMOS PA chip. The PAs with and without IPD transformer are designed for performance comparison. The IPD CMOS-PA achieves an output power of 28 dBm, power added efficiency (PAE) of 25% under a 1.8-V supply voltage. The measured output power and PAE of the CMOS-IPD PA is 1.3 dBm and 6% better than that of the typical CMOS PA at the same power consumption. Beside, at OFDM/64-QAM modulated signals, the measured adjacent channel power ratio (ACPR) and error vector magnitude (EVM) are -43 dBc and 1.6%, respectively.

[P1-29] 14:20 ~ 16:00

### A 77GHz CMOS Medium Power Amplifier with Transmission Line Transformers for Multi-mode Automotive Radar System 769

Juntaek Oh, Bonhyun Ku, Songcheol Hong, KAIST, Korea

A 77 GHz CMOS medium power amplifier (PA) with high efficient matching networks based on transformer is presented. The unit transistor size of a power cell is selected by analyzing its maximum available gain. The broadside-coupled Transmission-Line Transformers (TLTs) are implemented as matching networks for low insertion loss and wide band matching characteristics. The PA is fabricated using a 65-nm RF CMOS process. The saturated output power and the peak power-added efficiency at 76.5GHz is 12.8 dBm and 8%, respectively. The DC power consumption is 236 mW with a supply voltage of 2.0V.

[P1-30] 14:20 ~ 16:00

### Design of UWB CMOS LNA Based on Current-Reused Topology and Forward Body-Bias for High Figure of Merit 772

Meng-Ting Hsu, Yu-Hua Lin, Jing-Cheng Yang, National Yunlin University of Science and Technology, Taiwan

This paper presents an UWB low noise amplifier (LNA) based on current reused and forward body-bias topology to achieve high figure of merit. The circuit was fabricated in a TSMC 0.18  $\mu\text{m}$  CMOS process. The implemented LNA has a peak gain of 14.8 dB, the input reflection coefficient S11 is lower than -11.5 dB, and the output reflection S22 is lower than -10.7 dB, the minimum of the noise figure is 3.5 dB and the measurement of IIP3 is -13 dBm. It consumes 7.8mW power consumption from 1.1-V supply voltage. The figure of merit is 13.02.

## Poster Session I : Active Components & EM Field and Techniques

- Date: November 6, 2013 (Wednesday)
- Time: 14:20 ~ 16:00
- Room: Room 103

[P1-31]

14:20 ~ 16:00

### RF Parametric Study on AlGaIn/GaN HEMTs on Si-substrate for Millimeter-Wave PA 775

Jihoon Kim, Hongjoo Park, Donghwan Kim, Minseong Lee, Kwangseok Seo, Youngwoo Kwon, Seoul National University, Korea

Size-optimized AlGaIn/GaN HEMTs on Si-substrate are investigated for millimeter-wave power amplifier (PA) MMICs. The number of finger (2, 4, 8) and the unit finger width (25, 37.5, 50, 75, 100  $\mu\text{m}$ ) of devices are split in the AlGaIn/GaN HEMTs process on Si-substrate. For searching the best suitable size for millimeter-wave PA, the RF performances such as  $F_{\text{max}}$  and MAG (Maximum Available Gain) are investigated through S-parameter measurements and small signal model parameter extractions. Moreover, thermal resistances are extracted through pulsed IV measurement to evaluate thermal degradation on GaN HEMTs. Through these experiments and parametric analyses,  $4 \times 37.5 \mu\text{m}$  or  $8 \times 37.5 \mu\text{m}$  GaN HEMTs show the best RF performance keeping not larger thermal resistances ( $R_{\text{th}}$ ). Thermal resistance and MAG are dependent on the gate pitch of GaN HEMTs. The selection of the proper gate pitch parameter of device is expected to bring the optimal power device performance in the millimeter-wave frequencies.

[P1-32]

14:20 ~ 16:00

### A Dual-Mode RF CMOS Power Amplifier with Nonlinear Capacitance Compensation 778

Seunghoon Kang, Bonhoon Koo, Songcheol Hong, KAIST, Korea

A fully integrated dual-mode CMOS power amplifier (PA) with nonlinear MOS capacitance compensation is presented using 0.18- $\mu\text{m}$  RF CMOS process. The proposed technique is used to implement dual mode structure as well as reduces AM-PM distortion. Dual-mode output matching network using transmission line transformer (TLT) is implemented for efficient dual mode operation. With a supply voltage 3.5V, the PA has the power gain of 26.2 and 14.2dB in low power mode (LPM) and high power mode (HPM), respectively. The quiescent current is only 28mA at LPM. The maximum linear output power satisfying 3GPP WCDMA modulated signal is 28/16.3dBm with a PAE 33.8/10.2% in the HPM/LPM.

[P1-33]

14:20 ~ 16:00

### A Wide-Band RF Front-End with Linear Active Notch Filter for GSM Inter-operability 781

Sang Gyun Kim<sup>1</sup>, Seung Hwan Jung<sup>2</sup>, Yun Seong Eo<sup>1,2</sup>, <sup>1</sup>Kwangwoon University, Korea, <sup>2</sup>Silicon R&D, Korea

This paper presents a wide-band RF front-end for mobile TV applications covering VHF-III(174~248MHz) and UHF band(470~746MHz). The RF front-end consists of a single to differential LNA with low amplitude/phase mismatch and an active notch filter to suppress GSM transmitter signal in UHF band. The notch filter, which adopts linear active inductor and Q-enhanced structure, rejects 35/37 dB 850/900 GSM signal. The RF front-end has 11~15dB gain and 4~5dB NF. This is fabricated on 0.18 $\mu\text{m}$  CMOS technology and consumes 26.28 mW.

[P1-34]

14:20 ~ 16:00

### A K-Band Monolithic Broadband Low Phase Noise Voltage Controlled Oscillators using HBT-HEMT Cascode Topology 784

Shu-Yan Huang<sup>1</sup>, Chih-Chun Shen<sup>1</sup>, Yu-Cheng Liu<sup>1</sup>, Yen-Han Liao<sup>1</sup>, Hong-Yeh Chang<sup>1</sup>, Yo-Shen Lin<sup>1</sup>, Yu-Chi Wang<sup>2</sup>, <sup>1</sup>National Central University, Taiwan, <sup>2</sup>WIN Semiconductors Corp., Taiwan

In this paper, a K-band monolithic broadband low phase noise voltage controlled oscillator (VCO) using heterojunction bipolar transistor (HBT) and pseudomorphic high-electron mobility transistor (HEMT) cascode topology is presented. The frequency range of negative resistance can be enhanced, and the low phase noise performance can be achieved simultaneously by using the cascode HEMT-HBT topology. The proposed K-band VCO features a wide frequency tuning range of 6.61 GHz, and a phase noise of -100.3 dBc/Hz at 1-MHz offset with a dc power consumption of 31.5 mW. The chip size of the proposed VCO is  $1 \times 1 \text{ mm}^2$ .

[P1-35]

14:20 ~ 16:00

### RF Performance of Ultra Low Power Junctionless MOSFETs 787

Dipankar Ghosh, Mukta Singh Parihar, Abhinav Kranti, Indian Institute of Technology, India

In this work, we report on the doping dependence of RF performance metrics of junctionless transistors and compare the same with conventional undoped inversion mode MOSFETs. It is demonstrated that at low drive currents ( $\sim 25 \mu\text{A}/\mu\text{m}$ ), JL transistors outperform inversion mode MOSFETs as 20% to 40% higher values of cut-off frequency is obtained for all doping concentrations ( $10^{19} \text{ cm}^{-3}$  to  $3 \times 10^{19} \text{ cm}^{-3}$ ). It is shown that the junctionless device architecture is advantageous for ultra low power RF applications as parasitic capacitances are significantly reduced. Scaling trends for cut-off frequency (at lower drain currents) with respect to gate length highlights the potential of junctionless architecture for ultra low power applications.

## Poster Session I : Active Components & EM Field and Techniques

- Date: November 6, 2013 (Wednesday)
- Time: 14:20 ~ 16:00
- Room: Room 103

[P1-36] 14:20 ~ 16:00

### Wide-band Linear Characteristic Compensation for DPD Systems with Direct Learning 790

Zhijian Yu, Huan Xie, Erni Zhu, Shanghai Huawei Technologies Co., Ltd., China

Direct learning with ideal PA function assumption is an efficient method for adaptive DPD because the information of PA is not needed. However, high efficiency PA design results in worse amplitude response and group delay characteristic within the linearization bandwidth. Then underlying assumption may be not hold, and the direct learning is divergent. In the paper, we analyze condition for convergence using the direct learning with ideal PA assumption. Four schemes are proposed to compensate wide-band linear characteristic when condition is violated. Simulation results and experimental tests confirm the analysis and the effectiveness of proposed algorithms.

[P1-37] 14:20 ~ 16:00

### Phase Noise Suppression for Realistic LOS-MIMO Microwave Backhaul Systems 794

Rui Lv, Meng Cai, Zihuan Chen, Jun Ma, Xiaodong Li, Huawei Technologies Corporation, China

Phase noise (PN) in microwave (MW) systems greatly deteriorates Line-of-Sight (LOS) Multi-input Multi-output (MIMO) performance. To address the PN impairment, a least squares (LS) estimator for LOS-MIMO is derived based on a flat channel assumption, and the MIMO phase compensation strategy is also deduced to suppress the vital PNs. Then, more realistic radio frequency front-ends (RFFE) with non-flatness in frequency response are considered in a MW LOS-MIMO system. The normally shallow notches in RFFEs' bandwidth introduce some inter-symbol interference (ISI) into the system. Based on the ISI polluted MIMO system model, we prove that the effectiveness of LS MIMO PN suppression (PNS) is largely deteriorated by the fast varying component in adjacent symbols. A novel matrix-inversion-based method is then proposed to address the ISI impairment on MIMO PNS. The two PNS methods are evaluated in our MW LOS-MIMO receiver. Effectiveness of both methods on ideal RFFEs and the superior of the latter one on realistic RFFEs are verified.

[P1-38] 14:20 ~ 16:00

### Nonlinearity Estimation and Correction of VCO Based on Temperature-Varied Tuning Characteristic Model 797

Wang Hua, Song Qian, Zhou Zhi-min, National University of Defense Technology, China

As nonlinearity in voltage controlled oscillator (VCO) degrades the range resolution of frequency modulated continuous wave (FMCW) radar, a novel method to estimate and correct the nonlinearity is presented in this paper. Firstly, in order to provide a more accurate description of the nonlinear term, a temperature-varied tuning characteristic model of VCO (VCO-TT) is built. Afterwards, based on the VCO-TT model, a contrast of range profile optimization algorithm is adopted, which achieves the optimal estimation and correction of the nonlinearity. Without changing hardware system, this method which operates directly on the deramped data can refocus the range profile as well as nonlinearity removal simultaneously. Finally, experimental results from a commercial VCO convincingly validate the feasibility and effectiveness of the proposed method.

[P1-39] 14:20 ~ 16:00

### Preliminary Study of Wireless Power Transmission for Biomedical Devices inside a Human Body 800

SangWook Park, National Institute of Information and Communications Technology, Japan

As a preliminary study, the technique wirelessly transferring electromagnetic energies to an implant device within a human body has been investigated. The wireless power transmission (WPT) technique using magnetically coupled resonances has been adapted to obtain high transmission efficiency. The transmission efficiency into the inside of a human body has been estimated for open-type and closed-type WPT systems. It has been shown that the closed-type WPT system has higher transmission efficiency than the open-type WPT system.

[P1-40] 14:20 ~ 16:00

### Approximation for Measuring Complex Material Parameters at $\lambda/2$ Resonances in Transmission-Line Measurements 803

Sung Kim, James Baker-Jarvis, National Institute of Standards and Technology, USA

We propose an approximation for removing resonant artifacts that arise in permittivity and permeability measurements when using the transmission/reflection (T/R) method at frequencies where the test sample length is an integer multiple of a half wavelength. In order to address this issue, we approximate the input impedance of the transmission-line fixture around the  $\lambda/2$  resonance with a simple algorithm based on a 1st-order regression. The characteristic impedance of the sample-loaded section of the fixture is computed from those regression coefficients, and the permittivity and permeability can be computed by assuming that the refractive index obtained from the conventional T/R method does not suffer from resonant artifacts. Our approximate results are validated when compared with those from one of the conventional T/R methods, the Nicolson-Ross-Weir (NRW) method.

## Poster Session I : Active Components & EM Field and Techniques

- Date: November 6, 2013 (Wednesday)
- Time: 14:20 ~ 16:00
- Room: Room 103

[P1-41] 14:20 ~ 16:00

### Circuit Tuning Elements-Less Tuning Space Mapping Optimization 806

Bo Zhou, Weixing Sheng, Nanjing University of Science and Technology, China

Tuning space mapping (TSM) without circuit tuning elements (CTE) is proposed. A section of design interest in the electromagnetic (EM) model is replaced by 'n' pieces cascaded EM-based unit cells (EUC). The tuning parameter of proposed TSM is the quantity of cascaded EUC instead of conventional CTE components (e.g., capacitors, inductors, or microstrip-line models). Finally the optimal quantity parameter is transferred to original design variables. The advantage of the proposed TSM is the needless of CTE components. The method is useful when no corresponding CTE components of structures available in the circuit simulators' libraries. Verification example, comparisons and discussions are also implemented.

[P1-42] 14:20 ~ 16:00

### Miniaturized C-EBG Power/Ground Planes on Substrate Integrated Artificial Dielectric with Stopband Enhancement 809

Yongrong Shi<sup>1</sup>, Sheng Liu<sup>1</sup>, Cheng Wang<sup>1</sup>, Wanchun Tang<sup>2</sup>, <sup>1</sup>Nanjing University of Science and Technology, China, <sup>2</sup>Nanjing Normal University, China

A miniaturized C-EBG power/ground planes on the substrate integrated artificial dielectric (SIAD) with stopband enhancement is studied in this paper. Since the SIAD is also an EBG structure, the additional stopband of the SIAD can be effectively used to broaden the stopband bandwidth of C-EBG. The simulation results show that the stopband bandwidth is enhanced 65% as well as reducing the C-EBG unit cell size by 55% without deteriorating the lower bound cutoff frequency in the sub GHz region of the original C-EBG.

[P1-43] 14:20 ~ 16:00

### Evaluation of Electromagnetic Fields Levels in vicinity of Broadcasting Transmitters 812

Byung Chan Kim, Hyung-Do Choi, ETRI, Korea

In this paper, electromagnetic field levels in the vicinity of UHF-band TV/FM stations are presented. Measurements were performed in order to determine the compliance with exposure limits for the general public. The total exposure levels from eighteen stations at seven sites at distances of 183 to 5,406 m were within a range of 0.03 to 1.62 V/m. The highest level was found to correspond to about 0.3 % compared with ICNIRP guidelines.

[P1-44] 14:20 ~ 16:00

### Optimized Higher Order 3-D (2,4) FDTD Scheme for Isotropic Dispersion in Plasma 815

Inkyun Jung<sup>1</sup>, Il-Young Oh<sup>1</sup>, Yongjun Hong<sup>2</sup>, Jong-Gwan Yook<sup>1</sup>, <sup>1</sup>Yonsei University, Korea, <sup>2</sup>Agency for Defense Development, Korea

In this paper, an optimized higher order (2,4) 3-dimensional finite-difference time-domain (FDTD) method is applied in plasma. The optimized scheme uses the scaling factors and weighted sum of the standard FDTD method (Yee's scheme) and the standard (2,4) higher order FDTD method (H(2,4)) proposed by Fang. The proposed scheme improves performance of phase and attenuation constant error over propagation angle without additional computational complexity compared with H(2,4). The maximum phase constant error of the proposed scheme is reduced by 98.7% of the H(2,4)'s error.

[P1-45] 14:20 ~ 16:00

### Extraction of Vibration Components from a Rotating Propeller Model Based on Complex Empirical Mode Decomposition 818

Ji-Hoon Park<sup>1</sup>, Woo-Yong Yang<sup>1,2</sup>, Jun-Woo Bae<sup>2</sup>, Noh-Hoon Myung<sup>1</sup>, <sup>1</sup>Korea Advanced Institute of Science and Technology, Korea, <sup>2</sup>Samsung Thales, Korea

In this paper, we present extraction of vibration components embedded in signatures from rotating propellers. In order to deal with complex-valued signatures, complex empirical mode decomposition (CEMD), an extended version of EMD, is employed to extract the vibration components. With FEKO simulation, we obtain composite signatures induced by both rotation and vibration of the simply modeled propeller for two different cases. Then CEMD is applied to these signatures and the reconstructed vibration components are analyzed in the joint time-frequency domain. The estimated vibration-related parameters showed reasonable agreement with actual motion parameters. This paper shows good possibility of predicting new characteristics from rotating propellers.



## Poster Session I : Active Components & EM Field and Techniques

- Date: November 6, 2013 (Wednesday)
- Time: 14:20 ~ 16:00
- Room: Room 103

[P1-46] 14:20 ~ 16:00

### Transmission Characteristic of Electromagnetic Wave between the Ground and the Air 821

Sangmu Lee<sup>1</sup>, Dongho Kim<sup>2</sup>, Pyung-Dong Cho<sup>1</sup>, <sup>1</sup>Electronics and Telecommunications Research Institute, Korea, <sup>2</sup>Sejong University, Korea

When an electromagnetic wave comes into the ground from the air, it drops vertically from an incident point. Vice versa, an electromagnetic wave directs 45° from an incident point when it transmits into the air from the ground. The direction of transmission from the ground to the air has a useful meaning in that a sort of cavity phenomenon occurs in the area just right over the source in the ground due to the obliqueness of wave direction. This means that the effect of electromagnetic field decreases in that area. When an interference to another source in the air is analyzed, this phenomenon is worthwhile to be considered.

[P1-47] 14:20 ~ 16:00

### EM Optimization using Coarse and Fine Mesh Space Mapping 824

Chao Zhang<sup>1</sup>, Feng Feng<sup>1</sup>, Qi Jun Zhang<sup>1,2</sup>, <sup>1</sup>Tianjin University, China, <sup>2</sup>Carleton University, Canada

Space mapping is an effective method for electromagnetic (EM) optimization. The method normally assumes the availability of an equivalent circuit as the coarse model. This paper addresses the situation when an equivalent circuit coarse model is not available. We propose a space mapping optimization algorithm with coarse mesh EM simulation as coarse model. Our technique uses mostly coarse mesh EM evaluation and occasionally fine mesh EM evaluation to achieve optimal EM solutions with fine mesh accuracy. In our optimization, the surrogate model training and optimization are both done in the EM simulator. This technique is illustrated by two microwave filter examples.

[P1-48] 14:20 ~ 16:00

### Vertical Signal Transmission by Non-contact Technology Application for 3DIC 827

Jun-Kai Wang<sup>1</sup>, Ren-Fang Hsu<sup>1</sup>, Wen-Te Chien<sup>1</sup>, Sung-Mao Wu<sup>1</sup>, Cheng-Chang Chen<sup>2</sup>, Ming-Shan Lin<sup>2</sup>, <sup>1</sup>National University of Kaohsiung, Taiwan, <sup>2</sup>Bureau of Standards, Metrology and Inspection, Ministry of Economic Affairs, Taiwan

In order to solve the problem of process and cost in 3D-IC, novel non-contact signal transmission with coupling loops have been presented. In this study, we design the broadband, well reproducibility, well directivity and low loss coupling loops to transmit signal between different chips or ICs in 3DIC application, and establishing physical model up to 10GHz with coupling effect and loop effect to restore the signal radiation. By this method, the overall signal transmission of TSV can be the same as the non-contact technology. People can use this design to replace the TSV technology in the future.

[P1-49] 14:20 ~ 16:00

### Experimental Studies on Power Control Microwave Ablation in Vitro Animal Tissues with Microwave Percutaneous Coagulator 830

M. Chaichanyut, P. Lerprasert, S. Tungjitkusolmun, King Mongkut's Institute of Technology Ladkrabang, Thailand

Microwave coagulation therapy (MCT) has been used mainly for the treatment of small-size tumors. The operating frequency is 2450 MHz for the present MCT. In this paper, we analyzed the heating characteristics (temperature distributions patterns, lesion on size and etc.) of an applicator composed of thin microwave antenna. The configurations of thin microwave monopole antennas were considered: Coaxial Quarter Conductor Antennas (CQCA). Experimental protocol was composed by a radiation system and a thermometry system. We apply the microwave power during experiments was 10W, 20W, 40W and 80W which microwave power all case will vary the duration time for ablation were 60s 120s 240s and 480s respectively; Thermal sensors were placed next to the antenna at 1mm, a large number of experiments on porcine liver are carried out, the temperature distribution within the liver are measured and illustrated, for cases of different injected microwave power and ablation time. From our experimental results, if we considered the region where temperature exceeds 50°C, the threshold for successful hepatic ablation. The CQCA has lesion size was larger, with a lesion width of approximately 20 mm. In addition, the ablation areas in cases of different input microwave powers are measured also. All these results indicate the potential validity of this system on medical treatment of liver cancer of human body.

[P1-50] 14:20 ~ 16:00

### Solid State 448GHz Frequency Doubler using Intergrated Schottky Membrane Technology 833

F. Yang<sup>1,2</sup>, J. Treuttel<sup>2</sup>, A. Maestrini<sup>2</sup>, L. Gatilova<sup>3</sup>, <sup>1</sup>Southeast University, China, <sup>2</sup>Observatoire de Paris, France, <sup>3</sup>Laboratoire de Photonique et de Nanostructures, France

The design is to accomplish a frequency doubler by using thin membrane sub-millimeter wave integrated circuit fabrication technology. The Goubau line theory is firstly incorporated here to predefine the dimension of the channel, which is the key to the doubler's performance. The detailed linear and nonlinear co-simulation method is presented as followed, usually several iterations are needed during the optimization flow. Finally, the expected pass-band of doubler is from 430GHz to 470GHz over 22% efficiency. And the mesa size is 10umx8.2um and the membrane thickness is 5um. It shows that we can realize high efficiency frequency multipliers even up to several THz in the future by using this thin membrane fabrication technology.

## Poster Session I : Active Components & EM Field and Techniques

- Date: November 6, 2013 (Wednesday)
- Time: 14:20 ~ 16:00
- Room: Room 103

[P1-51] 14:20 ~ 16:00

### Investigation of The Assessment Method for Human Exposure from A Wireless Power Transfer System 836 Woo-Geun Kang<sup>1</sup>, Hae-Young Jun<sup>2</sup>, Yong-Ho Park<sup>2</sup>, Jeong-Ki Park<sup>1</sup>, <sup>1</sup>Chungnam National University, <sup>2</sup>Samsung Electronics, Korea

Various types of wireless power transfer devices have been developed recently and active researches are ongoing in each country. In this paper, we investigated the limitations and difficulties in the exposure assessment for wireless power transfer devices, and proposed a new assessment method based on the correlation characteristics between SAR and external magnetic field. As a typical example, the exposure from a wireless mobile-phone charger were analyzed in detail, assessed for the basic restrictions and reference levels of ICNIRP, FCC and Korean guideline, and problems related to the exposure assessment were discussed. The correlation characteristics between SAR and external magnetic field of the wireless charger, on which the new method is based, are presented. The proposed method is quite reasonable and can get around the difficulties in the exposure assessment of wireless power transfer devices.

[P1-52] 14:20 ~ 16:00

### Convolutional Perfectly Matched Layer (CPML) for Fundamental LOD-FDTD Method with 2nd Order Temporal Accuracy and Complying Divergence 839

Theng-Huat Gan, Eng Leong Tan, Nanyang Technological University, Singapore

This paper extends the unconditionally stable locally one-dimensional finite-difference time-domain method with second-order temporal accuracy and complying divergence (denoted as LOD2-CD-FDTD) by incorporating the convolutional perfectly matched layer (CPML). To further enhance efficiency, the LOD2-CD-FDTD method with CPML is formulated into the fundamental form with the simplest and most concise right-hand sides free of matrix operators. The explicit output processing of the LOD2-CD-FDTD method has complying divergence, and it is also independent of the CPML media. Numerical results are presented to validate the formulation.

[P1-53] 14:20 ~ 16:00

### Attenuation of a Horn Antenna for Thermal Noise Measurement 842

Tae-Weon Kang, Jeong-Hwan Kim, Jin-Seob Kang, No-Weon Kang, Korea Research Institute of Standards and Science, Korea

A cryogenic noise reference standard consists of an antenna, a cavity, an electromagnetic absorber, and a liquid nitrogen container. The horn antenna is installed at the upper part of the cavity to measure the thermal noise radiated from the absorber carefully placed at the bottom of the cavity. By filling liquid nitrogen to an appropriate level the electromagnetic absorber is maintained at approximately 77 K. In this paper, some design considerations are discussed to minimize the diffraction from the internal surface of the horn antenna. Using the resultant dimension of the horn, the attenuation of the overall horn-flare configuration is evaluated to be 0.034 dB to 0.037 dB in the frequency range of 75 GHz to 110 GHz. The calculated attenuation with other relevant parameters is used to obtain the calculable output noise temperature of the cryogenic noise reference standard.

[P1-54] 14:20 ~ 16:00

### On the Late-Time Instability of Perfectly Matched Layers in the Meshless Radial Point Interpolation Method 845

Zahra Shaterian, Thomas Kaufmann, Christophe Fumeaux, The University of Adelaide, Australia

The time-domain behavior of the Uniaxial Perfectly Matched Layer (UPML) in the 3D meshless Radial Point Interpolation Method (RPIM) is investigated in this paper. It is theoretically shown that the UPML will become unstable after a very long time when the energy in the computational almost completely vanishes. A timed introduction of loss terms in the equations inside the UPMLs, i.e. at a time after absorption of most of the energy, can significantly delay the occurrence of this instability without compromising the accuracy of the solution.

[P1-55] 14:20 ~ 16:00

### Reduction of Field Penetration through Narrow Slots by Conducting Strip 848

Byung-Ho Cho<sup>1</sup>, Sung-Min Lim<sup>2</sup>, Sung-Woo Jung<sup>3</sup>, Ki-Chai Kim<sup>1</sup>, <sup>1</sup>Yeungnam University, Korea, <sup>2</sup>SL Corporation, Korea, <sup>3</sup>Gyeongbuk Research Institute of Vehicle Embedded Technology, Korea

This paper considered the electromagnetic field reduction which penetrated into the slot by adding the conducting strip around the slot on the infinite conducting plane. In addition, the study examined how the structural changes in the additional conducting strip affected the reduction characteristics of the penetrated electromagnetic field by calculating the penetrated electric field depending on the gap and the length of the additional conducting strip.

## Poster Session I : Active Components & EM Field and Techniques

- Date: November 6, 2013 (Wednesday)
- Time: 14:20 ~ 16:00
- Room: Room 103

[P1-56] 14:20 ~ 16:00

### Development of Smart EM Wave Absorber with Heat Radiating Function 851

Dongsoo Choi, Dong Il Kim, Korea Maritime University, Korea

With the rapid progress of electronics and radio communication technology, human enjoys greater freedom in information communications. However, EMW (Electro-Magnetic Wave) environments have become more complicate and difficult to control. Thus, the international organizations, such as the American National Standard Institution (ANSI), Federal Communications Commission (FCC), the Comite Internationale Special des Perturbations Radio Electrique (CISPR), etc, have provided standards for controlling the EM wave environments and for the countermeasures of the electromagnetic compatibility (EMC). In this paper, the status of EMW absorbers and the goal of the smart EMW absorber for the future were described and discussed. Furthermore, a smart EMW Absorber with heat radiating function was suggested and designed, which has the absorption ability of more than 20 dB from 2 GHz to 2.45 GHz frequency band, and the optimum aperture (hole) size, the space between the adjacent holes, and the thickness of which were 6 mm, 9 mm, and 6.5 mm, respectively. Thus, it is respected that these results can be applied as various EMC devices in electronic, communication, and controlling systems.

[P1-57] 14:20 ~ 16:00

### Down-Converted Mixer Verification using The Measured X-Parameter for System Engineering Designers 854

Hsu-Feng Hsiao, Chih-Ho Tu, Hann-Huei Tsai, Hsu-Chen Cheng, Da-Chiang Chang, Ying-Zong Juang, National Applied Research Laboratories, Taiwan

This paper investigates the down-converted mixer verification using the measured X-parameter in future system-level simulation. The X-parameter measurement system utilizing Agilent's nonlinear vector network analyzer (NVNA) and the external RF signal generator can provide the desired stimulus to device under test (DUT) at the specified port in order to measure and respond to the non-linear DUT characteristic. The X-parameter of the down-converted mixer may include the measured nonlinear output power and phase at the specified frequencies. Also, the down-converted mixer utilizing with nonlinear device characteristic to convert RF to intermediate frequency (IF) can be described by the X-parameter with good consistency.

[P1-58] 14:20 ~ 16:00

### Adaptive Load Impedance Matching using 5-port Reflectometer With Computationally Simple Measurement 857

Hyeong-Seok Jang, Won-Seok Lee, Tae-dong Yeo, Jong-Won Yu, Korea Advanced Institute of Science and Technology, Korea

Five-port architectures are investigated as a reflectometer for adaptive load impedance matching. The proposed reflectometer requires computationally simple control loop. Moreover, the adaptive load impedance matching system in RFID UHF band are proposed. Using simulation and measurement studies, it is shown that the five-port architecture can be used as a low-cost, simple and high-performance reflectometer in adaptive load matching systems.

[P1-59] 14:20 ~ 16:00

### Effect of Signal PAPR on Efficiency of Envelope Tracking Power Amplifiers 860

Jonmei J. Yan<sup>1</sup>, Chan-Sei Yoo<sup>2</sup>, Elizabeth M. Trask<sup>1</sup>, Dongsu Kim<sup>2</sup>, Peter M. Asbeck<sup>1</sup>, <sup>1</sup>University of California, USA, <sup>2</sup>Korea Electronics Technology Institute, Korea

Although envelope tracking power amplifiers have significantly higher efficiency in back-off than constant supply Class AB amplifiers, there is nonetheless an impact of modulation peak-to-average power ratio (PAPR) on the overall system efficiency. This paper provides experimental results and analysis of efficiency of a GaN RF amplifier with peak power 100W under envelope tracking, as a function of PAPR over the range 6.5dB to 10dB. The analysis shows that the RF transistor knee voltage relative to its maximum drain voltage, and the output power of the envelope amplifier relative to its maximum output power, are major determinants of the efficiency roll-off.

[P1-60] 14:20 ~ 16:00

### Improved Accuracy of Asymmetric Ground-plane Cloak 863

Yongjune Kim<sup>1</sup>, Ilsung Seo<sup>2</sup>, Yongshik Lee<sup>1</sup>, <sup>1</sup>Yonsei University, Korea, <sup>2</sup>Agency for Defense Development, Korea

This paper demonstrates improving method of asymmetric ground-plane cloak by applying unequally generated initial grids and compensating the notorious lateral shift of the ground-plane cloak. By generating initial grids unequally, broken grids of quasi-conformally mapped grids are corrected. Thus, an error of reflection angle of asymmetric ground-plane cloak is compensated. Moreover, by increasing the height of the bump and cloak, and shifting down the cloaking material below the reference ground plane, the lateral shift of the ground-plane cloak is compensated effectively. The proposed method is verified via the ray tracing simulation results using commercial software, the Comsol multiphysics.

## [W2A] Novel RF Transceivers

- Date: November 6, 2013 (Wednesday)
- Time: 16:30 ~ 18:30
- Room: Room A (Room 101)
- Session Chairs: Chien-Nan Kuo (National Chiao Tung University)  
Sanggeun Jeon (Korea University)

[W2A-1]

16:30 ~ 17:00

### [Invited] Wireless Body Area Network and its Healthcare Applications 89

Hoi-Jun Yoo, KAIST, Korea

With a paradigm shift in advent of u-healthcare era, the wireless body area network (WBAN) has been recently emerged. In this paper, we overview the WBAN technology and summary its three types of physical layers (PHYs). Among three PHYs, we introduce the human body communication (HBC) which uses the human body as a communication channel to transmit the electric signal. Through the clear understanding of the body channel with T-shaped body channel model and theoretical channel analysis, we present 6 HBC transceiver implemented with CMOS technology, including a world-first WBAN transceiver satisfying all of the specifications for IEEE 802.15.6 standard. Through the implemented transceiver, we successfully demonstrate the MP3 player, and smart patch system for entertainment, and healthcare application, respectively.

[W2A-2]

17:00 ~ 17:30

### [Invited] ULP Receiver Design Methodologies for Wireless Sensor Network Applications 92

Jae-Seung Lee, Joo-Myoung Kim, Seok-Kyun Han, Sang-Gug Lee, KAIST, Korea

This paper presents an overview of design methodologies for the ultra-low power (ULP) receivers for the wireless sensor network (WSN) applications. The advantages and limitations of the most widely used ULP receiver architectures, tuned-RF, super-regenerative, uncertain-IF, and low-IF, are reviewed. The guidelines for the ULP RF circuit designs are also described.

[W2A-3]

17:30 ~ 17:50

### A Low Power, Area Efficient Frequency Acquisition Circuit with Array Oscillator for Pulse-Based Inductive-Coupling Transceiver 95

Teruo Jyo, Tadahiro Kuroda, Hiroki Ishikuro, Keio University, Japan

This paper presents a low power, small area Frequency Acquisition Circuit (FAC) for a pulse-based inductive coupling transceiver. Multiphase clock which is generated in array oscillator is used to control the pulse width. To solve the problem of oscillation frequency change by PVT variation, FAC is proposed to control the oscillating frequency. FAC uses multiphase clock in array oscillator. By sharing the multiphase clock for both the pulse generation and the frequency control, low power and small area can be achieved. The fabricated test chip in 65nm CMOS occupies 0.045mm<sup>2</sup>. The array oscillator generates 1GHz, 20 phase clock at the supply voltage of 0.8V. The RMS of cycle-to-cycle jitter is 3.3ps and the power consumption is 1.1mW.

[W2A-4]

17:50 ~ 18:10

### A Low Leakage Pull-Down Network for PLL with 6.7 dB Improvement in Reference Spur 98

Pawan Agarwal, Suman P. Sah, Deukhyoun Heo, Washington State University, USA

A leakage current reduction technique is proposed for the pull-down network (PDN), which is used to hibernate the Phase-locked loop (PLL). Due to the low leakage current, the PDN results in PLL with lower reference spur. The switch leakage is minimized by biasing the MOSFET with  $V_{GS} < 0$ . Proposed method reduces the leakage current by at least an order of magnitude. A prototype PLL was built in TSMC 0.18  $\mu\text{m}$  CMOS technology. An improvement of 6.7 dB in reference spur is measured compared to the conventional PLL.

[W2A-5]

18:10 ~ 18:30

### Novel Substrate Integrated Waveguide (SIW) Type High Power Amplifier using Microstrip-to-SIW Transition 101

Zhebin Wang, Chan-Wang Park, University of Quebec in Rimouski, Canada

In this paper, a novel 10W substrate integrated waveguide (SIW) high power amplifier (HPA) designed with SIW matching network (MN) is presented. The SIW MN is connected with microstrip line using microstrip-to-SIW transition. An inductive metalized post in SIW is employed to realize impedance matching. At the fundamental frequency of 2.14 GHz, the impedance matching is realized by moving the position of the inductive metalized post in the SIW. Both the input and output MNs are designed with the proposed SIW-based MN concept. One SIW-based 10W HPA using GaN HEMT at 2.14 GHz is designed, fabricated, and measured. The proposed SIW-based HPA can be easily connected with any microstrip circuit with microstrip-to-SIW transition. Measured results show that the maximum power added efficiency (PAE) is 65.9 % with 39.8 dBm output power and the maximum gain is 20.1 dB with 30.9 dBm output power at 2.18 GHz. The size of the proposed SIW-based HPA is comparable with other microstrip-based PAs designed at the operating frequency.

## [W2B] Transitions and Packaging

- Date: November 6, 2013 (Wednesday)
- Time: 16:30 ~ 18:30
- Room: Room B (Room 102)
- Session Chairs: Albert Chin (National Chiao Tung University)  
Ikmo Park (Ajou University)

[W2B-1]

16:30 ~ 16:50

### Experimental Verification of Coplanar-to-Substrate-Integrated-Waveguide Interconnect on Low-Permittivity Substrate 104 Farzaneh Taringou<sup>1</sup>, Jens Bornemann<sup>1</sup>, Ke Wu<sup>2</sup>, <sup>1</sup>University of Victoria, Canada, <sup>2</sup>Ecole Polytechnique de Montreal, Canada

An interconnect between coplanar waveguide (CPW) and substrate integrated waveguide (SIW) is designed and experimentally verified. Common to regular SIW circuits is a low-permittivity substrate, whereas design formulas CPW usually assume a high permittivity. Therefore, commercially available field solvers are used in a parametric study to optimize the interconnect over a wide bandwidth between 18 GHz and 28 GHz. Cross-sectional field plots demonstrate its basic operation. The individual interconnect achieves return and insertion losses better than 20 dB and 0.5 dB, respectively, over the entire frequency range. The respective values for a measured back-to-back transition are 17 dB and 1.45 dB which are in good agreement with simulations.

[W2B-2]

16:50 ~ 17:20

### [Invited] High Performance RF Passive Devices and Noise-Shielding MOSFET on IC-Standard Si Wafer for Sub-THz Applications 107

Albert Chin<sup>1</sup>, Hsuan-Ling Kao<sup>2</sup>, <sup>1</sup>National Chiao Tung University, Taiwan, <sup>2</sup>Chang Gung University, Taiwan

The operation frequency of a MOSFET is approaching THz as continuously scaling down into 1X nm. Nevertheless, the very high power loss of transmission line on IC-Standard Si wafer (~5 dB/mm at 110 GHz) is the fundamental limitation for Si-based sub-THz IC. Using a simple method to translate standard 10 Ω-cm low resistivity into semi-insulating, very low loss transmission line and broad filters have been realized on Si wafer to 110 GHz, with performance near ideal devices by EM design. The noise coupling of CPW-layout RF MOSFET can also be filtered using a microstrip line design, and a low min. noise figure (NF<sub>min</sub>) of 0.5 dB at 10 GHz was measured in a 90 nm MOSFET. Both ion-implantation translated semi-insulating Si and microstrip line noise shielding methods have been successfully implemented in IC foundry.

[W2B-3]

17:20 ~ 17:40

### Wideband Transition from Coaxial Line to Half-Mode Substrate Integrated Waveguide 110 Nghia Nguyen-Trong, Thomas Kaufmann, Christophe Fumeaux, The University of Adelaide, Australia

In this paper, a perpendicular transition from coaxial cable to Half-Mode Substrate Integrated Waveguide (HMSIW) is proposed for wideband operation. The design places emphasis on the robustness and manufacturability of the transition, in particular with a reproducible realization of a matching capacitive gap. A prototype of back-to-back transitions with 64 mm length of HMSIW in-between is realized for operation in the frequency range of 10 GHz to 16 GHz. The return loss of the back-to-back transitions is measured to be close to 20 dB. A reasonable agreement between experimental and simulation results is achieved, validating the proposed transition geometry.

[W2B-4]

17:40 ~ 18:10

### [Invited] Development of Millimeter-wave Passive Components and System-in-Packages by LTCC Technology 113 Ruey-Beei Wu, Tze-Min Shen, Ting-Yi Huang, National Taiwan University, Taiwan

This paper addresses the recent development of millimeter-wave passive components for radar and wireless communication applications by the low-temperature co-fired ceramic (LTCC) technology. Several new design ideas which fully utilize the LTCC multilayer features and the existence of multiple cavity modes in realizing some special performance are summarized, including multi-band filters with flexible band assignments, compact diplexers with single branch configurations, couplers and antennas design with filtering characteristics. Finally, two system-in-package application examples have been demonstrated in 60 GHz frontend phased array for dense wireless communications and micro-radar module for noncontact vital sign detection.

[W2B-5]

18:10 ~ 18:30

### An Optimized Process of High-performance Integrated Passive Devices (IPDs) on SI-GaAs Substrate for RF Applications 116 Yang Li, Cong Wang, Nam-Young Kim, Kwangwoon University, Korea

An integrated passive device (IPD) technology by semi-insulating (SI) GaAs-based fabrication has been developed to meet the ever increasing needs of size and cost reduction for RF and microwave applications. In this paper, we develop an advanced optimized process for realizing IPDs to reduce fabrication time and total cost and to increase RF performances. The critical characteristics of lumped elements thin film resistor (TFR), spiral inductor and metal-insulator-metal (MIM) capacitor are optimized in this advanced process. A low-pass filter (LPF) for global system for mobile communications (GSM) is demonstrated by using this IPD process; it shows very good RF performances in spite of its small chip size and low cost, when compared with the recently reported literature.

## [W2C] Theoretical Analysis

- Date: November 6, 2013 (Wednesday)
- Time: 16:30 ~ 18:10
- Room: Room C (Room 104)
- Session Chairs: Hiroshi Shirai (Chuo University)  
Yongbae Park (Ajou University)

[W2C-1]

16:30 ~ 16:50

### Genetic Algorithm to Formulate Fourth Order Debye Model of Main Head Tissues 119

S. Mustafa<sup>1,2</sup>, A. Abbosh<sup>2</sup>, <sup>1</sup>Salahaddin University, Iraq, <sup>2</sup>The University of Queensland, Australia

A fourth order Debye model is derived using genetic algorithms to represent the dispersive properties of the main tissues that form the human head. The derived model gives accurate estimation of the electrical properties of those tissues across the frequency band from 0.1 GHz to 3 GHz that can be used in microwave systems for head imaging.

[W2C-2]

16:50 ~ 17:10

### Multi-GPU Accelerated P-FFT Method for Efficient Modeling of Antennas Mounted on Complex and Large Platform 122

Shaoxin Peng, Chao-Fu Wang, National University of Singapore, Singapore

This paper presents a multi-GPU accelerated fast integral equation solver for efficient modeling of antennas mounted on complex and large platform. The antenna system with surface-wire configuration is characterized using surface wire integral equation (SWIE). The SWIE is solved using the Precorrected-FFT (P-FFT) method on multi-GPUs. Special mapping schemes are proposed to efficiently map the P-FFT algorithm to multi-GPU platform. Very good performance achieved validates the proposed multi-GPU mapping schemes.

[W2C-3]

17:10 ~ 17:30

### Radiation from a Circular Aperture Surrounded by Corrugations 125

Ji Hyung Kim<sup>1</sup>, Dong Yeop Na<sup>1</sup>, Yong Bae Park<sup>1</sup>, Kyung-Young Jung<sup>2</sup>, <sup>1</sup>Ajou University, Korea, <sup>2</sup>Hanyang University, Korea

Electromagnetic radiation from a cavity-backed circular aperture surrounded by corrugations is investigated. An electromagnetic boundary-value problem of the cavity-backed circular aperture surrounded by corrugations in a conducting plane is solved based on the Green's function and mode matching method. The radiated fields are computed in terms of corrugation geometry to illustrate radiation behaviors and measured to validate the computation.

[W2C-4]

17:30 ~ 17:50

### Excitation of Electromagnetic Waves in a Thin Water Layer using a Coaxial Probe 128

Zhenxin Hu<sup>1</sup>, Zhongxiang Shen<sup>2</sup>, Wen Wu<sup>1</sup>, <sup>1</sup>Nanjing University of Science and Technology, China, <sup>2</sup>Nanyang Technological University, Singapore

In this paper, two transitions between a coaxial line and a thin water layer are presented: one with symmetric structure and the other for a unidirectional wave propagation. In order to have a smooth transition and to achieve a wide bandwidth, an inverted glass cone is employed in the axially symmetric transition between a coaxial probe and a thin water layer. For the unidirectional design, a parabolic cavity made of a thin glass layer is added at one side of the water layer to reflect the electromagnetic waves to the desired direction. Simulation results show that omnidirectional and unidirectional propagation of electromagnetic waves can be successfully excited in the thin water layer through these two transitions respectively. The 10 dB bandwidths from 497 MHz to 897 MHz (57.4%) for the symmetric transition and from 463 MHz to 887 MHz (62.8%) for the unidirectional transition are obtained.

[W2C-5]

17:50 ~ 18:10

### On the Shielding Effectiveness of Dual Plates with Narrow Slots 131

Sung-Woo Jung<sup>1</sup>, Ki-Chai Kim<sup>2</sup>, <sup>1</sup>Gyeongbuk Research Institute of Vehicle Embedded Technology, Korea, <sup>2</sup>Yeungnam University, Korea

This paper presents the shielding effectiveness (SE) of a dual plates with narrow slots when the plane wave is incident. In the theoretical analysis, coupled integral equations for aperture magnetic currents on slots are derived. The solutions obtained by applying method of moments (MoM). The numerical results show that the SE depends on plate spacing for a given frequency. Also shows that the SE fluctuates with the spacing of the plate, and the fluctuation period is about  $0.5\lambda$ .

## [W2D] Broadband and Multiband Antennas I

- Date: November 6, 2013 (Wednesday)
- Time: 16:30 ~ 18:20
- Room: Room D (Room 105)
- Session Chairs: Kin-Lu Wong (National Sun Yat-sen University)  
Kyeong-Sik Min (Korea Maritime University)

[W2D-1]

16:30 ~ 17:00

### [Invited] 4G/Multiband Handheld Device Ground Antennas 134

**Kin-Lu Wong, National Sun Yat-sen University, Taiwan**

Promising internal handheld device ground antennas are presented. Using the ground antenna concept, the antenna element functions mainly as an exciter and can have a very small size to achieve 4G/multiband operation. In this paper, ground antenna structures for handheld devices including the use of a loop strip, a half-loop strip, a simple shorted strip, or an inverted-F strip with the aid of a capacitive element to achieve decreased resonant length and the use of a small-size strip or patch with an inductive element to combine with the device ground plane to form as an asymmetric dipole structure are discussed. By aided with proper matching circuits, the ground antennas are promising to provide wideband operations. A small corner strip antenna with its resonant length 29 mm only (less than  $0.08\lambda$  at 750 MHz) is also demonstrated for the LTE/WWAN tablet computer application. The ground antennas are also very promising to form high-isolation antenna systems for MIMO and diversity operation in the slim handheld devices.

[W2D-2]

17:00 ~ 17:20

### Multi-band Reconfigurable Antennas Embedded with Lumped-Element Passive Components and Varactors 137

**Shoichi Onodera, Ryo Ishikawa, Akira Saitou, Kazuhiko Honjo, The University of Electro-Communications, Japan**

Frequency reconfigurable dual-band antennas with varactor diodes have been demonstrated. An equivalent circuit, taking the coupling with free space and antenna's conductor embedded with lumped-elements, is proposed to design the reconfigurable antennas. By means of the equivalent circuit, reconfigurable antennas to control dual-band resonant frequencies independently were designed and fabricated with a parallel circuit of an inductor and a varactor. The lower resonant frequency was successfully controlled between 1.60 and 1.91 GHz, and the upper resonant frequency was controlled between 3.32 and 3.71 GHz. Measured gains were more than -9.8 dBi in the lower band, and more than -7.3 dBi in the upper band, respectively. To improve the gain, a reconfigurable antenna with a series circuit of an inductor and a varactor was also fabricated for the lower band. Measured gains have been improved to more than -4 dBi in the lower band.

[W2D-3]

17:20 ~ 17:40

### Circularly Polarized Tripleband Patch Antenna for Non-Linear Junction Detector 140

**In-hwan Kim, Kyeong-sik Min, Jae-hwan Jeong, Sung-min Kim, Korea Maritime University, Korea**

This paper presents a design of broadband circular polarization patch antenna for non-linear junction detector system. A patch antenna with inclined slots, two rectangular grooves on circular disc patch, asymmetry gap of the CPW feeding structure and truncated corner of ground plane was considered for circular polarization. By applying the CPW feeding, broad bandwidth is realized.

[W2D-4]

17:40 ~ 18:00

### Multiband Spiral Antenna with High Gain by Conical Wall 143

**Jae-Hwan Jeong, Kyeong-Sik Min, In-Hwan Kim, Sung-Min Kim, Korea Maritime University, Korea**

This paper presents design for high gain spiral antenna with conical wall. To improve the gain of spiral antenna, the angle and length of conical wall is newly designed for the conventional antenna with circular cavity wall. The good axial ratio of 2.4 dB below and the improved gain of 10.5 dBi above are measured by the added conical wall. The measured E-field radiation patterns and main beam directivity toward +z axis direction are agreed well with the simulated results. The proposed antenna will be applied for the NLJD system.

[W2D-5]

18:00 ~ 18:20

### Offset Quad Ridged Ortho-Mode Transducer with a 3.4:1 Bandwidth 146

**Alex Dunning, Mark Bowen, Yoon Chung, CSIRO Astronomy and Space Science, Australia**

We describe the design and measured parameters of an offset probe, quad ridged, ortho-mode transducer (OMT). The OMT operates over a 3.4:1 bandwidth from 3.6-12.4GHz. The OMT exhibits a return loss of greater than 15dB and an isolation of greater than 50dB across the full band. Simulations predict spurious mode production at the circular waveguide port to be greater than 15dB below the TE<sub>11</sub> mode.

## [W2E] System Applications

- Date: November 6, 2013 (Wednesday)
- Time: 16:30 ~ 18:00
- Room: Room E (Room 203)
- Session Chairs: Kiyomichi Araki (Tokyo Institute of Technology)  
Mardeni Roslee (Multimedia University)

[W2E-1]

16:30 ~ 17:00

**[Invited] A 77GHz CMOS Array Receiver, Transmitter and Antenna for Low Cost Small size Automotive Radar 149**  
Cheonsoo Kim<sup>1</sup>, Piljae Park<sup>1</sup>, Dong-Young Kim<sup>1</sup>, Seong-Do Kim<sup>1</sup>, Hyun-Kyu Yu<sup>1</sup>, Moon-Kyu Cho<sup>2</sup>, Jeong-Geun Kim<sup>2</sup>, Yun Seong Eo<sup>2</sup>, Joonhong Park<sup>3</sup>, Donghyun Baek<sup>3</sup>, Jun-Teag Oh<sup>4</sup>, Songcheol Hong<sup>4</sup>, <sup>1</sup>ETRI, Korea, <sup>2</sup>Kwangwoon University, Korea, <sup>3</sup>Chung-Ang University, Korea, <sup>4</sup>KAIST, Korea

A 77GHz CMOS Centric 4-channels receiver, transmitter with 3-outputs and array antenna were proposed for low cost/small size automotive radar system, and implemented by using 65nm CMOS and LTCC substrate respectively. Measured performance of CMOS transceiver showed that it has the comparable performances but it includes more functions that can't find in commercial chip, especially, it also can be operated with one third lower power compared with commercial SiGe chips. These results confirm that it can be a promising candidate for low cost/small size car radar system.

[W2E-2]

17:00 ~ 17:20

**A New Architecture for Concurrent Dual-Band Digital PreDistortion 152**  
Ikuma Ando<sup>1</sup>, Gia Khanh Tran<sup>1</sup>, Kiyomichi Araki<sup>1</sup>, Takayuki Yamada<sup>2</sup>, Takana Kaho<sup>2</sup>, Yo Yamaguchi<sup>2</sup>, Kazuhiro Uehara<sup>2</sup>, <sup>1</sup>Tokyo Institute of Technology, Japan, <sup>2</sup>NTT Corporation, Japan

This paper proposes a new power amplifier's linearization architecture for a unified access point uses a wideband power amplifier and transmits multi-band signals concurrently for system's flexibility. To achieve high power efficiency and low interference of the access point, we evaluate a concurrent dual-band digital predistortion (DPD) technique for the wideband amplifier using a feedback loop. A concurrent dual-band mixer is applied in the feedback loop to reduce the complexity and the cost. In addition, DPD is operated at low IF to reduce nonsymmetrical spectral regrowth. The simulation result shows the validity of this architecture and a good linearization performance.

[W2E-3]

17:20 ~ 17:40

**A 60 GHz LTCC Antenna in Package with Low Power CMOS Radio 155**  
Hong Yi Kim, Chul Woo Byeon, Jae Jin Lee, Seong Jun Cho, In Sang Song, Chae Jun Lee, Hae Jin Lee, Joong Ho Lee, Chong Hyun Yoon, Ki Chan Eun, In-Yeal Oh, Chul Soon Park, Korea Advanced Institute of Science and Technology, Korea

A 60 GHz LTCC Antenna in Package with low power CMOS Radio solution for high data-rate and short-range wireless mobile communication are presented in this paper. For low power consumption, a new type of OOK system is proposed. The 60 GHz OOK transmitter and receiver are designed in 90 nm CMOS process. The transmitter with an OOK modulator and a VCO added an output buffer consumes 27.32 mW power and is able to modulate over 2 Gbps. The receiver with a LNA, a de-modulator and a baseband amplifier consumes 12.92 mW and has ability to recover up to 5 Gbps. The OOK system is integrated with low loss compact LTCC AiP. The low loss AiP techniques mainly consist of inter-connection and antenna design methods. The direct wire bonding inter-connection with matched elements has under 1 dB insertion loss. The 60 GHz micro-strip patch antenna has over 90 percent efficiency with LTCC substrate. In the end, high data rate video demonstration using the low power wireless system are presented.

[W2E-4]

17:40 ~ 18:00

**A Novel Delay-Based GFSK Demodulator in 65 nm CMOS for High Resolution Epi-retinal Prosthesis N/A**  
Meng Fu, Stan Skafidas, Iven Mareels, University of Melbourne, Australia

This paper presents a low power Gaussian frequency shift keying (GFSK) demodulator designed for Medical Implant Communications Service (MICS) band Receiver. This work employs a new demodulator architecture, which shows great immunity to frequency offset. The demodulator draws 650uA from a 1 V power supply. A maximum data rate of 400 Kbits/s can be achieved within the 300KHz channel bandwidth defined by MICS. A simulated signal-to-noise ratio (SNR) of 15dB at AWGN channel is obtained to achieve 0.1% bit error rate (BER). This demodulator is fabricated on 65nm CMOS. The demodulator occupies 0.12 mm<sup>2</sup> silicon area.



## [W2F] Microstrip Antennas and Array

- Date: November 6, 2013 (Wednesday)
- Time: 16:30 ~ 18:00
- Room: Room F (Room 208)
- Session Chairs: Naobumi Michishita (National Defense Academy)  
Young Joong Yoon (Yonsei University)

[W2F-1] 16:30 ~ 17:00

### [Invited] Researches on Radiation Performance Improvement of Microstrip Reflectarray Antennas 161

Ji Hwan Yoon<sup>1</sup>, Jae-sik Kim<sup>1</sup>, Young Joong Yoon<sup>1</sup>, Jinwoo Shin<sup>2</sup>, Joon-ho So<sup>2</sup>, <sup>1</sup>Yonsei University, Korea, <sup>2</sup>The Agency of Defense Development, Korea

The performances of reflectarrays are mainly determined by the characteristics of the elements. In this communication, various microstrip reflectarray elements to improve reflectarray performances are reviewed. Based on the figures of merits of the element (reflection phase range, sensitivity, and bandwidth) multi-layer elements, concentric multi-ring / patch element, and subwavelength elements are reviewed. Also, reflectarrays with elements having bandgap characteristic to reduce mutual coupling between the elements are reviewed.

[W2F-2] 17:00 ~ 17:20

### Reflectarray with Logarithmic Spiral Lattice of Elementary Antennas on its Aperture N/A

M. Wasif Niaz, Zubair Ahmed, Mojeeb Bin Ihsan, National University of Sciences and Technology, Pakistan

A reflectarray with logarithmic spiral lattice of elementary antennas on its aperture is presented. In logarithmic spiral lattice, elementary antennas are arranged in a grid of an outwardly spiral so as to have no translational periodicity. Infinite array approach has been used to determine reflection phase curve as in the aperiodic logarithmic spiral array, the equivalent unit cell remains the same. Simulated results of this reflectarray show improvements in side lobe level and gain as compared to reflectarray with rectangular lattice of elementary antennas on its aperture.

[W2F-3] 17:20 ~ 17:40

### Conformal Array Pattern Synthesis on a Curved Surface with Quadratic Function using Adaptive Genetic Algorithm 167

Cheol-Min Seong<sup>1</sup>, Myung-seok Kang<sup>2</sup>, Cheol-Soo Lee<sup>3</sup>, Dong-Chul Park<sup>1</sup>, <sup>1</sup>Chungnam National University, Korea, <sup>2</sup>Microwave Technologies Group Co., Ltd., Korea, <sup>3</sup>Agency for Defense Development, Korea

Investigations on conformal phased array pattern synthesis using adaptive genetic algorithm are presented. The array antenna is assumed to be located on a curved surface with quadratic function. In order to get a desired pattern with low sidelobe level faster, the amplitude of Taylor distribution and the phase obtained by the phase delay of the conformal elements are used as the initial current excitation set. As a synthesis algorithm, a real-number coded genetic algorithm that simultaneously adapts several parameters is used to optimize the amplitude and the phase of the current excitation of the conformal array. The comparison between the optimized patterns by the algorithm and the EM simulated patterns by CST's MWS (Microwave Studio) shows the validity of our synthesis method.

[W2F-4] 17:40 ~ 18:00

### An Investigation of Circular Patch Antenna on Pin-bed type RIS 170

Swati Vaid, Ashok Mittal, A.I.A.C.T.R, G.G.S.I.P University, India

This paper presents analysis of circular microstrip patch antenna placed over a thin grounded pin bed type reactive impedance surface (RIS). Effect of the variation in the height of the pins on the resonant frequency and the radiation properties of antenna have been studied. 3D EM simulation tools based on finite element method (Ansoft's HFSS) and finite integration technique (CST Microwave Studio) are used to model the structure. Magnetic field distribution within the pin-bed substrate has also been studied. 26% compactness has been achieved with the pin bed structure maintaining the gain within an appreciable limit.

## [T1A] Frequency Conversion Circuits

- Date: November 7, 2013 (Thursday)
- Time: 09:00 ~ 10:40
- Room: Room A (Room 101)
- Session Chairs: Huei Wang (National Taiwan University)  
Sungho Lee (Korea Electronics Technology Institute)

[T1A-1]

09:00 ~ 09:20

### High Linear Even Harmonic Mixer Driven by the Pulsed LO 173

Jun Hashimoto, Kenji Itoh, Keisuke Noguchi, Tetsuo Hirota, Shigeru Makino, Shin-ichi Betsudan, Kanazawa Institute of Technology, Japan

This paper presents the high linear even harmonic mixer driven by the pulsed LO for achieving high power and low distortion performance. For the objectives, positive and negative pulses pump an anti-parallel diode pair as LO voltage. Duty ratio of each pulse is 25% for the LO period. This means that pumped conductance  $G_j$  of the anti-parallel diode pair includes the highest level of the second order harmonic. This can reduce LO dependence on conversion efficiency of the even harmonic mixer. Theoretical and experimental investigations confirm effectiveness on high power and low distortion performance of the even harmonic mixer with the proposed LO waveform.

[T1A-2]

09:20 ~ 09:40

### Design of Wide-IF-Band CMOS Mixer with LO Multiplier 176

Han-Ting Tsai<sup>1</sup>, Pei-Ling Tseng<sup>1</sup>, Che-Wei Chang<sup>2</sup>, Robert Hu<sup>2</sup>, Christina F. Jou<sup>1</sup>, <sup>1</sup>National Chiao-Tung University, Taiwan, <sup>2</sup>National Chiao-Tung University, Taiwan

This paper reports the development of K-band wide-IF-band CMOS mixer with LO multiplier suitable for wideband applications. To achieve such broad bandwidth, several design techniques—such as current-reuse differential-pair with LC resonance circuit, and simultaneous in-band gain peaking and off-band gain tailoring—have been analyzed and employed. The on-wafer measurement of this 17.4-26.1GHz TSMC 0.18 $\mu$ m CMOS mixer with LO doubler shows a -1dB conversion gain, 11dB noise figure, -6dBm input-referred 1dB compression point, 40dB RF-IF isolation, and 45dB LO-IF isolation at 8.7GHz. The chip size is 1400 1300 $\mu$ m<sup>2</sup>.

[T1A-3]

09:40 ~ 10:00

### 15 GHz Wideband CMOS Gilbert Up-Converter With Stacked Spiral-CPS Phase-Inverter Rat-Race Coupler at RF Port 179

Yu-Chih Hsiao<sup>1</sup>, Chinchun Meng<sup>1</sup>, Po-Yi Wu<sup>1</sup>, Guo-Wei Huang<sup>2</sup>, <sup>1</sup>National Chiao Tung University, Taiwan, <sup>2</sup>National Nano Device Laboratories, Taiwan

A miniaturized phase-inverter rat-race and its wideband Gilbert up-converter is demonstrated in 0.13- $\mu$ m CMOS technology. The common-mode LO leakage can be absorbed by the isolated port of the rat-race coupler while the rate-race employed at RF port to combine the mixer differential output. A phase-inverter rat-race coupler with a stacked spiralshape coplanar stripline (CPS) by multi-layer metals can highly reduce the chip size. Finally, the experimental results of upconverter shows the 1-dB conversion gain and 15 GHz RF bandwidth. The IF-to-RF isolation is about 50 dB and LO-to-RF isolation is about 23 dB, respectively.

[T1A-4]

10:00 ~ 10:20

### 60-GHz Dual-Conversion Down-Converter using Schottky Diode and Dual-Band Rat-Race Coupler in Standard 0.18- $\mu$ m CMOS Process 182

Yu-Chih Hsiao<sup>1</sup>, Chinchun Meng<sup>1</sup>, Hung-Ju Wei<sup>1</sup>, Ta-Wei Wang<sup>1</sup>, Guo-Wei Huang<sup>2</sup>, <sup>1</sup>National Chiao Tung University, Taiwan, <sup>2</sup>National Nano Device Laboratories, Taiwan

A 60 GHz dual-conversion down-converter is demonstrated using Schottky diode in 0.18- $\mu$ m CMOS technology. The high cut-off frequency of the Schottky diode helps lowering the conversion loss and noise figure. The first down-converted sub-harmonic mixer consists of a rat-race coupler with the Chebyshev response and diodes in anti-parallel configuration. Both RF and LO ports of the rat-race coupler can achieve matching because of the dual-band Chebyshev response. Thus, 0-dBm LO pumping power is enough to make the mixer reach fully switching. A double balanced resistive mixer with RC-CR polyphase filter is used at the second down-converted mixer to produce precise output signals and subsequently a shunt-shunt feedback buffer amplifier is connected to compensate the conversion loss of the passive mixer. To reduce the noise contribution from the resistive mixer and the subsequent wideband amplifier, a low-noise buffer is inserted between two mixers. As a result, the conversion gain is around 6 dB in the frequency range of 45 ~ 67 GHz. IP1dB is around -5-dBm and IIP3 is around 5-dBm at 45 ~ 67 GHz. The single sideband noise figure with respect to IF frequency is around 20 dB and IF bandwidth is over 1 GHz. The total power consumption is 71 mW at 2.5 V.

[T1A-5]

10:20 ~ 10:40

### A K-Band SiGe BiCMOS Fully Integrated Up-Conversion Mixer 185

Cuong Huynh, Jaeyoung Lee, Cam Nguyen, Texas A&M University, USA

The design of a fully integrated 0.18- $\mu$ m SiGe BiCMOS up-conversion mixer in K-band is presented. The mixer consists of a single-ended-to-differential active balun, double-balanced Gilbert mixer cell, differential amplifier and band pass filter. The input active balun is used to facilitate on-wafer characterization from a single-ended IF signal. With an LO power of -2 dBm, the mixer exhibits a conversion gain of 25.7 dB, 1-dB input power of -23 dBm, 1-dB output power of 1.36 dBm, and maximum output power of 2.7 dBm at 24.5 GHz, while consuming a DC current of 40 mA from a supply voltage of 1.8V. Design procedure, parameter trade-off, simulation, and layout issues of the mixer are discussed.

## [T1B] Tunable Components

- Date: November 7, 2013 (Thursday)
- Time: 09:00 ~ 10:40
- Room: Room B (Room 102)
- Session Chairs: Yasushi Horii (Kansai University)  
Taek-Kyung Lee (Korea Aerospace University)

[T1B-1]

09:00 ~ 09:20

### Center Frequency and Bandwidth Tunable Filter Employing MEMS Digitally Tunable Capacitors 188 Kunihiro Kawai, Hiroshi Okazaki, Shoichi Narahashi, NTT DOCOMO, INC., Japan

This paper proposes a novel multi-pole bandpass filter that is suitable for applying micro electromechanical systems (MEMS). The proposed bandpass filter employs parallel resonance circuits with tunable capacitors, and can independently tune its center frequency and bandwidth by only tunable capacitors. The proposed bandpass filter comprises tunable ring resonators which are coupled by J-inverters. Since the tunable resonator can change its bandwidth by itself, it is not required to tune the characteristics of the J-inverters for changing the bandwidth, which helps to simplify a bandwidth tuning scheme. This paper shows the circuit configuration of the proposed filter. A two-pole filter is fabricated using MEMS digitally tunable capacitors. Measured results show that the fabricated bandpass filter changed its bandwidth from 1.7% to 7.4% at the center frequency of 1.77 GHz, and changed its center frequency from 1.37 GHz to 1.77 GHz.

[T1B-2]

09:20 ~ 09:40

### Design of Tunable Bandpass Filter using PIN Diode With Constant Absolute Bandwidth 191 Jong-Hyun Lee, Jae-Won Choi, Xu-Guang Wang, Sang-Won Yun, Sogang University, Korea

This paper presents a tunable bandpass filter(BPF) for cognitive radio applications. The proposed two-pole BPF is implemented using lumped elements and the frequency tuning is realized by PIN diodes. Due to the L-C parallel circuit J-inverter, constant absolute bandwidth is achieved. 4 PIN diodes in each resonator and the capacitor bank are used to cover the desired frequency tuning range from 480MHz to 687MHz with 20MHz bandwidth. The circuit is theoretically analyzed, and the complete design process is described. The fabricated filter shows wide tuning range of 42.5% with insertion loss varying from 2.7dB to 3.8dB and good linearity. The 1-dB bandwidth of the filter is kept  $20 \pm 1$  MHz.

[T1B-3]

09:40 ~ 10:00

### Reduction of Insertion Loss in Millimeter-Wave Tunable Filter Over 100 GHz 194 Takashi Kawamura, Hiroshi Shimotahira, Akihito Otani, Anritsu Corporation, Japan

Rapid advances in millimeter-wave wireless communication technologies require accurate spectrum analysis in the frequency domain over 100 GHz. A tunable pre-selection filter is a key device in building such a spectrum analyzer. We have prototyped a new tunable filter in the frequency range from 110 to 140 GHz, but it suffered significant insertion losses around 116 and 140 GHz. This paper clarifies structural causes of these losses and presents the correct dimensions of the filter. Computer simulation of the redesigned filter gives reduced and flattened insertion loss in the working range.

[T1B-4]

10:00 ~ 10:20

### Negative Group Delay Circuit with Independently Tunable Center Frequency and Group Delay 197 Junhyung Jeong<sup>1</sup>, Kolet Mok<sup>1</sup>, Jeayeon Kim<sup>1</sup>, Yongchae Jeong<sup>1</sup>, Jongsik Lim<sup>2</sup>, <sup>1</sup>Chonbuk National University, Korea, <sup>2</sup>Soonchunhyang University, Korea

In this paper, a design of negative group delay circuit (NGDC) with independently tunable center frequency and group delay (GD) is presented. Since the proposed structure consists of a parallel RLC resonance circuit, it is possible to obtain a variable negative GD by using a variable resistor and an adjustment of center frequency of GD is possible due to a variable inductor. To get the pure variable resistor, the transmission line (TL) terminated with the PIN diode is used. Similarly, the variable inductor is realized by TL terminated with the varactor diode. To show the effectiveness of the proposed NGDC, it is designed at 2.14 GHz of WCDMA downlink band. The measured negative GD time is  $-2 \sim -20$  ns, and are able to change the center frequencies of negative GD in the range of 2.04 ~ 2.24 GHz.

[T1B-5]

10:20 ~ 10:40

### A Compact 1.9-2.9 GHz Tunable Bandpass Filter with Wide Stopband Range 200 Yi-Ming Chen, Sheng-Fuh Chang, Zuo-Ming Tsai, Tai-Chuan Chao, National Chung Cheng University, Taiwan

This paper presents a compact broadband tunable bandpass filter with wide stopband range. The combline topology is adopted, where the varactor-loaded stepped-impedance resonator is used for frequency tuning. A double-stub parallel-line transformer at input/output port is used for generating multiple transmission zeros and matching port and resonator impedances. The measured performances show that the tuning frequency range of 1.9 to 2.9 GHz (51% tuning range) is achieved. The insertion loss is between 2.9 dB and 1.5 dB and the return loss is better than 18.5 dB. The stopband suppression greater than 20 dB is obtained up to 10 GHz. The circuit design, EM simulation and experimental comparison are described.

## [T1C] Special Session on EUMA

- Date: November 7, 2013 (Thursday)
- Time: 09:00 ~ 10:30
- Room: Room C (Room 104)
- Session Chairs: Roberto Sorrentino (University of Perugia)  
Songcheol Hong (KAIST)

[T1C-1]

09:00 ~ 09:30

### [Invited] Terahertz Monolithic Integrated Circuits Based on Metamorphic HEMT Technology for Sensors and Communication 203

Axel Tessmann<sup>1</sup>, Michael Schlechtweg<sup>1</sup>, Daniel Bruch<sup>1</sup>, Ulrich J. Lewark<sup>2</sup>, Arnulf Leuther<sup>1</sup>, Hermann Massler<sup>1</sup>, Sandrine Wagner<sup>1</sup>, Matthias Seilmann-Eggebert<sup>1</sup>, Volker Hurm<sup>1</sup>, Rolf Aidam<sup>1</sup>, Ingmar Kalfass<sup>3</sup>, Oliver Ambacher<sup>1</sup>, <sup>1</sup>Fraunhofer Institute for Applied Solid State Physics IAF, Germany, <sup>2</sup>Karlsruhe Institute of Technology, Germany, <sup>3</sup>University of Stuttgart, Germany

For the next generation of sensors and communication systems operating at frequencies up to 600GHz and above, the Fraunhofer IAF is developing a broad variety of millimeter-wave and terahertz monolithic integrated circuits (MMICs and TMICs) and modules. The monolithic integrated circuits are realized using the advanced metamorphic high electron mobility transistor (mHEMT) technology in the InGaAs/InAlAs material system on 4" GaAs substrates. The potential of this technology is demonstrated in this paper by two TMICs operating at 600GHz: a high-gain amplifier and an active frequency multiplier-by-six.

[T1C-2]

09:30 ~ 10:00

### [Invited] Emerging Ferroelectric Ceramic-Polymer Composites for Sub-THz Tunable Devices 206

Y. Yashchyshyn, J. Modelski, K. Godziszewski, P. Bajurko, E. Pawlikowska, B. Bogdańska, E. Bobryk, M. Szafran, Warsaw University of Technology, Poland

The paper presents the recent research in ferroelectric ceramic-polymer composites for sub-THz tunable devices. Developed composites are a very promising group of materials due to the possibility of fabrication of materials with desired electrical and mechanical properties. Appropriate selection of components for ceramic slurry enables to obtain composites with low losses and high tunability. Using tape-casting technology and water-dispersible polymers environmentally friendly thin and flexible ferroelectric tapes can be realized. Particular emphasis is made on measurement methods of electrical properties in sub-THz range. In addition, various composites, process of fabrication and characterization of developed ferroelectric ceramic-polymer composites are discussed.

[T1C-3]

10:00 ~ 10:30

### [Invited] Integrated mm-Wave Sensors in a Package 209

Reinhard Feger, Abouzar Hamidipour, Andreas Stelzer, Johannes Kepler University, Austria

We present integrated 160-GHz sensors in a package which combine SiGe-based mm-wave circuits with an antenna inside single embedded wafer level ball grid array (eWLB) packages. The eWLB technology provides a platform to realize miniaturized antennas and to easily combine them with other building blocks to create a full mm-wave system in package. With this approach no external mm-wave connections or special low-loss laminates are required. An imaging system based on the packaged sensors was realized and measurements were carried out to demonstrate the easy applicability of the realized components.

## [T1D] Broadband and Multiband Antennas II

- Date: November 7, 2013 (Thursday)
- Time: 09:00 ~ 10:40
- Room: Room D (Room 105)
- Session Chairs: Hiroyuki Arai (Yokohama National University)  
Kangwook Kim (Gwangju Institute of Science and Technology)

[T1D-1]

09:00 ~ 09:20

### Experimental Validation of Removal of Sharp Ends in Sinuous Antenna Arms 212

Yunsu Kang, Kangwook Kim, Gwangju Institute of Science and Technology, Korea

The effect of the removing the sharp ends of the sinuous antenna arms are experimentally validated. The method of removing the sharp ends of the sinuous antenna arms is presented. The gains of the two antennas are measured in an anechoic chamber. The calibration procedure for the feeding network is presented and its validity is proved through comparison with simulation results. The measured results of the original and the modified antennas show that the gains are relatively flat above 1 GHz. The original antenna shows a dip in the gain at approximately 2.1 GHz, which is not observed with the modified antenna. Thus, the removal of the sharp ends is found to improve the gain flatness

[T1D-2]

09:20 ~ 09:40

### Double Side Axe Shaped UWB Antenna With Reduced RCS 215

Cengizhan M. DİKMEN, Gonca ÇAKIR, Kocaeli University, Turkey

In this study, an ultra wide band (UWB) antenna which radiates at 3.4-15.5 GHz is designed. The patch of the antenna is designed asymmetrically and the effect of the asymmetric structure to radiation performance is examined. The size of the antenna is 28×35 mm and the fractional bandwidth is 128%. At the second stage, the radar cross section (RCS) of the designed antenna is reduced by modifying the physical structure. RCS of the antenna is reduced approximately 10 dB. The proposed antenna is fabricated and the experimental results of the radiation performance are in a good agreement with the simulation results.

[T1D-3]

09:40 ~ 10:00

### A Novel Miniaturized Wide Bandwidth LPDA Antenna N/A

Tenigeer, Ning Zhang, Jinghui Qiu, Pengyu Zhang, Hua Zong, Harbin Institute of Technology, China

A miniaturized log-periodic dipole array (LPDA) antenna is proposed in this paper. Elliptical dipoles are adopted in this design to realize wideband impedance bandwidth of each dipole, leading to a miniaturized structure. The dimensions of the antenna in three dimensions are 300mm, 80mm and 350mm respectively. VSWR is less than 2 from 0.4GHz to 2GHz. Stable radiation patterns can be obtained in the whole frequency band. Gain changes from 4.4dB to 8dB along with the change of frequency.

[T1D-4]

10:00 ~ 10:20

### Compact Printed Monopole UWB Antenna loaded with Non – Concentric Open – Ended Rings for Triple Band – Notch Characteristic 221

G Shrikanth Reddy, Anil Kamma, Jayanta Mukherjee, Indian Institute of Technology Bombay, India

A compact, ultra – wideband monopole antenna with triple band-notch characteristic is presented. Proposed antenna consists of an elliptical radiator for achieving UWB bandwidth. For rejecting WiMAX (3.3 – 3.6 GHz) and WLAN (5.15 – 5.3 GHz, 5.7 – 5.825 GHz) bands, antenna is loaded with Non-concentric open ended rings. The effective lengths for these non-concentric rings are approximately half wavelength for the respective notch frequencies. Overall surface dimension of the fabricated antenna is 25×18 mm<sup>2</sup>. The proposed antenna is simulated, fabricated and tested experimentally for its performance. A good agreement between simulated and experimental results ensures the suitability of the proposed antenna for various UWB applications.

[T1D-5]

10:20 ~ 10:40

### Wideband Rectangular Dielectric Resonator Antenna with Novel Array of Square Shaped Slots 224

Pragati Patel, Biswajeet Mukherjee, Jayanta Mukherjee, Indian Institute of Technology Bombay, India

A wideband rectangular dielectric resonator antenna with novel array of square shaped slots has been designed and proposed. The number of symmetrical square shaped array is optimized to 5×5 elements. The dielectric material used is a Teflon based ceramic, Rogers RT/ Duroid 6010.2LM having dielectric constant of  $\epsilon_r = 10.2$ . Advantage of drilling square shaped slots from solid rectangular dielectric resonator antennas (RDRAs) is twofold; one reduction of the effective dielectric constant and second is antenna weight reduction. As a result improvement in impedance bandwidth from 9.3 % to 31 % is achieved. The proposed antenna operates in the frequency range of 2.6 GHz to 3.5 GHz at the resonant frequency of 2.9 GHz and offers a peak gain of 6.5 dBi at 3.4 GHz. A good agreement between simulated and measured results predicts that the proposed antenna can be used for applications in wireless communications.

## [T1E] mm-wave Circuits and Systems

- Date: November 7, 2013 (Thursday)
- Time: 09:00 ~ 10:50
- Room: Room E (Room 203)
- Session Chairs: Tadao Nagatsuma (Osaka University)  
Byung-Wook Min (Yonsei University)

[T1E-1]

09:00 ~ 09:30

**[Invited] Recent Advances in Q-LINKPAN/IEEE 802.11aj (45GHz) Millimeter Wave Communication Technologies** 227  
Wei Hong, Haiming Wang, Jixin Chen, Nianzu Zhang, Yan Zhang, Guangqi Yang, Pinpin Yan, Chen Yu, Zhe Chen, Wenfeng Liang, Fang Zhu, et. al, Southeast University, China

In this talk, the recent research advances in channel characteristic measurement, IC design etc. for the newly proposed millimeter wave high data rate wireless communication standard Q-LINKPAN or IEEE802.11aj (45GHz) are reviewed.

[T1E-2]

09:30 ~ 09:50

**60-GHz Band Beam Forming Receiver RFIC for Broadband Communication Phased Array Antenna Module** 230

Tuan Thanh Ta, Mikoto Nakamura, Osamu Wada, Katsunori Gomyo, Yuya Suzuki, Satoshi Yoshida, Shoichi Tanifuji, Suguru Kameda, Noriharu Suematsu, Tadashi Takagi, Kazuo Tsubouchi, Tohoku University, Japan

In order to extend the communication range of the 60-GHz band broadband communication system, beam forming technology has been introduced. Due to the relatively high insertion loss and high phase/amplitude errors of 60-GHz band radio frequency (RF) phase shifter, broadband baseband (BB) phase shifter has been focused. In this paper, we have developed a beam forming CMOS receiver RF integrated circuits (RFIC) with 5-bit BB phase shifter for the use in phased array antenna (PAA) receiver module employing 3-dimensional (3-D) system in package (SiP) technology. The receiver RFIC consists of a 7-stages low noise amplifier (LNA), an on-chip balun, a down-mixer, a quadrature-mixer, and a 5-bit BB phase shifter. To obtain the broadband characteristic of 2GHz at RF (i.e., 1GHz at BB), BB phase shifter has been carefully designed. By using fixed-gain amplifier matrix configuration instead of variable gain amplifiers, broadband and low phase/amplitude errors are obtained. The fabricated receiver RFIC in 90-nm CMOS process exhibits performance applicable to 60-GHz band broadband communication such as IEEE 802.15.3c (channel 2).

[T1E-3]

09:50 ~ 10:10

**77-110GHz 90nm-CMOS Receiver Design** 233

Jo-Han (Judy) Yu<sup>1</sup>, Chien-Hsiung Liao<sup>1</sup>, Cheng-Huang Hsieh<sup>1</sup>, Robert Hu<sup>1</sup>, Dow-Chih Niu<sup>2</sup>, <sup>1</sup>National Chiao-Tung University, Taiwan, <sup>2</sup>Chung-Shan Institute of Science and Technology, Taiwan

This manuscript details our latest 90nm-CMOS W-band receiver design where the RF LNA, resistive mixer, IF differential amplifier and LO tripler have been integrated, thus allows the whole 77–110GHz spectrum to be down-converted into quasi-DC–33GHz using a much lower microwave frequency. In addition to being used in our broadband receiver array project, this W-band circuit is also eligible for the conventional 77/94GHz vehicular and surveillance applications. This 90nm-CMOS receiver with LO tripler has around -0.4dB conversion gain, 18dB noise figure, 48dB LO-IF isolation, and its chip size is 950-times-750 $\mu\text{m}^2$ , with 114mW power dissipation at 1.3V DC bias.

[T1E-4]

10:10 ~ 10:30

**A Low-Power 77 GHz Transceiver for Automotive Radar System in 65 nm CMOS Technology** 236

Seong-Kyun Kim<sup>1</sup>, Chenglin Cui<sup>1</sup>, Sangwook Nam<sup>2</sup>, Byung-Sung Kim<sup>1</sup>, <sup>1</sup>Sungkyunkwan University, Korea, <sup>2</sup>Seoul National University, Korea

A fully-integrated low power 77 GHz radar transceiver in 65 nm CMOS process is presented. It consists of a low-noise amplifier (LNA), a down-conversion mixer, a power amplifier (PA), and a frequency synthesizer based on a tripler. The receiver front-end provides a conversion gain of 21 dB, and the PA has an output power over 10 dBm. The phase noise of VCO is -75 dBc/Hz at 1-MHz offset. The total dc power dissipation of the transceiver is 217 mW and the size of the chip is 0.8 $\times$ 1.1 mm<sup>2</sup>.

[T1E-5]

10:30 ~ 10:50

**CMOS Power Amplifier with Temperature Compensation for 79 GHz Radar System** 239

Takeshi Yoshida, Kyoya Takano, Chen yang Li, Mizuki Motoyoshi, Kosuke Katayama, Shuhei Amakawa, Minoru Fujishima, Hiroshima University, Korea

We have developed a 79 GHz CMOS power amplifier (PA) with temperature compensation implemented using 40 nm CMOS technology that suppresses the variation of small-signal gain and the degradation of linearity within 0.8 dB in the temperature range from 0 to 100°C. The PA consists of an on-chip temperature sensor and four-stage common-source NMOS amplifiers. The temperature-compensated PA operating at 100°C achieved a small-signal gain of 15.7 dB, a 12 GHz bandwidth and a saturated output power (Psat) of 6.8 dBm with 96.2 mW power consumption at a supply voltage of 1.1 V.

## [T1F] RFID

- Date: November 7, 2013 (Thursday)
- Time: 09:00 ~ 10:40
- Room: Room F (Room 208)
- Session Chairs: Wen-Shan Chen (Southern Taiwan University of Science and Technology)  
Jong-Won Yu (KAIST)

[T1F-1]

09:00 ~ 09:20

### Novel Design of UHF RFID Near-Field Antenna for Smart Shelf Applications 242

Andrey S. Andrenko, Manabu Kai, Fujitsu Laboratories Ltd., Japan

This paper presents the design of UHF RFID read/write (R/W) antenna to be used in a variety of smart shelf retail applications. The design principle based on the EM coupling between open-ended MS feed line and periodic planar metal strips is presented. The proposed antenna can be easily customized for the required area of smart shelf RFID interrogation. Several antenna prototypes have been designed, produced and measured. The antenna performance has been evaluated in UHF RFID system for the simultaneous detection of arbitrary oriented tagged apparel items placed on the antenna surface. The proposed antenna demonstrates excellent ability to provide strong and uniform E-field distribution at the distances up to 50 cm from the antenna surface.

[T1F-2]

09:20 ~ 09:40

### Design of A Novel Circularly Polarized Annular-Ring RFID Tag Antenna for Metallic Surfaces 245

Ran Liu<sup>1</sup>, Yuan Yao<sup>1</sup>, Youbo Zhang<sup>1</sup>, Hongbin Ge<sup>1</sup>, Wenjing Lee<sup>1</sup>, Junsheng Yu<sup>1</sup>, Xiaodong Chen<sup>2</sup>, <sup>1</sup>Beijing University of Posts and Telecommunications, China, <sup>2</sup>University of London, UK

A novel circularly polarized tag antenna designed for RFID UHF band is proposed. An annular-ring microstrip patch with a pair of inserted slits is used to achieve circularly polarized operation. By choosing the proper lengths of two short-circuited arc microstrip lines and its coupling distance, good complex impedance matching can be obtained. The 10 dB return-loss bandwidth of the tag antenna is measured to be 215 MHz (720-935MHz), while its 3 dB axial-ratio bandwidth is 6 MHz (919-925 MHz). Further experiment shows that the tag antenna could provide better reading range when mounted on a metallic surface.

[T1F-3]

09:40 ~ 10:00

### Electronically Controlled 2 by 1 Arrayed Beam Forming Antenna for UHF RFID Reader 248

Soo-Ji Lee, Dong-Jin Lee, Wang-Sang Lee, Sol-Ji Yoo, Jong-Won Yu, Korea Advanced Institute of Science and Technology, Korea

In this paper, a 2 by 1 array antenna for beam forming based on a feeding network composed of 2 low temperature cofired ceramic (LTCC) hybrid coupler, a 90 degree delay line and 4 Single-pole double-throw (SPDT) switch with 50  $\Omega$  termination is proposed. By combining these elements, the feeding network can operate as many kinds of power dividers such as wilkinson power divider, quadrature hybrid coupler and ring hybrid coupler depending on the switching condition. This feeding network can make different kinds of the phase difference between the divided signals which leads to different direction of beams of the antenna. The antenna used for the array is the quadrifilar spiral antenna (QSA) which can radiate right hand circular polarization (RHCP) beam. The measured results show that the proposed antenna has 5 directional beams of 2.5°, 25°, -25°, 40° and -42.5°.

[T1F-4]

10:00 ~ 10:20

### Dual Band Circularly Polarized Diamond-Shaped Antenna with Directional Capabilities for RFID Application 251

M. I. Sabran, S. K. A. Rahim, T. A. Rahman, M. Z. M. Nor, M. S. A. Rani, Universiti Teknologi Malaysia, Malaysia

A simple and novel diamond-shaped structure capable of producing dual band antenna with circular polarized enhancement is presented. The proposed antenna operates at both UHF and ISM bands which is suitable for RFID application. A pair of slots is introduced at the blended edge within the radiating element with optimum width and length, which can excite circular polarized antenna for both frequencies. The proposed antenna's gain is improved by using a fixed air gap between substrate and ground plane. It is observed that there is good measure of agreement between the simulation and measurement return loss result, when compared.

[T1F-5]

10:20 ~ 10:40

### Hemispheric Coverage Multi-beam Switched Antenna Array using a 4-Port Feeding Network for UHF RFID Dead Zone Avoidance 254

Wang-Sang Lee<sup>1</sup>, Seung-Tae Khang<sup>2</sup>, Won-Seok Lee<sup>2</sup>, Jong-Won Yu<sup>2</sup>, <sup>1</sup>Korea Railroad Research Institute, Korea, <sup>2</sup>Korea Advanced Institute of Science and Technology, Korea

For ultra-high frequency (UHF) radio frequency identification (RFID) dead zone avoidance from the viewpoint of antenna configurations and radiation characteristics, a hemispheric coverage multi-beam switched square quadrifilar spiral antenna (QSA) array using a 4-port feeding network is presented. The proposed antenna array consists of a 2x2 circular polarized QSA array and a 4-port feeding network for multiple beams. It generates single-, dual-, and quad-beams with a hemispheric coverage by a beam switching, and its maximum beam gains and directions are 8.4 dBic and 65°, respectively. By switching multi-beams with the hemispheric coverage, the proposed 2x2 QSA array with a 4-port feeding network improves the tag identification in the dead-zone read area within the reading range.

## [T2A] Low Noise Amplifiers

- Date: November 7, 2013 (Thursday)
- Time: 11:10 ~ 12:50
- Room: Room A (Room 101)
- Session Chairs: Zuo-Ming Tsai (National Chung Cheng University)  
Tae Wook Kim (Yonsei University)

[T2A-1]

11:10 ~ 11:30

### A Concurrent Dual-band Low-Noise Amplifier for K- and Ka-band Applications in SiGe BiCMOS Technology 258 Jaeyoung Lee, Cam Nguyen, Texas A&M University, USA

A 24/35-GHz BiCMOS concurrent dual-band low-noise amplifier (DBLNA) has been developed. The proposed concurrent DBLNA was designed using new active notch filters embedded into a wideband LNA. The concurrent DBLNA has measured peak gains of 21.9/16.6 dB at 23.5/35.7 GHz, respectively. The measured 3-dB bandwidths of the low and high pass-bands are 7.7 GHz (18.8–26.5 GHz) and 8.8 GHz (32.8–41.6 GHz), respectively. The best noise figures measured in the pass-bands are 5.1/7.2 dB at 22/35.6 GHz, respectively. The measured  $IP_3$  performances are -10.4/-8.3 dBm at 24/35 GHz, respectively.

[T2A-2]

11:30 ~ 11:50

### Cryogenic 8-18 GHz MMIC LNA using GaAs PHEMT 261

Chau-Ching Chiong<sup>1</sup>, Ding-Jie Huang<sup>2</sup>, Ching-Chi Chuang<sup>1</sup>, Yuh-Jing Hwang<sup>1</sup>, Ming-Tang Chen<sup>1</sup>, Huei Wang<sup>2</sup>, <sup>1</sup>Institute of Astronomy and Astrophysics, Taiwan, <sup>2</sup>Department of Electrical Engineering and Graduate Institute of Communication Engineering, Taiwan

An 8-18 GHz MMIC LNA is designed and fabricated using 0.15- $\mu$ m GaAs pHEMT process. The peak LNA is more than 23 dB gain at room temperature and more than 27 dB gain at 17.5 K. At 18 GHz, the room temperature noise figure is 1.5 dB, and the best effective noise temperature at 17.5 K is 20 K. The measured noise data of the LNA are then fitted for the two temperature model. The derived drain temperature is proportional to the drain current, independent of the ambient temperature.

[T2A-3]

11:50 ~ 12:10

### A High-gain Low-power Balun-LNA for 6-9GHz UWB System 264

Zhi Li, Ligu Sun, Lu Huang, University of Science and Technology of China, China

This paper presents a balun-LNA for 6-9GHz UWB system. The LNA uses common-gate (CG) stage before active balun stage for input matching, also it utilizes current reuse technology to reduce power consumption. Capacitor-cross-coupled (CCC) buffer is cascaded to improve the differential signal amplitude and phase balance. The balun-LNA is designed and fabricated by a standard 0.13- $\mu$ m CMOS technology. This balun-LNA can achieve differential gain above 22dB from 6.5GHz to 9.0GHz with 5.5mA current consumption under a 1.3-V supply. The core area of the LNA is 0.53mm<sup>2</sup>. The noise figure of the LNA is under 3.2dB.

[T2A-4]

12:10 ~ 12:30

### A Broadband Low-Noise Wide Dynamic Range SiGe Front-end Receiver IC for Multi-band Access Points 267

Takana Kaho, Yo Yamaguchi, Hiroyuki Shiba, Munenari Kawashima, Hideki Toshinaga, Kazuhiro Uehara, NTT Corporation, Japan

A broadband, low-noise, wide dynamic range front-end receiver IC is reported. It uses 0.25  $\mu$ m SiGe BiCMOS process technology and consists of broadband variable gain low noise amplifiers (VGLNAs), down-conversion mixers, step attenuators, and buffer amplifiers. It can receive triple-band signals concurrently, and the chip size is only 3mm $\times$ 3mm. Its measured noise figure was under 3.2 dB and the measured conversion gain was around 30 dB in the broad frequency range from 300 MHz to 3 GHz. It has a wide gain control range of around 100 dB; 50 dB is controlled by the VGLNA and the step attenuator, and 50 dB by the mixer with novel relative power control method using dual LO signal. The gain control enhances the input 1dB compression point from -40 dBm to -21 dBm.

[T2A-5]

12:30 ~ 12:50

### 2.4 GHz Low Cost Low Noise Amplifier on Flexible Organic Substrate 270

Fan Cai, A. Çağrı Ulusoy, John Papapolymerou, Georgia Institute of Technology, USA

In this paper a low cost 2.4 GHz low noise amplifier on organic flexible substrate, that is widely used for organic light-emitting diodes (OLED) and flexible printed circuits, is presented. The amplifiers were fabricated by two ways, one with aerosol jet printing technology and the other with copper tape for reduced cost fabrication. Using the aerosol jet printing approach, the amplifier exhibits a measured performance of 12.09 dB gain and 2.4 dB noise figure compared with the copper tape implementation which exhibits 10.55 dB gain and 3.2 dB NF. This demonstration paves the way for low cost ISM sensors on flexible substrates utilized for a variety of functions (LEDs etc.) using digital manufacturing technology.



## [T2B] Balun, Coupler and Combiners I

- Date: November 7, 2013 (Thursday)
- Time: 11:10 ~ 12:50
- Room: Room B (Room 102)
- Session Chairs: Eko Tjipto Rahardjo (Universitas Indonesia)  
Nam-Young Kim (Kwangwoon University)

[T2B-1]

11:10 ~ 11:30

### A G-Band (140-220 GHz) Planar Stubbed Branch-Line Balun in BCB Technology 273

Sona Carpenter, Morteza Abbasi, Yogesh Karandikar, Per-Åke Nilsson, Herbert Zirath, Chalmers University of Technology, Sweden

A G-Band planar stubbed branch-line balun is designed and fabricated in 3 $\mu$ m thick BCB technology. This topology of the balun does not need thru-substrate via hole or thin-film resistor which makes it extremely suitable for realization on single-layer high-resistivity substrates commonly used at millimeter-wave or post-processed BCB layers on top of standard semi-insulating wafers. The design is simulated and validated by measurements. Back to back balun measured results have better than 10 dB input and output return loss and 3.2 dB insertion loss from 140 to 220 GHz.

[T2B-2]

11:30 ~ 11:50

### A Compact X-Band CPW Branch-Line Coupler using Glass Integrated Passive Device (GIPD) Technology 276

Yu-Tzu Chen, Chih-Lin Chang, Chao-Hsiung Tseng, National Taiwan University of Science and Technology, Taiwan

In this paper, a compact X-band CPW branch-line coupler is proposed using the glass integrated passive device (GIPD) technology. To reduce the circuit size and retain a similar return-loss bandwidth to that of conventional coupler, the asymmetrical CPW branch-type T-structures are employed to implement the proposed coupler. Each T-structure is realized by two sections of high-impedance lines with unequal lengths and a set of branch-type shunt stubs. The developed coupler has a 31.5 % 10-dB return loss bandwidth and only occupies a 17.79 % circuit size of the conventional one. The measured results of the developed branch-line coupler are in a good agreement with simulated results.

[T2B-3]

11:50 ~ 12:10

### W-band Waveguide 3dB Directional Coupler Based on E- plane Branch Line Bridge 279

Pei Zheng<sup>1</sup>, Hou-Jun Sun<sup>1</sup>, Meng-Jia Luo<sup>1</sup>, Zhi-Lei Wen<sup>1</sup>, Hong Deng<sup>2</sup>, <sup>1</sup>Beijing Institute of Technology, China, <sup>2</sup>Xi'an Modern Control Technologies Research Institute, China

In this paper, a W-band waveguide 3dB directional coupler based on E-plane branch line bridge is proposed. The structure of this coupler and the formulas used to determine the critical design parameters have been given. The measurement and simulation results show that all the features of the 3dB coupler, such as equal power split, reflection coefficient, isolation, are satisfied over 85-96 GHz.

[T2B-4]

12:10 ~ 12:30

### Miniaturized Dual-Band Composite Right/Left-Handed Crossover 282

Sheng-Yu Hsieh, Pei-Ling Chi, National Chiao Tung University, Taiwan

In this paper, an arbitrary dual-band and miniaturized crossover is proposed using the composite right/left-handed (CRLH) transmission structures. The proposed crossover is based on the two-section CRLH branch lines of three different characteristic impedances where one degree of design freedom can be used for implementation convenience. Combining the CRLH implementation approach with the even- and odd-mode analysis results, a simple design procedure is developed. To support our idea, a dual-band crossover operating at 0.9 GHz and 2.45 GHz was fabricated and tested. The experimental results are in good agreement with the simulated data. Compared to the reported dual-band crossovers based on the printed-circuit-board (PCB) technology, our presented crossover shows a significant size reduction by about 59% with respect to the smallest footprint found in the literature.

[T2B-5]

12:30 ~ 12:50

### Analysis of Shorted Coaxial Peripheral Feeding Networks for Conical Line Power Combiners 285

Ryno D. Beyers, Dirk I. L. de Villiers, Stellenbosch University, South Africa

A simple equivalent circuit model for the peripheral ports of conical line power combiners is presented. Standard feeding pins present a series inductance in the feeding lines which limits the operating bandwidth of the structure. The presented circuit model is used to illustrate how stepping to a thickened feeding post in the conical line may reduce the feed pin inductance by introducing a shunt step capacitance in the feed line. The validity of the circuit model is confirmed by favorable comparisons with full wave simulations. Since the inductance of the feeding pins increase with length, the stepped feeding posts are crucial for good performance - especially for electrically large conical line combiners with higher impedances.

## [T2C] Computational Electromagnetics

- Date: November 7, 2013 (Thursday)
- Time: 11:10 ~ 12:50
- Room: Room C (Room 104)
- Session Chairs: Chi Hou Chan (City University of Hong Kong)  
Jong-Gwan Yook (Yonsei University)

[T2C-1]

11:10 ~ 11:30

### FDTD Method for the Analysis of the EM Field from a Moving Source 288

Shafrida Sahrani<sup>1</sup>, Tatsuya Akata<sup>2</sup>, Michiko Kuroda<sup>2</sup>, <sup>1</sup>Universiti Malaysia Sarawak, Malaysia, <sup>2</sup>Tokyo University of Technology, Japan

A numerical technique for the analysis of the EM field by a moving source or a moving body can be significantly important for the realization of new optical/nanotechnology devices. We have previously proposed the Overset Grid Generation method coupled with FDTD method for the analysis of the EM field with moving boundaries considering Doppler Effect. By overlapping one moving sub-mesh on a static main mesh, each mesh is calculated alternately by using interpolation technique. For higher velocity value, Lorentz transformation is applied to the FDTD method. In this paper, this technique is proposed for solving the EM field when the input source is moving. As a bench mark, the received wave at the observation point is calculated when the source moves for x-direction in free space intersect at right angle by the dielectric object. The numerical results are compared with the stationary case and the moving case.

[T2C-2]

11:30 ~ 11:50

### FDTD Modeling of Diurnal/Seasonal Variations of Schumann Resonance 291

Xiao Yuan, Yi Wang, Jinzhi He, Qunsheng Cao, Nanjing University of Aeronautics and Astronautics, China

A three-dimensional geodesic finite difference time domain (G-FDTD) algorithm is employed to model the diurnal/seasonal variations of the first five Schumann resonance parameters (SRs), including resonance frequencies and quality factors, in the Earth-ionosphere (E-I) system. In order to make the results more accurate, Prony's method is introduced to obtain these parameters. Through several simulations the SRs shift with time/locations are found and compared with reference results. Besides, different conductivity profiles of the ionosphere including the two-exponential profile and the "knee" profile are also considered in the simulations to assure the results.

[T2C-3]

11:50 ~ 12:10

### High Frequency Scattering Analysis of Dielectric Surfaces- TM Incidence Case- 294

An Nguyen Ngoc, Hiroshi Shirai, Chuo University, Japan

Electromagnetic TM polarized plane wave scattering by dielectric surfaces is analyzed by high frequency asymptotic method. The scattering field is estimated from the equivalent currents induced by reflected plane wave on the dielectric surface. Effects of material nature, polarization and finiteness of the dielectric bodies are included in a multiple reflection coefficient. A comparison between theoretical estimations and measurement in the case of a rubber cube suggests a strong connection between the thickness of the body and its RCS values.

[T2C-4]

12:10 ~ 12:30

### Concise Analytical Expressions for Evaluating Time Domain Potentials in Time Domain Integral Equations 297

Xuezhe Tian<sup>1</sup>, Gaobiao Xiao<sup>1</sup>, Jinpeng Fang<sup>2</sup>, <sup>1</sup>Shanghai Jiao Tong University, China, <sup>2</sup>Shanghai Key Laboratory of Electromagnetic Environmental Effects for Aerospace Vehicle, China

New and concise analytical formulae for calculating time domain potentials from Rao-Wilton-Glisson (RWG) type sources are derived in this paper, which can be applied to efficiently evaluate the interaction between two RWG elements in time domain, as is required in methods such as marching-on-in-time (MOT) for time-domain-integral-equations (TDIEs). Compared with previous analytical expressions, formulae in this paper are readily deduced through the RWG coordinates which are very compact to program without finding and paring the intersecting points between the concentric time spheres and the RWG triangles or categorizing the geometric relations of the observation point and the triangles into different occasions. Undifferentiated EFIE, MFIE and CFIE are applied to provide numerical examples that verify the efficacy of these formulae.

[T2C-5]

12:30 ~ 12:50

### Spectral-Domain Analysis of Electromagnetic Scattering by Periodically Corrugated Surfaces with Local Deformation 301

Koki Watanabe, Fukuoka Institute of Technology, Japan

This paper considers the electromagnetic scattering from a periodically corrugated surface, in which the reference level is locally deformed, and presents a spectral-domain formulation based on the coordinate transformation method (C-method). The C-method is originally developed to analyze the plane-wave scattering from perfectly periodic structures, and based on the pseudo-periodicity of the fields. The fields in imperfectly periodic structures do not have the pseudo-periodic property and the conventional C-method is not applicable. This paper introduces the pseudo-periodic Fourier transform to convert the fields in imperfectly periodic structures to pseudo-periodic ones, and the C-method becomes then applicable.

## [T2D] Millimeter-Wave Antennas

- Date: November 7, 2013 (Thursday)
- Time: 11:10 ~ 13:00
- Room: Room D (Room 105)
- Session Chairs: Jiro Hirokawa (Tokyo Institute of Technology)  
Kwai-Man LUK (City University of Hong Kong)

[T2D-1]

11:10 ~ 11:40

### [Invited] Magneto-electric Dipole Antennas for Millimeter-wave Applications 304 Kwai-Man Luk, Mingjian Li, City University of Hong Kong, Hong Kong

In this paper, we present a new millimeter-wave wideband magneto-electric dipole antenna which consists of four metal patches, four sets of vias and an L-shaped probe. This antenna, operating at 60GHz, achieves a wide impedance bandwidth of over 50%, a maximum gain of 9.5dBi and relative high antenna efficiency. The antenna is made of low-cost printed circuit board. Two kinds of feeding technique for this antenna is investigated.

[T2D-2]

11:40 ~ 12:00

### 43dBi Gain, 60% Efficiency and 10% Bandwidth Hollow-waveguide Slot Array Antenna in the 120GHz Band 307 Jiro Hirokawa<sup>1</sup>, Dongjin Kim<sup>1</sup>, Makoto Ando<sup>1</sup>, Jun Takeuchi<sup>1,2</sup>, Akihiko Hirata<sup>2</sup>, <sup>1</sup>Tokyo Institute of Technology, Japan, <sup>2</sup>NTT Corporation, Japan

We propose high gain antennas with a broad bandwidth for the 120 GHz band. The proposed antennas are fabricated by diffusion bonding of laminated thin copper plates which has the advantages of high precision and low loss even in a high frequency region such as 120 GHz. For the stable fabrication using the diffusion bonding technique, we propose a new feeding structure with a double layer. A 32x32-element array shows 38 dBi gain with 70% antenna efficiency over 13 GHz bandwidth and a 64x64-element array shows 43 dBi gain with 60% antenna efficiency over 13 GHz bandwidth, respectively.

[T2D-3]

12:00 ~ 12:20

### Antenna Array in eWLB for 61 GHz FMCW Radar 310 M. Pour Mousavi<sup>1</sup>, M. Wojnowski<sup>2</sup>, R. Agethen<sup>1</sup>, R. Weigel<sup>1</sup>, A. Hagelauer<sup>1</sup>, <sup>1</sup>University of Erlangen-Nuremberg, Germany, <sup>2</sup>Infiniteon Technologies, Germany

In this article we present an antenna array concept in embedded wafer level ball grid array (eWLB) package for mm-wave applications. The eWLB package has an excellent performance for high frequency and the additional fan-out area around the silicon chip enables the realization of passives and antennas. Moreover, integration of the antenna in package increases the efficiency and reduces cost. For some applications a single antenna in package is unable to achieve the required gain and directivity. Combining several antenna elements as an array in a package can be a possible solution. A two elements differential dipole antenna array in an 8 mm x 8 mm eWLB package at IMS (Industrial, Medical and Scientific) band about 61 GHz is analyzed and successfully implemented. A 100  $\Omega$  differential feeding system is designed for the array. The measured reflection coefficient is -25 dB and the designed antenna array has a gain of 11 dB and radiates in broadside.

[T2D-4]

12:20 ~ 12:40

### A Differentially-Fed Complementary Antenna for WiGig Applications 313 Kung Bo Ng, Chi Hou Chan, City University of Hong Kong, Hong Kong

A differentially-fed complementary antenna array is introduced in this paper. Coplanar waveguide (CPW)-fed planar slot antennas are inherently narrow in bandwidth. Modification on widening open-ends of the slot is the most popular technique for bandwidth enhancement. An alternative approach is to use complementary sources. In this paper, a new stacked structure of complementary antenna is proposed which utilizes a regular slot antenna to act as a magnetic source and a parasitic dipole allocated across the slot to act as an electric source. This antenna array, fabricated on generic microwave substrate with simple plated-through-hole printed-circuit technology, achieves an impedance bandwidth of 25% from 53 to 68 GHz for VSWR < 2. It also yields a stable gain of 11.5 dBi across the entire operating band from 56 to 67GHz.

[T2D-5]

12:40 ~ 13:00

### Surface Micro-machined High Efficient and Wideband Cavity-backed Patch Antenna Array for 60GHz Radios 316 Hua Zhu<sup>1,2</sup>, Nan Li<sup>1,2</sup>, Qi Zhang<sup>1,2</sup>, Weiwei Feng<sup>1,2</sup>, Xiuping Li<sup>1,2</sup>, Yang Tian<sup>3</sup>, Hong Wang<sup>3</sup>, <sup>1</sup>University of Posts and Telecommunications, China, <sup>2</sup>State Key Laboratory of Millimeter Waves, China, <sup>3</sup>Nanyang Technological University, Singapore

A wideband V-band cavity-backed circular patch antenna array is designed using a surface micromachining. The antenna array is excited by T-power divider. The T-power divider is designed using rectangular micro-coaxial transmission line. The antenna array with the specified size of 6.1mmx3mmx0.42mm and bandwidth shows around 10.3GHz (56.5 ~ 66.2GHz) under the condition of voltage standing wave ratio (VSWR) less than 2, which covers full-band standard of frequency range. Gain of the antenna array is up to 10.7 dBi gain at 61GHz, and the efficiency is 90%.

## [T2E] Novel Oscillators

- Date: November 7, 2013 (Thursday)
- Time: 11:10 ~ 12:30
- Room: Room E (Room 203)
- Session Chairs: Tah-Hsiung Chu (National Taiwan University)  
Dongha Shim (Seoul National University of Science & Technology)

[T2E-1] 11:10 ~ 11:30

### Striped Inductor for Quasi Millimeter Wave Voltage-Controlled Oscillator 319

Nobuyuki Itoh<sup>1</sup>, Yuka Itano<sup>1,2</sup>, Shotarou Morimoto<sup>1</sup>, Sadayuki Yoshitomi<sup>2</sup>, <sup>1</sup>Okayama Prefectural University, Japan, <sup>2</sup>Toshiba Corporation, Japan

Striped inductor has been implemented to quasimm-wave voltage-controlled oscillator (VCO) to improve Qfactor. Since skin effect is significantly degrades Q-factor of inductor in this frequency region, the phase noise of VCO is degraded. Proposed striped inductor can be improved its Qfactor, hence, the phase noise of VCO is improved. The phase noise of designed and fabricated VCO shows -106 dBc/Hz at 1-MHz offset from 21-GHz oscillation frequency. It exhibits 5 dB better phase noise compare than conventional inductor's VCO. The process technology of designed and fabricated VCO is 65-nm standard CMOS with thick Cu metal.

[T2E-2] 11:30 ~ 11:50

### A Ka-Band YIG-based Local Oscillator for Astronomical Heterodyne Receiver 322

Yue-Fang Kuo, Yuh-Jing Hwang, Academic Sinica Institute of Astronomy and Astrophysics, Taiwan

A Ka-band local oscillator generator based on YIG-tuned oscillator is designed, fabricated and measured for astronomical telescope applications. The optimized bandwidth analysis can overcome high phase noise problems caused by poor microwave photonic source noise and to improve the out-band phase noise of LO by at least 10.5 dB. The experimental results show that the 33.8 GHz LO phase noise of -107 dBc/Hz is achieved at offset frequency of 700 kHz and exhibits a reference spurs of -71 dBc.

[T2E-3] 11:50 ~ 12:10

### 2.4 GHz-Band Ultra-Low-Voltage Class-C LC-VCO IC in 65 nm CMOS Technology 325

Xin Yang, Yorikatsu Uchida, Kangyang Xu, Wei Wang, Toshihiko Yoshimasu, Waseda University, Japan

A novel LC-VCO IC is proposed to achieve ultra-low-voltage low-power operation even at a supply voltage below the threshold voltage. The LC-VCO consists of a VCO circuit, a power detector circuit and a comparator circuit. A feedback loop consisting of the power detector and the comparator controls the bias condition of the LC-VCO to realize class-C operation and robust start-up. The class-C LC-VCO IC has been designed, fabricated and fully evaluated using 65 nm CMOS technology. The fabricated VCO IC has an oscillation frequency band from 2.22 to 2.43 GHz at an operation voltage of only 0.3 V with dc current consumption of 1.92 mA. The fabricated VCO IC exhibits a measured phase noise of -111 dBc/Hz at 1 MHz offset from the 2.43 GHz carrier frequency at an operation voltage of only 0.3 V.

[T2E-4] 12:10 ~ 12:30

### Low Power and Low phase Noise CMOS VCO Based on Cross-Coupled Topology with Capacitor Filter 328

Meng-Ting Hsu, Yu-Tuan Hsu, Yao-Yen Lee, National Yunlin University of Science and Technology, Taiwan

The paper presents a low power and low phase noise voltage controlled oscillator (VCO) for IEEE 802.11a applications. The quality enhancement and reducing current architecture is designed to improve phase noise and power. The measured results exhibited phase noise -115.62 dBc/Hz at 1MHz offset frequency and measured tuning range is about 14.5% from 5.26GHz to 6.08GHz. The power dissipation is 2.26mW and FOM is -187dBc/Hz. The chip fabrication of VCO is made by TSMC 0.18μm 1P6M CMOS standard process.

## [T2F] Metamaterials Novel EM Structures

- Date: November 7, 2013 (Thursday)
- Time: 11:10 ~ 12:50
- Room: Room F (Room 208)
- Session Chairs: Atsushi Sanada (Yamaguchi University)  
Bomson Lee (Kyung Hee University)

[T2F-1] 11:10 ~ 11:40

### [Invited] Adjustable Metamaterial Cloaking using an Elastic Crystal 331

Dongheok Shin<sup>1</sup>, Yaroslav Urzhumov<sup>2</sup>, Youngjean Jung<sup>1</sup>, Kyoungsik Kim<sup>1</sup>, David R. Smith<sup>2</sup>, <sup>1</sup>Yonsei University, Korea, <sup>2</sup>Duke University, USA

We introduce a microwave cloak composed of smart metamaterials whose electromagnetic properties can be effectively changed by mechanical deformation. Against mechanical deformations, our smart metamaterials self-adjust own flexible elasto-electromagnetic crystal structure for obeying transformation optics rules. With this idea, we built microwave cloak made of flexible silicone rubber tube array and experimentally demonstrated self-adjustable carpet cloak in broadband ranges (8-12GHz) with variable deformations.

[T2F-2] 11:40 ~ 12:00

### Negative Group Delay Circuit based on a Multisection Asymmetrical Directional Coupler 333

Chung-Tse Michael Wu, Sam Gharavi, Tatsuo Itoh, UCLA, USA

In this paper, we present a novel passive negative group delay (NGD) circuit based on directional couplers. By cascading several directional couplers with appropriate coupling coefficients, we are able to synthesize negative group delay with a broad bandwidth at the coupled port of the multisection directional coupler. Unlike conventional NGD circuits that use bandstop structures with lumped elements, such as inductors and capacitors, to realize negative group delay, the proposed design provides a fully distributed realization of NGD circuit. Therefore, this novel NGD circuit is very promising to be integrated into high frequency designs.

[T2F-3] 12:00 ~ 12:20

### Angle Selective High Absorption by a Mushroom Metasurface at V-Band 336

Shotaro Nagai<sup>1</sup>, Atsushi Sanada<sup>1</sup>, Munenari Kawashima<sup>2</sup>, Tomohiro Seki<sup>2</sup>, <sup>1</sup>Yamaguchi University, Japan, <sup>2</sup>NTT Corporation, Japan

A metasurface consisting of a periodic array of mushroom structures is designed and tested to demonstrate a strong angle selective absorption for TM incident waves from free space at V-band. An absorption as high as 35.6 dB is experimentally obtained with the incident/reflection angle of  $\theta = 7$  deg at 67.3 GHz. Time domain measurements reveal that there exist reradiated waves with a longer decay than that of the direct specular reflection and the absorption is considered to be due to a cancellation of the direct specular reflected waves and the reradiated waves.

[T2F-4] 12:20 ~ 12:40

### Combining Method of Two Filtering Circuits Based on Isolation Circuits for Five-Channel Multiplexers 339

Hanseung Lee, Tatsuo Itoh, University of California, USA

This paper presents a design method of combining two multiplexers using isolation circuits such that the number of channels is increased. An isolation circuit is composed of a synthesized (metamaterial) transmission line (TL) connected to a multiplexer, while the combination of two isolation circuits has multiplexer functionality. Using this concept, the number of channels can easily be increased because the number is the sum of the channels of two isolation circuits. The freedom to choose any commercial band-pass filter or multiplexer is another positive aspect. Furthermore, it is not necessary to use a complex optimization process because of the straightforward design method. In this paper, a composite right/left-handed (CRLH) TL (having dual-band characteristics), and a double-Lorentz (DL) TL (having tri-band characteristics) are used for a five-channel multiplexer.

[T2F-5] 12:40 ~ 13:00

### Dual-band Circularly Polarized Hybrid Metamaterial Patch Antenna 342

Seung-Tae Ko<sup>1,2</sup>, Byung-Chul Park<sup>1</sup>, Jeong-Hae Lee<sup>1</sup>, <sup>1</sup>Hongik University, Korea, <sup>2</sup>Samsung Electronics, Korea

In this paper, a small dual-band circularly polarized (CP) hybrid metamaterial (HMTM) patch antenna is presented by utilizing the first positive (+1) mode and the first negative (-1) mode. The -1 mode is generated on the periodic mushroom structures that provide a left-handed (LH) property of the metamaterial (MTM). Similarly, the CP radiation can be also obtained by using two orthogonal -1 modes, because the -1 mode has the same property with the +1 mode. To obtain two +1 modes and two -1 modes simultaneously, the trimmed patch antenna and 2+2 mushroom antenna are employed, respectively, and two antennas are united into one. It is measured that the CP radiations of the +1 and -1 modes appear 2.846 GHz ~ 2.887 GHz and 3.829 GHz ~ 3.835 GHz, respectively. Finally, the radiation efficiencies are measured to be 87 % and 47 % of the +1 mode and -1 mode, respectively.

## Poster Session II: Passive Components & Systems and Applications

- Date: November 7, 2013 (Thursday)
- Time: 14:20 ~ 16:00
- Room: Room 103

[P2-1] 14:20 ~ 16:00

### Design of UWB Bandpass Filter with Embedded Open-Circuited Stub Multi-mode Resonator 866

Yunxiu Wang, Hankui Liu, Qianshu Zhang, Shunwen Xiao, Huaibing Qi, Xianzhi Dai, China West Normal University, China

A compact microstrip ultra-wideband (UWB) bandpass filter (BPF) with a narrow notched band in the passband is presented in this letter. To achieve a notched band, an embedded open-circuited stub multi-mode resonator is utilized in the filter design. The bandwidth of the notched filter can be controlled by adjusting the width of the stub. The length of the stub can be tuned to select a specific frequency for the notched band. Predicted frequency responses are verified by the simulation and measurement.

[P2-2] 14:20 ~ 16:00

### A Compact Tri-band Antenna Switch Module for Compass Satellite Positioning Application 869

Liu Wanzong, Huang Yong, Zhang Xiaopeng, Wang Jie, Wang Xiao, Liu Weiyong, Suzhou Bohai Micro-system Co., Ltd., China

In this paper, a compact tri-band antenna switch module is presented. The module consists of a high rejection triplexer embedded in LTCC board and three surface mounted SPDT switches. The module operates at B3, L and S channel of Compass Satellite Positioning System. Experimental results show that the insertion loss of the switch module is less than 3.5dB and the rejection between B3 and L is more than 35dB. Well agreement between simulated and experimental result is achieved.

[P2-3] 14:20 ~ 16:00

### A constant absolute bandwidth Tunable Filter using Varactor-Loaded Open-Loop Resonators 872

Xiaoguo Huang<sup>1,2</sup>, Quanyuan Feng<sup>1</sup>, Lei Zhu<sup>2</sup>, Qianyin Xiang<sup>1</sup>, <sup>1</sup>Southwest Jiaotong University, China, <sup>2</sup>Nanyang Technological University, Singapore

This paper presents a new type of larger tuning rate tunable filters using varactor-loaded open-loop resonators. The filter is based on capacitively loaded folded  $\lambda/2$  resonators that are coupled to each other with mixed electrical and magnetic coupling. By adjusting the value of the varactors between the open gaps in a mixed coupled filter, the coupling coefficients and external quality can be tuned to meet the requirement of constant absolute bandwidth. The fabricated filter shows a tuning rate of 460 MHz/pF. To our knowledge, this planar tunable filter represents state-of-the-art tuning rate characteristics among the varactor-tuned filter.

[P2-4] 14:20 ~ 16:00

### Short Stub Band-pass Filter using Stepped Impedance Resonator for Size Reduction 875

Jaegook Lee, Ki-Cheol Yoon, Hyunwook Lee, Tae-Sung Jung, Tae-Young Kim, Jong-Chul Lee, Kwangwoon University, Korea

This paper shows a short stub narrow bandpass filter using a stepped impedance resonator (SIR). A SIR is adopted instead of transmission line to reduce the size of the BPF on the low dielectric substrate. The size of the conventional narrow BPF is reduced by more than 30 % of its length of the transmission line within the inverter. The experimental results show that the insertion loss is 1.6 dB, return loss is 16 dB, and the fractional bandwidth is 10% at the center frequency of 5.8 GHz. The size of the filter is 22x8.7 mm<sup>2</sup>.

[P2-5] 14:20 ~ 16:00

### Superconducting Narrow-band Filter for 2 GHz-band Transmitter 878

Noritsugu Shiokawa, Tamio Kawaguchi, Kohei Nakayama, Mutsuki Yamazaki, Hiroyuki Kayano, Toshiba Corporation, Japan

We have developed a superconducting microstrip resonator for the narrow-band transmitting filter application, in order to achieve both high power handling capability and high unloaded Q value. For the superconducting microstrip resonator, it is necessary to suppress the radiation loss of the resonator in order to achieve high unloaded Q value and to reduce the maximum current density in the resonator to achieve high power handling capability, too. Therefore, by adopting an interdigital resonator consisting of two coupled comb resonators, we have reduced current density and suppressed the radiation loss. Using the interdigital resonators, we have fabricated an 8-pole pseudo-elliptic function filter that has about 2.0 GHz center frequency and 0.975% fractional bandwidth, and evaluated the power handling capability. As a result, we have confirmed that the power handling capability of the filter exceeds 40 W.

## Poster Session II: Passive Components & Systems and Applications

- Date: November 7, 2013 (Thursday)
- Time: 14:20 ~ 16:00
- Room: Room 103

[P2-6] 14:20 ~ 16:00

### A Study On RF Characteristics of Polyether Sulfone Substrate for Application to Flexible Mobile Communication Device 881 Young Yun, Jang-Hyeon Jeong, Sung-Jo Han, Ki-Jun Son, Korea Maritime University, Korea

In this work, coplanar waveguide was fabricated on flexible PES substrate, and their RF loss characteristics were extracted using transmission line theory. Concretely, several Qfactors of the coplanar waveguides were extracted using transmission line theory. Firstly,  $Q_L$  was characterized using the equivalent RLGC circuit. According to measured result, the  $Q_L$  was 25.7 at 49.8 GHz. Q-factor was also extracted from a resonant tank built using a one-quarter of a wavelength long line at the resonance frequency  $f_0$ . According to the measured result, the Q-factor measured from one port open stub resonant circuit was 38.3 at a resonance frequency of 49.8 GHz, which was much higher than the open stub on silicon substrate.

[P2-7] 14:20 ~ 16:00

### A Basic Study on RF Characteristics of Inverted Comb-Type Capacitive Transmission Line Structure on MMIC 884 Young Yun, Jang-Hyeon Jeong, Sung-Jo Han, Ki-Jun Son, Korea Maritime University, Korea

In this work, the inverted comb-type capacitive transmission line (ICCTL) structure on GaAs monolithic microwave integrated circuit (MMIC) was proposed and its RF characteristics were investigated for application to a development of miniaturized on-chip passive components. According to the results, the ICCTL structure showed short wavelength characteristic due to an enhancement of its periodic capacitance. Concretely, the wavelength of the ICCTL structure was only 11.85 % of conventional microstrip line on MMIC. The insertion loss of the ICCTL with a length of  $\lambda/8$  was less than 0.36 dB up to 6 GHz, which was comparable to conventional microstrip line. Using the ICCTL structure, a highly miniaturized impedance transformer was fabricated on GaAs MMIC. The impedance transformer showed good RF performances in a broad band from S to X band, and its size was  $0.012 \text{ mm}^2$ , which was only 1.7 % of the size of the transformer fabricated by conventional microstrip line on GaAs MMIC.

[P2-8] 14:20 ~ 16:00

### A Multi-mode Cavity Filter with Jerusalem Cross Structure Resonator 887 J. J. Liu, Y. J. Chen, N. Xu, Y. H. Ren, G. X. Xu, C. L. Ji, Z. Y. Zhao, Y. Y. Zhang, R. P. Liu, Kuang-Chi Institute of Advanced Technology, China

In this paper, a novel multi-mode dielectric resonator sandwiched by a Jerusalem Cross metal structure in the middle is proposed. This resonator has one degenerate dual modes and another nearby mode. These three modes are smartly used in a cylindrical cavity to generate two transmission zeros and one transmission pole. Therefore a single-cavity multi-mode bandpass filter is designed. In order to excite the three modes, two ports are placed orthogonally and another two tuning screws are needed to provide similar capacitance effects as the port pins. Simulation results show that the cavity with the resonator successfully becomes a bandpass filter and measurement results also prove this concept.

[P2-9] 14:20 ~ 16:00

### Novel Ultra-wide Bandpass Filter with Notched Band using Multimode Resonator and Open Stubs 890 Fang Xu<sup>1</sup>, Zongjie Wang<sup>1</sup>, Kaiyi Ye<sup>2</sup>, Ju Mu<sup>3</sup>, <sup>1</sup>Tianjin University, China, <sup>2</sup>Brown University, USA, <sup>3</sup>Southeast University, China

In this letter, a novel ultra-wideband bandpass filter with notched band is proposed. This filter is based on multi-mode resonator (MMR) and coupled with the special feed-line structure. The main structure creates the UWB passband from 3.9GHz to 11.1GHz. The notched band was generated around 9GHz by connecting the open-stubs in original structure. Moreover, the theoretical analysis of the main resonator is given, briefly. The measured results shows the feasibility of the filter with the insertion loss lower than 2dB and the average group delay less than 0.4ns. Compared to the other UWB filter with notched band, the size of filter is 50% smaller and fabricated in just a single layer of the substrate.

[P2-10] 14:20 ~ 16:00

### Direct Coupled Quad-band Bandstop Filter Synthesis using Frequency Transformation 893 Seema Awasthi, Animesh Biswas, Mohammed Jaleel Akhtar, Indian Institute of Technology, India

In this paper we propose a design of quadband bandstop filter for the suppression of interfering signals in broadband applications. There are different approaches to implement multiband filters among which frequency transformation techniques is advantageous than other methods in terms of complexity to find the transfer functions. So it is applied here for finding the locations of poles and zeros of a direct coupled quadband bandstop filter. By properly combining several single-band filtering functions, the multiband filtering function of similar bandwidth are generated. For easy tuning, filter has been synthesized in cul-de-sac topology which eliminates the need for diagonal couplings. Finally 16-pole symmetric quadband bandstop filters have been synthesized to validate the proposed method.

## Poster Session II: Passive Components & Systems and Applications

- Date: November 7, 2013 (Thursday)
- Time: 14:20 ~ 16:00
- Room: Room 103

[P2-11] 14:20 ~ 16:00

### Design of a Broadband Coaxial to Substrate Integrated Waveguide (SIW) Transition 896

Soumava Mukherjee, Prasun Chongder, Kumar Vaibhav Srivastava, Animesh Biswas, Indian Institute of Technology, India

In this paper, a novel design of broadband coaxial to Substrate Integrated Waveguide (SIW) transition has been implemented. The difficulties to get impedance matching between SIW and excitation port especially for thin substrate has been investigated and design steps to overcome the problem has been discussed. A two port SIW section using back to back configuration of the proposed transition is designed to operate at X band (8-12 GHz) and fabricated. The measured result shows a broad bandwidth (30%) and an insertion loss of 1.2 dB in the operating band.

[P2-12] 14:20 ~ 16:00

### New Dual-Band Band-Pass Filter Design with Enhanced Dual-Band Skirt Characteristics 899

Juseok Bae, Cam Nguyen, Texas A&M University, USA

A new frequency transformation concept is proposed to overcome the skirt characteristic of dual-band band-pass filters (BPF) caused by the conventional frequency transformation method. The new frequency transformation incorporates an extra frequency parameter to achieve additional rejection function in the high-frequency stop-band. To realize the concept, the dual-band BPF's resonators are modified based on their frequency responses. A new dual-band BPF was also designed with the modified resonators, fabricated and measured, and achieved desired enhanced skirt characteristic.

[P2-13] 14:20 ~ 16:00

### Compact Quad-Mode Bandpass Filter with Sharp Cut-off using Folded Parallel-Coupled Microstrip Lines and Semi-annular Resonator 902

J. Marimuthu, A. Abbosh, The University of Queensland, Australia

A quad-mode microstrip bandpass filter with compact size, wide stopband and sharp lower and upper cut-off bands is designed. The proposed filter uses low impedance feeding network, folded parallel coupled microstrip lines (FPCML) and semi-annular middle resonator. The low impedance feeding network is utilized to enhance the coupling of the FPCML structure and to achieve a sharp lower and upper cut-off frequencies with extended upper stopband. Meanwhile, the low impedance semi-annular resonator is used to produce multiple resonant modes within the operating band and two transmission zeros to isolate that band from the stopbands. The proposed filter with a centre frequency of 2.45 GHz is designed and optimized using ADS Momentum. The filter shows excellent performance with 0.5 dB insertion loss, more than 26 dB attenuation at the wide stopband, more than 77 dB/GHz rate of cut-off at the edges of 35% fractional bandwidth passband.

[P2-14] 14:20 ~ 16:00

### A Dual-Mode Bandpass Filter with Tuning Transmission-Zero and Harmonic Suppression for RFID and WiMax Applications 905

Z. Yao, N. Y. Kim, Kwangwoon University, Korea

A dual-mode T-shape stub loaded bandpass filter (BPF) with wide stopband is proposed. To design a narrow BPF for suitable use in 5.8 GHz radio frequency identification (RFID) and worldwide interoperability for microwave access (WiMax) applications, a dual-mode T-shape stub-loaded resonator (TSSLR) is introduced and studied. Due to the symmetrical plane, odd-even mode theory can be adopted to characterize it. One transmission zero is located near the passband, which leads to a high selectivity. An extra transmission zero can be tuned at the second harmonic frequency to realize a wide stopband. The center frequency of the proposed BPF is 5.8 GHz, and the 3 dB fraction bandwidth is 8.9%. The super response is below 20 dB from 7.1-15.0 GHz.

[P2-15] 14:20 ~ 16:00

### Novel Size-Reduced Unit Cells for Uniplanar Chipless RFID Tags 908

Milan Polivka, Jan Machac, Czech Technical University in Prague, Czech

The paper introduces the two new size-reduced unit cells/scatterers for application in frequency spectrum-based uniplanar chipless RFID tags. They are derived from U-folded dipole loaded by either meander line inductor or interdigital capacitor. Radar cross section, and resonant frequency has been evaluated by EM simulation and s-parameters have been measured and calculated when scatterers have been placed in parallel-plate waveguide. The results clearly show the trade-off between size-reduction and radar cross section proportional to reading range of the proposed configurations. Their potential lies in the development of new smaller uniplanar chipless tags with higher information density.



## Poster Session II: Passive Components & Systems and Applications

- Date: November 7, 2013 (Thursday)
- Time: 14:20 ~ 16:00
- Room: Room 103

[P2-16]

14:20 ~ 16:00

### Design of Near-field Chipless RFID Tags and Reader Based on Transmission Line

Won-Seok Lee, Hyung-Seok Jang, Wang-Sang Lee, Kyung-sub Oh, Jong-Won Yu, Korea Advanced Institute of Science and Technology, Korea 911

A new method of reading chipless RFID tags in the near-field region using a microstrip transmission line and resonant coupling with the tags is proposed. A chipless tag consist of combinations of two resonant structures using different resonance methods and resonance frequencies. N-bit codes distinguish  $2^N$  types of items by passing over the microstrip transmission line as the reader system. This method can be used effectively in paper/plastic-based items, especially required to improve security as the additional security element. It will be the effective way to identify chipless RFID tags in the near-field region.

[P2-17]

14:20 ~ 16:00

### Multilayer Compact Hybrid Coupler based on Vertical Microstrip Transition 914

Young Kim<sup>1</sup>, Seok-Hyun Sim<sup>1</sup>, Young-Chul Yoon<sup>2</sup>, <sup>1</sup>Kumoh National Institute of Technology, Korea, <sup>2</sup>KwanDong University, Korea

This paper proposes a multilayer compact hybrid coupler based on vertical microstrip transition. This transition is a sandwich structure with via hole to connect two microstrip lines in different layer. For designing a compact microwave passive circuit, the microstrip line using via-hole transition is proposed to reduce a size of microwave circuit with long transmission line. For the validation of the microstrip line with via-hole transition, the multilayer hybrid coupler is implemented at center frequency of 2 GHz. The measured performances are in good agreement with simulation results and about 50% size reduction compare to conventional coupler.

[P2-18]

14:20 ~ 16:00

### Numerical Estimation on Intermodulation Distortion of a High-Temperature Superconducting Dual-Band Bandpass Filter 917

Kei Satoh, Yasunori Suzuki, Yuta Takagi, Shoichi Narahashi, NTT DOCOMO, INC., Japan

This paper proposes a method for numerically estimating the intermodulation distortion (IMD) of a high-temperature superconducting (HTS) dual-band bandpass filter (DBPF) when two-tone signals are simultaneously input to each passband of the HTS-DBPF. The numerical estimation method is based on the third-order polynomial approximation of the input-output characteristics of the HTS-DBPF when a two-tone signal is input to each passband. For the validation of the proposed method, a 2.0-/3.5-GHz band HTS-DBPF is used to measure its IMD characteristics when two tones with a 30-kHz separation are individually and simultaneously input to each passband. The calculated and measured results confirm that the proposed method is available for estimating the IMD characteristics.

[P2-19]

14:20 ~ 16:00

### Application of Transmission-resonant Aperture to the Waveguide Limiter Design 920

Jun-Seo Park<sup>1</sup>, Hyeok-Woo Son<sup>1</sup>, Jin-Young Choi<sup>1</sup>, Byung-Mun Kim<sup>2</sup>, Young-Ki Cho<sup>1</sup>, <sup>1</sup>Kyungpook National University, Korea, <sup>2</sup>Gyeongbuk Provincial College, Korea

H-shaped small resonant aperture is applied to the design of the combined structure of the band-pass filter and the limiter by incorporating PIN diode into the resonant aperture structure. Single stage and double stage limiters are designed and experimented and the utility of the proposed types is confirmed.

[P2-20]

14:20 ~ 16:00

### A High Performance C-Band FBAR Filter 923

Zhixin Zhang, Yao Lu, Wei Pang, Daihua Zhang, Hao Zhang, Tianjin University, China

In this paper a RF band pass filter in C-band based on film bulk acoustic resonator (FBAR) technology is developed. The measured insertion loss is less than 2.0 dB at the center frequency (5.2GHz) of the filter, and the signal attenuation near the pass band of the filter is greater than 50 dB. The measurement data are in good agreement with the design employing three dimensional electromagnetic simulation techniques. A method to move the transmission zeros of the FBAR filter is proposed by adding a capacitor element between the two shunt branches of the filter. Using the technique, an FBAR filter chip can be configured to meet different rejection specifications potentially.

## Poster Session II: Passive Components & Systems and Applications

- Date: November 7, 2013 (Thursday)
- Time: 14:20 ~ 16:00
- Room: Room 103

[P2-21] 14:20 ~ 16:00

### Feasibility Study on Comblin Filter for Tunable Filters 927 Changsoo Kwak, Manseok Uhm, Inbok Yom, ETRI, Korea

In this paper, a combline filter is studied to see if the filter can be used for a reconfigurable filter that covers a frequency range of 2.0 GHz to 2.7 GHz and a bandwidth ranging from 50 MHz to 80 MHz. Since the bandwidth as well as the center frequency should vary in a wide range, the coupling between the load/source and the first/last resonator must be changeable. This study proves that the combline filter can meet the frequency requirements by designing the combline filter that meets four extreme frequency requirements using full-wave electromagnetic simulations. The input/output coupling proves that it can be tuned enough to be used for the reconfigurable filter of interest.

[P2-22] 14:20 ~ 16:00

### Design of Highly Selective Open-Loop Tunable Bandpass Filters with Wide Tuning Range 930 Jun Chen, Xiao-Wei Zhu, Chuan Ge, Southeast University, China

This paper presents an open-loop tunable filter with a continuous tunability for both center frequency and bandwidth. Electric and magnetic mixed coupling is utilized to achieve one transmission zero in the lower stopband, while the source/load coupling introduces another zero in the upper stopband which totally improve the selectivity. The bandwidth tunability is achieved by placing a transmission line with one end shorted to ground and with a varactor loaded at the opposite end. Moreover, this new filter with novel input and output structure without any via-hole grounds which avoid parasitic inductance can reduce the design error validly. A two-pole filter with wide simultaneous and continuous tunings of center frequency (from 500MHz to 1025MHz, tuning range of 68.9%) and bandwidth (from 30 to 47 MHz around 800MHz) is presented. Measured results agree with simulated predications excellently.

[P2-23] 14:20 ~ 16:00

### A Novel Compact Capacitive Loaded Differential Bandpass Filter 933 Hui Wang<sup>1,2</sup>, Kam-Weng Tam<sup>2</sup>, Sut-Kam Ho<sup>2</sup>, Wen Wu<sup>1</sup>, <sup>1</sup>Nanjing University of Science and Technology, China, <sup>2</sup>University of Macau, China

A novel compact differential bandpass filter (BPF) with parallel coupled resonator and capacitive load is proposed in this paper. The differential- and common-mode equivalent half circuits are given and discussed. By properly designing the coupled resonator and the loaded capacitance, differential-mode passband responses and common-mode rejection can be obtained. In common-mode operation, loaded capacitive network offers wideband attenuation response suppressing common-mode signal. A prototype differential BPF operated at 4.2 GHz with more than 20 dB common-mode suppression from 0 to 9 GHz has been realized to validate the proposed concept and theory. In addition, the circuit size of this filter is merely  $0.09\lambda_0^2$ , showing its compactness advantage.

[P2-24] 14:20 ~ 16:00

### Post-wall Waveguide Transmission Loss Depending on Thickness of Porous Substrates and Its Evaluation of Leakage 936 Tatsuya Suzuki, Ryosuke Suga, Osamu Hashimoto, Aoyama Gakuin University, Japan

In this paper, the transmission and leakage loss of post-wall waveguide depending on the thickness of porous substrate was evaluated. The transmission loss for various thickness of the porous waveguide was simulated in millimeter-wave band by using EM simulator. The valid substrate thickness for improving transmission loss by air-holes was studied. The leakage of the waveguide was also evaluated as a function of substrate thickness, and the relationship between transmission loss and leakage was discussed.

[P2-25] 14:20 ~ 16:00

### Millimeter-Wave Non-Contact Flip-Chip Transitions with Chebyshev Filtering Response using Coupled Microstrip Resonators 939 Han-Yun Tsai, Ting-Yi Huang, Tze-Min Shen, Ruey-Beei Wu, National Taiwan University, Taiwan

The 77GHz automotive collision avoidance radar system is more important today. In this paper, a non-contact flip-chip transition design incorporating with the filter characteristic is proposed for the radar system. The transition is used to connect the RF signal path from a low-temperature co-fired ceramic (LTCC) substrate to a Teflon board. The concept of the transition is based on the design of coupled microstrip resonators, thereby accomplishing filtering transitions. The overall performance can also be improved, with bandwidth of 15 dB return loss from 74.4 GHz to 81.8 GHz, i.e., a 9.5% fractional bandwidth (FBW) and insertion loss of 1.3dB in the pass band.

## Poster Session II: Passive Components & Systems and Applications

- Date: November 7, 2013 (Thursday)
- Time: 14:20 ~ 16:00
- Room: Room 103

[P2-26] 14:20 ~ 16:00

### Design of Dual-Mode Substrate Integrated Hexagonal Cavity (SIHC) Filter for X-Band Application 942

Prasun Chongder, Soumava Mukherjee, Kumar Vaibhav Srivastava, Animesh Biswas, Indian Institute of Technology, India

A Dual-mode substrate integrated waveguide hexagonal cavity (SIHC) filter using hexagonal shaped cavity for X-Band application has been proposed in this paper. Use of perturbation technique to achieve dual mode response has been investigated. The field patterns of the degenerate modes and the mode splitting characteristics are also studied. The theoretical analysis with the help of coupling matrix is shown and experimental verification is also presented.

[P2-27] 14:20 ~ 16:00

### Compact Dual Mode Switchable BPF–BSF using RF PIN Diodes and DGS 945

Hesham A. Mohamed<sup>1</sup>, Heba B. El-Shaarawy<sup>2</sup>, Esmat. A. F. Abdallah<sup>1</sup>, Hadia El-Hennawy<sup>3</sup>, <sup>1</sup>Electronics Research Institute, Egypt, <sup>2</sup>Cairo University, Egypt, <sup>3</sup>Ain Shams University, Egypt

This work presents a novel frequency miniaturized reconfigurable dual-mode stub-loaded resonator switchable from BPF to single/double notched bandpass filter. The proposed filter topology employs RF PIN diodes as the switching device. Based on the odd and even-mode equivalent circuits, the resonant characteristics of the proposed microstrip resonator are investigated. RF PIN diodes are used to switch the passband between GSM (1.83GHz) and BSF to reject much application, and when changing the location of diode, filter could switch its double notched band for 1.77GHz and tuned a second notch. Measured results show a very good agreement with the simulations where a 1.83 GHz center frequency with a 280 MHz bandwidth was obtained for the GSM state. The DGS patterned enhanced the performance such as a 3 dB bandwidth reached 63%, insertion loss of -0.5 dB and great sharpness 351dB/GHz in low frequency edge and 255 dB/GHz in high frequency edge.

[P2-28] 14:20 ~ 16:00

### A New Transition for SIW and Microstrip Line 948

Zheng Liu, GaoBiao Xiao, Shanghai Jiao Tong University, China

Transition is a critical component to integrate the substrate integrated waveguide and planar circuits. In this paper, a novel transition design method is presented. The new approach combines slots and multi-section stepped impedance transformers directly within a single section of microstrip line. Two new transitions working in U band and Ku band have been studied. The results show that these two transitions all have good performance and achieve good impedance matching in their operating frequency bands. The sizes of the new structures are more compact than the traditional tapered ones.

[P2-29] 14:20 ~ 16:00

### Ultra-wideband Phase Shifter using Broadside-Coupled Microstrip Coplanar Waveguide 951

L. Guo, A. Abbosh, The University of Queensland, Australia

A compact planar phase shifter with ultra-wideband (UWB) performance and 180 degree differential phase shift is proposed. It utilizes a broadside-coupled microstrip/coplanar waveguide (CPW). Thus, the proposed device can be fabricated using a simple double-side printed circuit board. Four open-ended stubs are added to the microstrip patches and CPW in order to achieve the required 180° phase shift. The designed phase shifter operates across the band from 4.2GHz to 11GHz with less than ±10° differential phase imbalance, and less than 1dB insertion loss.

[P2-30] 14:20 ~ 16:00

### Design of the Miniaturized Ultra-Wide Band (UWB) Filter using the Metamaterial Characteristic 954

Seung-Hun Oh<sup>1</sup>, Koon-Tae Kim<sup>1</sup>, Jeong-Hyeok Lee<sup>1</sup>, Sungtek Kahng<sup>2</sup>, Hyeong-Seok Kim<sup>1</sup>, <sup>1</sup>Chung-Ang University, Korea, <sup>2</sup>Incheon National University, Korea

In this paper, a filter for the ultra-wide band (UWB) ranging 3GHz~10.5GHz has been designed by taking the advantage of the metamaterial Composite Right & Left-Handed Transmission-line (CRLH-TL) with a Shorted Open Gap Ring Resonator(SOGR) structure and an inter-digital line. In order to bring the remarkable improvement in an attempt to reduce the total metamaterial cell size, only one cell of the SOGR with the inter-digital line is taken. This metamaterial filter will be shown to have the size of 15mmXx15mm, the fractional bandwidth over 100%, the insertion loss much less than 1dB, and an acceptable return loss.

## Poster Session II: Passive Components & Systems and Applications

- Date: November 7, 2013 (Thursday)
- Time: 14:20 ~ 16:00
- Room: Room 103

[P2-31] 14:20 ~ 16:00

### Design of Wideband Filters With High Skirt-Selectivity using Improved Parallel-Coupled Three-line Units 957

J. Oda<sup>1</sup>, C.-P. Chen<sup>1</sup>, K. Kamata<sup>1</sup>, T. Kato<sup>1</sup>, N. Kato<sup>1</sup>, T. Anada<sup>1</sup>, S. Takeda<sup>2</sup>, <sup>1</sup>Kanagawa University, Japan, <sup>2</sup>Antenna Giken Co., Ltd., Japan

An improved compound three-line unit is proposed to implement wideband bandpass filters with high skirt-selectivity and out-of-band characteristics. A corresponding two-step design/synthesis scheme is proposed to design the filter. Firstly, a filter consisting of two cascaded parallel-coupled lines with two short-circuited stubs loaded at input- and output- ports is synthesized based a Chebyshev Function. Then, in order to improve the skirt characteristics, two  $5/4$  wavelength SIRs are inserted into between the parallel-coupled lines, whereas two two-section open-circuited stubs are designed to replace the short-circuited ones loaded at the ports to create multiple transmission zeros. Finally, a wideband filter with a bandwidth of 3-5GHz (FBW:50%) is designed to validate the effectiveness of the proposed structure and corresponding design scheme.

[P2-32] 14:20 ~ 16:00

### Substrate Integrated Waveguide Switch Matrix in LTCC Technology 960

Yang Fei, Yu Hong-xi, Liu Rui-zhu, Sun Shu-feng, He Xin-Yang, China Academy of Space Technology, China

A novel implementation of high frequency switch matrix is proposed in this paper. The solution is based on substrate integrated waveguide (SIW) in low-temperature co-fired ceramic (LTCC) technology. The approach demonstrates significant benefit of using SIW as a connection and cross transmission of the Switch matrix, offering high isolation and good transition performance in high frequency. A K band 4x4 switch matrix is simulated and fabricated, with good performance demonstrated experimentally.

[P2-33] 14:20 ~ 16:00

### Bandstop Resonator using Electrically Coupled Open Stub for Compact Wideband Bandstop Filters 963

Hyun-Seung Lee<sup>1</sup>, Won-Gyu Lim<sup>2</sup>, Choul-Young Kim<sup>1</sup>, <sup>1</sup>Chungnam National University, Korea, <sup>2</sup>Korea Aerospace Research Institute, Korea

In this paper, a compact wideband bandstop resonator in the form of open stub combination is proposed. The wideband characteristic of the proposed bandstop resonator is due to electrical coupling at the ends of the two open stubs. A stopband is approximately improved by 52% (rejection depth: -20dB) compared with the case that the end of open stub is uncombined. Proposed structure increases the skirt selectivity and elastically controls the frequency bandwidth and rejection depth.

[P2-34] 14:20 ~ 16:00

### Compact and High-Isolation Microstrip Quadruplexer 966

Shih-Shan Lo, Ko-Wen Hsu, Wen-Hua Tu, National Central University, Taiwan

A microstrip quadruplexer with high isolation and compact size is proposed. The quadruplexer utilizes multi-mode resonators, stepped-impedance resonators, and distributed coupling technique. In this proposed quadruplexer, the first and third passbands are excited in odd modes, and the second and fourth passbands are of even modes. Then, the transmission zeros are controlled to other's channel to achieve high isolation in terms of the enhanced feeding line structures. The quadruplexer occupies only a small area of  $0.049\lambda_0^2$ , and the isolation is better than 31 dB.

[P2-35] 14:20 ~ 16:00

### Investigation of Isotropy for 3-D Metamaterial Bulk Structure 969

Gunyoung Kim, Bomson Lee, Kyung Hee University, Korea

In this paper, we investigate the isotropy of a 3-D metamaterial bulk structure consisting of ring resonators (RR) and thin wires based on the modeling of them using the definition of magnetization and polarization. The presented 3-D metamaterial bulk structure is shown to be synthesized to have the effective permeability and permittivity of near -1 at 8 GHz. Its refractive index is also about -1. The computed Brillouin dispersion diagram also showed that the proposed structure is almost near isotropic. The electrical length of the unit cell, examined based on the Brillouin zone, showed the deviation of about 20%.

## Poster Session II: Passive Components & Systems and Applications

- Date: November 7, 2013 (Thursday)
- Time: 14:20 ~ 16:00
- Room: Room 103

[P2-36] 14:20 ~ 16:00

### A Compressive Sensing Imaging Algorithm for Millimeter-wave Synthetic Aperture Imaging Radiometer in Near-field 972 Jianfei Chen, Yuehua Li, Jianqiao Wang, Yuanjiang Li, Nanjing University of Science and Technology, China

In order to overcome the disadvantage of large data amount and receiver number in near-field passive millimeter-wave synthetic aperture imaging radiometer (PMSAIR), an imaging algorithm based on Compressive Sensing (CS) theory is proposed in this paper. Due to the fact that the brightness temperature distributions of the observed target have a sparse representation in some proper transform domain (such as the spatial finite-differences and wavelet coefficients), we use the CS approach to reconstruct the brightness temperature images from very few visibilities. Thus the amount of data and number of receivers can be further reduced than those traditional methods based on the Fourier transform. The reconstruction is performed by minimizing the Total-Variation norm of brightness temperature image. Finally, the numerical simulation of synthetic aperture imaging demonstrates that the proposed algorithm is an efficient, feasible imaging algorithm for near-field PMSAIR.

[P2-37] 14:20 ~ 16:00

### Direction Finding Fuze Sensor: Assessment in a real scenario 975 Jae-Hyun Choi<sup>1</sup>, Myung-Suk Jung<sup>1</sup>, Kyung-Whan Yeom<sup>2</sup>, <sup>1</sup>Agency for Defense Development, Korea, <sup>2</sup>Chungnam National University, Korea

This paper presents the implementation and assessment of a direction finding proximity fuze sensor for anti-aircrafts or anti-air missiles. A higher rejection of clutter signals is achieved by employing a BPSK (Binary Phase Shift Keying) modulation using Legendre sequence. The direction finding is implemented by comparing received powers from six receiving antennas equally spaced by an angle of 60° around a cylindrical surface. In addition, target detection algorithms have been developed for a robust detection of the target taking the wide variation of target related parameters into considerations. The performances of the developed fuze sensor are experimentally verified by constructing the fuze-specific encounter simulation test apparatus which collects and analyzes reflected signals from a standard target. To assess realistic operation, the fuze sensor was tested using 155 mm gun firing test setup. Through the gun firing test, the successful fuzing range and direction finding performances were demonstrated.

[P2-38] 14:20 ~ 16:00

### A Wide-Band Programmable Radio Frequency Feed Network 978 Sameir Deif<sup>1</sup>, Mohammad S. Sharawi<sup>1</sup>, Elias Ghafari<sup>2</sup>, Daniel N. Aloi<sup>2</sup>, <sup>1</sup>King Fahd University of Petroleum and Mineral, Saudi Arabia, <sup>2</sup>Oakland University, USA

The design and fabrication of a Wide-Band programmable radio-frequency (RF) feed network is proposed. The design architecture is composed of four main stages, switching, phase shifting, amplification/attenuation and control. The proposed feed network is designed to cover a wide band from 2.5 to 6 GHz over two separate paths, one covers from 2.5 to 3 GHz and the other covers 3 to 6 GHz. Digitally controlled phase shifters are used to control the phase. A digital control unit is used to provide the required control signals for all the feed network stages. Digitally controlled wideband variable gain amplifiers are used to set the appropriate amplitude to the signal in both paths. The feed network is simulated and fabricated on an FR-4 substrate with thickness of 0.8mm. Good matching between simulation and measurement results is achieved. The measured amplitude and phase resolutions were approximately 0.55 dB and 6.4°, respectively.

[P2-39] 14:20 ~ 16:00

### Detection of Concealed Objects in Passive Millimeter Wave Imaging based on CS Theory 981 Yilong Zhang, Yuehua Li, Jianfei Chen, Nanjing University of Science and Technology, China

This paper reports development of a passive millimeter wave imaging system for detection of concealed objects using sparse characterization and reconstruction algorithm based on CS theory. By measuring the radiometric temperatures of different objects, passive millimeter wave imaging can acquire images of objects concealed underneath clothing. In this system a millimeter wave antenna controlled by revolving table receives the passive millimeter signal from target object. As passive millimeter wave images have poor contrast and low signal to noise ratio, traditional segmentation algorithms are unable to detect concealed objects, so this system uses a method which transforms the image signal by a non-adaptive base matrix. The high-dimensional signal will be transformed to a lower dimensional space, and then solve an optimization problem for the highest sparsity of the signal through the gradient projection. We present experimental results of 94GHz passive millimeter wave images.

[P2-40] 14:20 ~ 16:00

### A Simple and Efficient Method of Millimeter-wave Image Formation using Back-projection Algorithm 984 Z. Hu<sup>1</sup>, M. F. Karim<sup>2</sup>, L. C. Ong<sup>2</sup>, B. Luo<sup>2</sup>, T. M. Chiam<sup>2</sup>, <sup>1</sup>University of Western Ontario, Canada, <sup>2</sup>Institute for Inforcomm Research, Singapore

This paper presents a simple and efficient method of millimeter-wave image formation using back-projection algorithm. A commercial Vector Network Analyzer transmits and receives a wideband signal centered at 35GHz. The millimeter-wave signal illuminates and reflects off the surface of the target. A widely employed algorithm in computed tomography is used to perform imaging processing, specifically, the back-projection algorithm.

## Poster Session II: Passive Components & Systems and Applications

- Date: November 7, 2013 (Thursday)
- Time: 14:20 ~ 16:00
- Room: Room 103

[P2-41] 14:20 ~ 16:00

**RF Bio-Radar System using a Compact Lumped Six-Port Demodulator and Quadrifilar Helix Antenna 987**  
Han Lim Lee<sup>1</sup>, Dong-Hoon Park<sup>2</sup>, Hyung-Seok Jang<sup>1</sup>, Hyun-Jun Dong<sup>2</sup>, Moon-Que Lee<sup>2</sup>, Jong-Won Yu<sup>1</sup>, <sup>1</sup>Korea Advanced Institute of Science and Technology, Korea, <sup>2</sup>University of Seoul, Korea

This paper presents a bio-radar system using a compact lumped six-port demodulator and a Quadrifilar Helix Antenna (QHA) for remote respiration and heartbeat monitoring. Since bio-radar applications require low power characteristics and six-port structure has an advantage in low power operation, the proposed system is configured with a six-port demodulator replacing active frequency mixers. For the compactness and minimization in size at low frequency applications, the six-port demodulator which consists of three hybrid couplers and a power divider is implemented by lumped elements. Also, the proposed system adopts a QHA module that has high Tx and Rx isolation characteristics. The system performance is verified at 917 MHz by monitoring respiration and heartbeat.

[P2-42] 14:20 ~ 16:00

**An Analog-Based GFSK Demodulator for 60GHz Direct-Conversion Receiver Applications 990**  
Mu-Tsung Lai, Hen-Wai Tsao, National Taiwan University, Taiwan

An analog-based GFSK demodulator for 60GHz direct-conversion receiver is presented. Using a standard 90nm CMOS process, the demodulator successfully achieves demodulation at data rate of 1 Gb/s. At a supply voltage of 1.2 V, the fabricated circuit consumes a dc power of 40 mW with a chip area of 0.78x0.84 mm including the pads.

[P2-43] 14:20 ~ 16:00

**Road Watch Radar System Development 993**  
Jung S. Jung<sup>1</sup>, Chul H. Jung<sup>2</sup>, Jung Kim<sup>1</sup>, Young K. Kwag<sup>1</sup>, <sup>1</sup>Korea Aerospace University, Korea, <sup>2</sup>Solid inc., Korea

Multi-mode road watch radar system has been designed and implemented using pulse Doppler and monopulse technique. This paper gives an overview of RWR system and shows the operation of the system as well as several results. The system operation modes are traffic monitoring and collision avoidance. The algorithms of traffic monitoring are MTI, CFAR, FFT, angle estimation, and tracking. IMTI, pulse integration, and change detection is applied to collision avoidance mode. The field campaign is successfully performed on test highway after validation of system performance. The performance of collision avoidance mode shows 99.9 % of detection probability and 10<sup>-3</sup> of false alarm rate at a distance of 500 m using the reference RCS of 30x30 cm. The tests result of traffic monitoring mode show that RWR detect vehicles at 500m and is possible to lane discrimination at about 350m.

[P2-44] 14:20 ~ 16:00

**Reliable Estimation of Respiration Rate using UWB Impulse Radar 997**  
Jae-Mo Kang<sup>1</sup>, Dong-Woo Lim<sup>1</sup>, Jae-Hwan Lee<sup>1</sup>, Changdon In<sup>1</sup>, Hyung-Myung Kim<sup>1</sup>, Sung-Chul Woo<sup>2</sup>, Cheonsoo Kim<sup>2</sup>, <sup>1</sup>Korea Advanced Institute of Science and Technology, Korea, <sup>2</sup>Electronic and Telecommunications Research Institute, Korea

In this paper, we present a procedure for reliable estimation of the respiration rate using UWB impulse radar. We initially extract the respiratory signal using the energy detector to reduce the effect of the multipath impulse response of the human body. Then, the noise subspace methods are applied to estimate the respiration-rate more accurately. The experimental results show that the proposed method is more reliable than the conventional method.

[P2-45] 14:20 ~ 16:00

**Interference detection using wireless LAN based MIMO transmission 1000**  
Masaaki Kawahara<sup>1</sup>, Kentaro Nishimori<sup>1</sup>, Ryochi Kataoka<sup>1</sup>, Takefumi Hiraguri<sup>2</sup>, Hideo Makino<sup>1</sup>, <sup>1</sup>Niigata University, Japan, <sup>2</sup>Nippon Institute of Technology, Japan

This paper proposes an interference detection method in MIMO transmission, which utilizes periodical preamble signals in a frequency domain. The signals are mapped in only several subcarriers in short preamble signals of IEEE802.11 based OFDM signals and the signal in a frequency domain is transformed by IFFT at the transmitter. We assume the collision due to multiple short preamble signals. In the propose method, second antenna receives the preamble signals while first antenna transmits the preamble signals. The interference can be detected by subtracting the short preamble signal which is multiplied by the estimated channel response using the received signal after the FFT processing. Moreover, we utilize the dual polarization to reduce the mutual coupling between the transmitter and receiver. By a computer simulation, it is shown that the proposed method can successfully detect interference in OFDM signal when the interfering power is greater than the noise power.

## Poster Session II: Passive Components & Systems and Applications

- Date: November 7, 2013 (Thursday)
- Time: 14:20 ~ 16:00
- Room: Room 103

[P2-46] 14:20 ~ 16:00

### Simultaneous Data and Power Transmission in Resonant Wireless Power System 1003

Yong-Ho Son, Byung-Jun Jang, Kookmin University, Korea

A simultaneous digital data and power transmission method in a resonant wireless power transfer system is suggested. Especially, we suggested a new amplitude shift keying (ASK) transmitter architecture, where a drain bias of class E power amplifier is switched alternatively between two voltage levels with respect to input data. The suggested method has a variety of advantages such as simple architecture, easy to adjust of modulation index and duty rate, and constant efficiency characteristics. A maximum 5 W class E power amplifier with the suggested ASK transmitter was designed using a low cost IRF510 power MOSFET at the frequency of 6.78 MHz.

[P2-47] 14:20 ~ 16:00

### Human Detection Based on the Condition Number in the Non-stationary Clutter Environment using UWB Impulse Radar 1006

Changdon In<sup>1</sup>, Dong-Woo Lim<sup>1</sup>, Jae-Mo Kang<sup>1</sup>, Jae-Hwan Lee<sup>1</sup>, Hyung-Myung Kim<sup>1</sup>, Seongdo Kim<sup>2</sup>, Cheonsoo Kim<sup>2</sup>, <sup>1</sup>Korea Advanced Institute of Science and Technology, Korea, <sup>2</sup>Electronics and Telecommunications Research institute, Korea

In this paper, we propose a human detection method in non-stationary clutter environment using ultra-wideband (UWB) impulse radar. We treat the foliage swaying in the wind as the non-stationary clutter. It is observed that the signal from the human body is more correlated than the signal from the non-stationary clutter. The method based on the condition number of correlation matrix is used to distinguish the human from the non-stationary clutter. The experimental results show that the proposed method shows better detection probability than the conventional method.

[P2-48] 14:20 ~ 16:00

### Intelligent Circular Collaborative Beamforming Array in Wireless Sensor Network for Efficient Radiation 1009

N. N. N. Abd Malik, M. Esa, S. K. Yusof, M. K. H. Ismail, S. A. Hamzah, Universiti Teknologi Malaysia, Malaysia

This article presents a novel method of optimizing sensor node location of wireless sensor network (WSN) in a circular arrangement. Appropriate selection of active collaborative beamforming (CB) nodes and cluster are needed each time to perform CB in WSNs. The nodes are modeled in circular array location in order to consider it as a circular antenna array (CAA). This newly proposed intelligent circular sensor node array (ICSA) is further presented to solve the problem. In particular, the selected collaborative nodes and the desired objective can vary significantly. Analyses obtained are compared to those from previous work. The findings demonstrate a better beamforming performance, and the difference is shown in normalized power gain.

[P2-49] 14:20 ~ 16:00

### Turn-on Analysis of Quantum Cascade Lasers 1012

Kelvin S. C. Yong<sup>1</sup>, Manas K. Haldar<sup>1</sup>, Jeffrey F. Webb<sup>2</sup>, <sup>1</sup>Swinburne University of Technology, Malaysia, <sup>2</sup>The University of Nottingham, Malaysia

An analytical analysis on turn-on delay and rise time for quantum cascade laser upon switching on is presented here. Numerical solution for the rate equations is presented and comparison between analytical and numerical solution shows good agreement. Effect of varying injected current value on turn-on delay and rise time is observed. Variation of bias current from zero up to threshold value is used.

[P2-50] 14:20 ~ 16:00

### Advanced Class-S Transmitter with Tri-level Delta-Sigma Modulator 1015

Young-Kyun Cho, Sung Jun Lee, Seung Hyun Jang, Bong Hyuk Park, Jae Ho Jung, Kwang Chun Lee, Electronics and Telecommunications Research Institute, Korea

An advanced Class-S transmitter based on a tri-level delta-sigma modulator (DSM) is presented. The second order DSM shows a signal-to-noise and distortion ratio (SNDR) of 44.7 dB and a spurious-free dynamic range (SFDR) of 63.6 dB with a 3.1-MHz sinusoidal input at 522.24-MHz using an offset cancellation scheme. The proposed technique improves the SFDR and SNDR over 10 dB and 3 dB, respectively. The proposed scheme can effectively control the input referred offset voltage of the DSM, resulting in the improvement of spectrum efficiency. The power consumption of the modulator is 13.4 mW from a 1.2 V supply. Measurements with a mixer show that the proposed modulator modulates a 10-MHz long-term evolution signal which has an 8.5 dB peak-to-average ratio with 3.30 % error vector magnitude and 38.7 dB adjacent channel leakage ratio at 2.6 GHz.

## Poster Session II: Passive Components & Systems and Applications

- Date: November 7, 2013 (Thursday)
- Time: 14:20 ~ 16:00
- Room: Room 103

[P2-51]

14:20 ~ 16:00

### A CMOS Impulse Radar DSP System for Human Detection 1018

Sungchul Woo, Piljae Park, Sungdo Kim, Cheonsoo Kim, Electronics and Telecommunications Research Institute, Korea

The real-time radar system is implemented using a prototype CMOS impulse radar and a DSP (Digital Signal Processor) chip for human detection. Human motions such as walk, breathing are successfully measured. The received signals of the prototype radar at high resolution (1.5 cm) with sufficient SNR are utilized. A commercial DSP chip is used to process received data. The radar signal processing for detecting a walking man and human respiration is proposed. The pulse integration as a part of radar signal processing is used for SNR improvement, also MTI (Moving Target Indicator) processing including maximum detector, comparator and direct coupling rejection is used for increasing detection probability about human target. The experiments on a walking man and human respiration are performed, and measurement results are discussed.

[P2-52]

14:20 ~ 16:00

### Three-dimensional Microwave Breast Imaging using Least Electrical Path Method 1021

Yifan Wang, Amin Abbosh, University of Queensland, Australia

A three-dimensional microwave imaging algorithm using least-electrical-path (LEP) method is presented. The algorithm is designed for the ultra-wideband imaging system for breast cancer detection and localization. By considering the signal refraction on the borders of the imaged breast, this developed algorithm provides an accurate estimation for the pulse delay from a hypothesis point within the imaged region. It, thus, provides an accurate estimation of the tumor's position. The proposed method is validated using full-wave simulations.

[P2-53]

14:20 ~ 16:00

### Generalized MED Blind Deconvolution of GPR Data and Its Sparsity-Promoted Solution 1024

Lianlin Li, Libo Wang, Yunhua Tan, Peking University, China

Over the past decades, numerous efforts have been attempted to enhance the resolution and accuracy of surface ground-penetrating radar (GPR) data by employing blind deconvolution techniques. The fact that most GPR source wavelets utilized in practice are non-minimum phase presents some challenges for blind deconvolution of GPR data. This letter formulates blind deconvolution of GPR data as a sparsity promoted optimization problem, which extends classical minimum entropy deconvolution (MED) strategy and provides a general-purpose framework of blind deconvolution of GPR data. And then an alternating iterative method is explored to solve the derived non-convex optimization problem. Experimental results demonstrate that the proposed methodology is very effective, efficient and flexible.

[P2-54]

14:20 ~ 16:00

### High Gain, Linear, Low Cost Digitally Controlled VHF-UHF Analog Transponder for Nano Satellites 1027

Osman Ceylan, Okan Emre Ozen, Hilal Hilye Canbey, Zehra Gulru Cam, Hasan Bulent Yagci, Istanbul Technical University, Turkey

Nano satellites are generally developed by universities for scientific researches because of low design cost and time. On the other hand a nano satellite has small power and limited volume; therefore there are several restrictions for circuit design. In this project, a digitally controlled VHF to UHF analog transponder is presented for nano satellites. System has -115 dBm receive sensitivity. Output power is 1W at 437.225 MHz with  $\pm 35$  kHz narrow bandwidth. Transponder is controlled by a microcontroller to keep output power stable as 30 dBm (1W) with  $\pm 1.5$ dB ripple. Circuit size is  $9 \times 9$  cm<sup>2</sup> and includes a metal shield. System was verified under space conditions such as vacuum and very high and low temperature. Circuit is pin to pin compatible with other commercial nano satellite devices' structure.

[P2-55]

14:20 ~ 16:00

### Isolation Analysis of Correlator Mixer for Digital Frequency Discriminator Error Improvement 1030

Won Choi<sup>1,2</sup>, Kyung Heon Koo<sup>1</sup>, <sup>1</sup>Incheon National University, Korea, <sup>2</sup>Victek Co., Ltd., Korea

This paper has presented the design of a phase correlator for digital frequency discriminator (DFD) that operates in the 2.0 to 6.0GHz frequency range. The frequency discrimination accuracy of the DFD with the isolation of correlator mixer are analyzed, and it is shown that LO-RF isolation has much effect on frequency discrimination error by deriving relating equations between LO-RF isolation and phase performance. More than 5.7° phase error and 1.27MHz frequency error will be happened from less than 20dB LO-RF isolation. The RMS phase error of the designed phase correlator is 4.57° and the frequency accuracy is 1.02MHz.



## Poster Session II: Passive Components & Systems and Applications

- Date: November 7, 2013 (Thursday)
- Time: 14:20 ~ 16:00
- Room: Room 103

[P2-56]

14:20 ~ 16:00

### Study on Measuring Cholesterol Level using Microwaves 1033

Yamato Kudo, Suguru Nakamura, Yoshio Nikawa, Kokushikan University, Japan

The glucose and cholesterol level is indicated as value of vital signs. This invasive measurement needs blood sample and cause a pain of the body as heavy burden to the patient. In this paper, reflection method which is applied for noninvasive microwave measurement for cholesterol is studied using microwaves. The cholesterol was dissolved in ethanol and make cholesterol solution. Relative permittivity and dielectric loss have measured and evaluated. Regression line is made to simplify the relation between the relative permittivity and dielectric loss versus cholesterol concentration, it become clear.

[P2-57]

14:20 ~ 16:00

### Design of Multiple Receiver for Wireless Power Transfer using Metamaterial 1036

Sungje Lee, Sanghwan Kim, Chulhun Seo, Soongsil University, Korea

In this paper, we analyze the characteristics of Wireless Power Transfer (WPT) between a transmitter coil and four receiver coils. There are different results such as efficiencies when we use one transmitter coil for one receiver coil and four receivers. The size of transmitter coil is 300mm×310mm×5mm. And size of receiver coil is 50mm×64mm×2mm. Operating frequency is 13.56MHz, distance between transmitter coil and receiver coil is 50mm. we simulate different number of receiver coil. There is big change in efficiency, depending on the distance between a receiver coil and others receiver coils. Characteristics of efficiency decrease as the number of the receiver is increased can be seen. In this case of a transmitter coil and receiver coil, efficiency is 60.6%. However, in the case of the transmitter coil and four receiver coils, the efficiency is about 20% after tuning. We have improved efficiency about 20% using metamaterial.

[P2-58]

14:20 ~ 16:00

### Omni-directional Circularly Polarized Microstrip Antenna using Dual-Patch Radiators 1039

Indu Jiji Rajmohan<sup>1</sup>, Nasimuddin<sup>2</sup>, Arokiaswami Alphones<sup>1</sup>, <sup>1</sup>Nanyang Technological University, Singapore, <sup>2</sup>Institute of Infocomm Research, Singapore

A circularly polarized microstrip antenna with omnidirectional radiation pattern is proposed using coplanar waveguide feed. The antenna consists of dual-patch radiators and in between a single feed. The design includes back to back configuration of radiating patches with respect to the ground plane. The metallic patches include circular slots and rectangular slots, where the slots in the metallic patches in the back to back arrangement appear as mirror images. The antenna is optimized for circularly polarized omnidirectional radiation. The antenna is prototype and measured. The measured axial ratio (AR) < 3dB is obtained in all direction over a 3-dB AR bandwidth with gain of 2.31 dBic. The measured results showed that the proposed design exhibit good CP characteristics in the omnidirectional radiation.

## [T3A] Sub-mm-wave and mm-wave Integrated Circuits

- Date: November 7, 2013 (Thursday)
- Time: 16:30 ~ 18:20
- Room: Room A (Room 101)
- Session Chairs: Chinchun Meng (National Chiao Tung University)  
Munkyo Seo (Sungkyunkwan University)
- 

[T3A-1]

16:30 ~ 17:00

### [Invited] Resonant Tunneling Diodes for Room-Temperature Terahertz Oscillators 345

Masahiro Asada, Safumi Suzuki, Tokyo Institute of Technology, Japan

Our recent results of THz oscillators using GaInAs/AlAs resonant tunneling diodes (RTDs) are reported. For high frequency oscillation, the dwell time in the resonant tunneling structure was reduced by a narrow well, and a fundamental oscillation up to 1.31 THz with the output power of 10  $\mu$ W was achieved at room temperature. Higher frequency is expected with the structures reducing both of the dwell time and collector transit time. For high output power, coherent power combining was demonstrated in a two-element array, and 610 $\mu$ W at 620 GHz was obtained. Spectral linewidth of a few megahertz and a frequency change with bias voltage were also obtained. Direct intensity modulation with bias voltage and wireless data transmission were investigated, and a transmission rate of 3 Gbps with the bit error rate of  $3 \times 10^{-5}$  was obtained in a preliminary experiment at 540 GHz.

[T3A-2]

17:00 ~ 17:20

### 135GHz CMOS Small-Signal Amplifier with Power-Efficient Bias Method 348

Mizuki Motoyoshi, Kyoya Takano, Kosuke Katayama, Minoru Fujishima, Hiroshima University, Japan

A 135GHz CMOS wideband amplifier is proposed with high power efficiency to achieve a high-speed D-band wireless receiver. The proposed amplifier was fabricated with standard 1P12M 40nm CMOS technology. From measurement, the peak gain is 25dB with the power consumption was 140mW with a supply voltage of 1.1V. The amplifier achieved figure of merits of 27fJ. As a result, the performance characteristics required to realize a low-power front-end amplifier for a D-band wireless receiver were obtained.

[T3A-3]

17:20 ~ 17:40

### A Wideband 215 - 255 GHz CB Differential Amplifier in a 0.25- $\mu$ m SiGe HBT Technology 351

Daekeun Yoon<sup>1</sup>, Namhyung Kim<sup>1</sup>, Ullich Pfeiffer<sup>2</sup>, Bernd Heinemann<sup>3</sup>, Jae-Sung Rieh<sup>1</sup>, <sup>1</sup>Korea University, Korea, <sup>2</sup>University of Wuppertal, Germany, <sup>3</sup>IHP GmbH, Germany

A wideband amplifier operating beyond 200 GHz has been developed in a 0.25- $\mu$ m SiGe HBT technology. The common-base (CB) amplifier consists of 5 differential stages and a pair of Marchand balun to allow single-ended S-parameter measurement. The amplifier shows a flat gain over 215 - 255 GHz, leading to a 3-dB bandwidth of 40 GHz with a peak gain of 10 dB. It consumes a total DC power of 153 mW with a 1.5 V supply voltage. The fabricated chip occupies an area of 400 $\times$ 600  $\mu$ m<sup>2</sup> including pads and baluns.

[T3A-4]

17:40 ~ 18:00

### A Broadband Amplifier MMIC with 105 to 140 GHz bandwidth 354

S. Diebold<sup>1</sup>, P. Pahl<sup>1</sup>, S. Wagner<sup>2</sup>, H. Massler<sup>2</sup>, A. Tessmann<sup>2</sup>, A. Leuther<sup>2</sup>, T. Zwick<sup>1</sup>, I. Kallfass<sup>3</sup>, <sup>1</sup>Karlsruhe Institute of Technology, Germany, <sup>2</sup>Fraunhofer Institute for Applied Solid-State Physics, Germany, <sup>3</sup>University of Stuttgart, Germany

A compact and broadband high-gain millimetre-wave monolithic integrated circuit (MMIC) amplifier has been developed. It employs an advanced power combining approach allowing for broadband designs. At 115GHz it provides a gain of 22 dB and at 125 GHz an output power of 10.4 dBm. Its 3 dB gain bandwidth spans from 105 to 140 GHz leading to an absolute (B) and relative (b) bandwidth of 35GHz and 29 %, respectively.

[T3A-5]

18:00 ~ 18:20

### A Low-power 71GHz-band CMOS Transceiver Module with on-board Antenna for Multi-Gbps Wireless Interconnect 357

Kensuke Nakajima<sup>1</sup>, Akihiro Maruyama<sup>1</sup>, Tadamasu Murakami<sup>1</sup>, Masato Kohtani<sup>1</sup>, Tsuyoshi Sugiura<sup>1</sup>, Eiichiro Otobe<sup>1</sup>, Jaejin Lee<sup>2</sup>, Shinhee Cho<sup>2</sup>, Kyusub Kwak<sup>2</sup>, Jeongseok Lee<sup>2</sup>, Minoru Fujishima<sup>3</sup>, Toshihiko Yoshimasu<sup>4</sup>, <sup>1</sup>Samsung R&D Institute Japan, Japan, <sup>2</sup>Samsung Electronics Corp., Korea, <sup>3</sup>Hiroshima University, Japan, <sup>4</sup>Waseda University, Japan

Fully integrated millimeter-wave transceiver ICs using 65nm CMOS technology and on-board antenna for high-speed/short-range wireless communication system are described. To realize high-speed and low power consumption for a mobile application, a simple transceiver architecture with non-coherent amplitude shift keying (ASK) modulation method is adopted. The transceiver ICs are flip-chip bonded on boards and connected with on-board antenna for a simple and low cost transceiver system. The developed transceiver system module demonstrates 5Gbps/3.8Gbps at wireless communication range of 5mm/10mm and power consumption of 79.6mW with a carrier frequency of 71GHz. To our best knowledge, this is the first report of a millimeter-wave, above 60GHz, CMOS transceiver module with on-board antenna for a high-speed/short-range wireless communication system.

## [T3B] Balun, Coupler and Combiners II

- Date: November 7, 2013 (Thursday)
- Time: 16:30 ~ 18:10
- Room: Room B (Room 102)
- Session Chairs: Yi-Hsin Pang (National University of Kaohsiung)  
Jong-Chul Lee (Kwangwoon University)

[T3B-1]

16:30 ~ 16:50

### Miniaturized Branch-Line Coupler with Coupling-Dependent Dual-Frequency Operation 360

Tse-Yu Chen, Pei-Ling Chi, Ting-Tsan Lin, National Chiao Tung University, Taiwan

A miniaturized branch-line coupler that is able to operate at two arbitrary frequencies is presented in this paper. The dual-band frequency ratio depends on the coupling coefficient in the proposed transmission line element. It will be shown later that the dual-band separation decreases as the coupling strength increases. By replacing the traditional quarter-wavelength lines with the proposed artificial transmission lines of a prescribed coupling coefficient, a size-reduced branch-line coupler can be implemented at dual frequencies of interest. An example of the 0.9- and 1.8-GHz branch-line coupler, which corresponds to a band ratio of 2, is experimentally developed and characterized. The presented coupler occupies only 44% footprint of the conventional coupler operating at the lower frequency of the dual-band operation. Excellent agreement between the simulated and measured results is obtained.

[T3B-2]

16:50 ~ 17:10

### Design of a Compact Ultra Wideband Balanced-to-Balanced Power Divider/Combiner 363

Hoa Thai Duong<sup>1</sup>, Hoang Viet Le<sup>2</sup>, Anh Trong Huynh<sup>2</sup>, Nhan Tran<sup>1</sup>, Efstratios Skafidas<sup>1,2</sup>, <sup>1</sup>University of Melbourne, Australia, <sup>2</sup>National ICT Australia, Australia

A compact ultra wideband balanced to balanced powerdivider/combiner based on Finite Ground Coplanar Waveguide (FGCPW) phase inverter is presented in this paper. By replacing the  $\lambda/2$  transmission lines in [1] by FGCPW phase inverters, circuit size of the power divider/combiner has been significantly reduced, from  $(0.75\lambda \times 0.5\lambda)$  to about  $(0.375\lambda \times 0.125\lambda)$ . With the wideband property of the FGCPW phase inverter, 3-dB fractional bandwidth of the proposed power divider/combiner can be obtained up to 200%. A -3.7 dB differential mode transmission coefficient  $|S_{ddAB}|$  and -0.25 dB common mode reflection coefficients  $|S_{ccAA}|$ ,  $|S_{ccBB}|$  have been obtained. Other mixed mode S-parameters are all less than -10 dB from 0.1 GHz to 1.75 GHz. The measurement results agreed well with the simulation results.

[T3B-3]

17:10 ~ 17:30

### A 5 GHz, Integrated Transformer based, Variable Power Divider Design in CMOS Process 366

Man-Chum J. Chik, Wei Li, Kwok-Keung M. Cheng, The Chinese University of Hong Kong, Hong Kong

This paper presents, for the first time, the realization of CMOS power divider with variable dividing ratio. Size reduction is attained by the adoption of lumped-LC networks based on on-chip capacitors and integrated differential transformers. The proposed design offers a tuning range of about 9dB with standard CMOS tuning diodes and low control voltage. For demonstration, both simulated and measured results of a 5GHz variable power divider implemented using 0.35 $\mu$ m CMOS process are shown.

[T3B-4]

17:30 ~ 17:50

### Filtering Power Divider for Differential Input and Output Signals 369

Chiau-Ling Huang, Yi-Hsin Pang, National University of Kaohsiung, Taiwan

A power divider with differential input and output ports is proposed in this paper. The proposed powerdivider consists of three coupled resonators and exhibits a bandpass filter response. Good frequency selectivity could hence be obtained. A 2.45-GHz differentially operated power divider has been fabricated on an RO4003C substrate and measured by a vector network analyzer. The measured data as well as the simulated results show that the power divider has a better frequency selectivity compared with a traditional one. From the simulated current distribution, the differential operation at the output ports with the differentially input signal could be validated.

[T3B-5]

17:50 ~ 18:10

### Generalized, Miniaturized, Dual-band Wilkinson Power Divider with Series RLC Circuit 372

Xiaolong Wang<sup>1,2</sup>, Iwata Sakagami<sup>3</sup>, Atsushi Mase<sup>1</sup>, <sup>1</sup>Kyushu University, Japan, <sup>2</sup>University of Tsukuba, Japan, <sup>3</sup>University of Toyama, Japan

In this paper, a generalized, miniaturized, dual-band Wilkinson power divider consisting of series RLC circuit and two-section transmission lines is presented. A coupled-line section is introduced for miniaturization under the assumptions of linear phase characteristics and equal phase velocities of the even- and odd-modes. Experimental results for miniaturized power divider showed good agreement with theoretical results.

## [T3C] Biomedical Applications

- Date: November 7, 2013 (Thursday)
- Time: 16:30 ~ 18:20
- Room: Room C (Room 104)
- Session Chairs: Zhongxiang Shen (Nanyang Technological University)  
Nam Kim (Chungbuk National University)
- 

[T3C-1]

16:30 ~ 17:00

### [Invited] Microwave Active Integrated Probes for Biomedical Applications 375

Kihyun Kim, Namgon Kim, Sung-Hyun Hwang, Taeyoon Seo, Yong-Kweon Kim, Youngwoo Kwon, Seoul National University, Korea

This paper introduces recently developed active integrated probes for biomedical applications. To realize broadband cancer detection and low-power cancer ablation, planar-type coaxial probes have been integrated with active circuits for measurement and microwave generation, respectively. A multi-state reflectometer (MSR) is employed for cancer detection based on broadband permittivity characteristics. Also, to achieve microwave hyperthermia, a Ku-band microwave source is integrated on the probe platform. Each active integrated probe is implemented on a single silicon platform using Microelectromechanical Systems (MEMS) and monolithic microwave integrated circuit (MMIC) technologies for miniaturization and integration. Through the experiments, the feasibilities of the active integrated probes for microwave cancer detection and ablation have been validated.

[T3C-2]

17:00 ~ 17:20

### Coherent Time Reversal Minimum Variance Beamforming for the Localization of Tissue Malignancies in Dense Breast Phantoms 377

Md. Delwar Hossain, Ananda Sanagavarapu Mohan, University of Technology Sydney, Australia

The time reversal (TR) based minimum variance beamforming, both the standard capon beamforming (SCB) and robust capon beamforming (RCB) techniques for microwave imaging of breast for early stage breast cancer detection is considered in this paper. The performance of coherent signal subspace processing for TR-SCB and TR-RCB techniques is investigated. We have used anatomically realistic numerical breast phantoms in FDTD simulations. We consider 2D sagittal slice of the breast phantom in 2D FDTD simulation. Our simulation results indicate that coherent signal subspace processing significantly improves the performance of TR based minimum variance beamforming techniques.

[T3C-3]

17:20 ~ 17:40

### Complex Rational Function for Frequency Dependent Complex Permittivity of Biological Tissues 380

Sang-Gyu Ha<sup>1</sup>, Sungmin-Park<sup>1</sup>, Eunki Kim<sup>1</sup>, Kyung-Young Jung<sup>1</sup>, Yong Bae Park<sup>2</sup>, <sup>1</sup>Hanyang University, Korea, <sup>2</sup>Ajou University, Korea

In this work, we accurately characterize frequency dependent complex permittivity of biological tissues in the frequency range from 100 kHz to 10 GHz. Toward this purpose, a fourth-order complex rational function (CRF) is employed for dispersive modeling of the relative permittivity of biological tissues. We also discuss how to improve the accuracy of their dispersion characteristics.

[T3C-4]

17:40 ~ 18:00

### Quick SAR Measurement System by 2D Array E-field Sensors 383

Yoon-myung Gimm<sup>1</sup>, Youngjun Ju<sup>2</sup>, Sungtek Kahng<sup>3</sup>, Yuri Lee<sup>2</sup>, Seungbae Lee<sup>2</sup>, <sup>1</sup>Dankook University, Korea, <sup>2</sup>EMF Safety Inc., Korea, <sup>3</sup>Incheon National University, Korea

The safety on human body against electromagnetic fields radiating from mobile devices has been investigated for a long time. The measurement method of RF power absorption to human body from wireless devices usually adopted robot scanning in the phantom in the past. But it takes a very long time to evaluate the SAR value of a mobile device. In this paper, a quick SAR measurement system using a 2D array of E-field probes having 3 axes isotropic characteristics is proposed. It is possible to fast estimate the volume SAR by a software with the 2D surface SAR data acquired by arrayed probes deleting robot moving time.

[T3C-5]

18:00 ~ 18:20

### Synthetic-Bandwidth Microwave System for Breast Imaging 386

Yifan Wang, Amin Abbosh, University of Queensland, Australia

A multi-channel ultra-wideband (UWB) system that employs the method of bandwidth synthesizing is presented. The method provides an effective solution to mitigate the challenges on UWB antenna's implementation. The proposed system operates across the band 3.0-10.0 GHz using three broadband antennas designed to cover three sub-bands (channels). The scattered signals captured by the three antennas are combined and used to form an internal image of the human breast for cancerous tumor detection and localization. The infrastructure of the proposed imaging system and the frequency-domain image reconstruction algorithm are illustrated with an analysis of the signal propagation model. The feasibility of the system is verified by two-dimensional finite-difference time-domain (FDTD) simulations conducted on heterogeneous dispersive breast model.

## [T3D] Mobile and Indoor Propagation

- Date: November 7, 2013 (Thursday)
- Time: 16:30 ~ 18:10
- Room: Room D (Room 105)
- Session Chairs: Yoshihide Yamada (National Defense Academy)  
Kyung-Young Jung (Hanyang University)
- 

[T3D-1] 16:30 ~ 16:50

### Fast FDTD Analysis of MIMO Channel using Spread Spectrum Technique 389

Kazuma Ouchida, Naoki Honma, Yoshitaka Tsunekawa, Iwate University, Japan

This paper proposes fast FDTD (Finite-Difference Time-Domain) analysis method that uses simultaneous excitation for multi-antenna systems. In this method, spread spectrum technique is employed for maintaining the orthogonality among the excited signals. Excitation signals are generated by multiplying the spreading codes that are different to each other. By assigning the different spreading codes to all transmitting antennas, the channels from multiple transmitting antennas to receiving antenna(s) can be calculated simultaneously. The simulation of a 2x2 multi-antenna system shows that the results of the proposed method agree well with those of the conventional method even though its computation speed is two times higher than that of the conventional method.

[T3D-2] 16:50 ~ 17:10

### Evaluation of Terminal Position Estimation by Position Fingerprinting Technique using Array Antenna 392

Mayu Ohtani, Hisato Iwai, Hideichi Sasaoka, Doshisha University, Japan

We experimentally evaluate the performance of the position estimation of wireless terminals by a position fingerprint method based on propagation properties. We adopt artificially-generated variation of received signal strength by array antennas. We carry out indoor experiment using the method and evaluate the estimation performance quantitatively.

[T3D-3] 17:10 ~ 17:30

### Study on Short-Range MIMO Transmission using Interference Cancellation by Antenna Directivities 395

Maki Arai, Tomohiro Seki, Ken Hiraga, Tadao Nakagawa, Kazuhiro Uehara, NTT corporation, Japan

In this paper, a simple method for canceling interference by using antenna directivities is proposed for short-range transmission systems. For higher data transmission systems the millimeter-wave frequency bands are useful because of their wide bandwidths. Also, Multiple-Input Multiple-Output (MIMO) technology can be applied to these bands because the application enables channel capacity to be increased by using multiple antennas at the transmitter and receiver without expanding the frequency bandwidth. However, since MIMO transmission schemes are complicated we consider parallel transmission, a simple method for transmitting multiple data streams that is suitable for short-range MIMO transmission. We propose a simple method for canceling interference by using antenna directivities and improving channel capacity in parallel transmission. Numerical analysis shows that the method maximizes channel capacity at the optimal spacing  $L^{\text{opt}} = 2\lambda_0$ . It is also found that the channel capacity of the method is 14 % higher than that of Eigenmode beamforming (EM-BF) for two transmission streams and 12 % higher for four streams.

[T3D-4] 17:30 ~ 17:50

### Quiet Zone Evaluation from Nonredundant Rectilinear Data for Trireflector Compact Antenna Test Range 398

Cheng Yang<sup>1</sup>, Junsheng Yu<sup>1</sup>, Yuan Yao<sup>1</sup>, Xiaoming Liu<sup>1</sup>, Xiaodong Chen<sup>2</sup>, <sup>1</sup>Beijing University of Posts and Telecommunications, China, <sup>2</sup>University of London, UK

The quiet zone performance of a tri-reflector Compact Antenna Test Range is evaluated by an efficient sampling strategy with rectilinear plane scanning. The method relies on the nonredundant sampling expression of the scattered fields and the optimal sampling interpolation. An evenly stepping sampling based on the nonredundant sampling is also adopted considering the difficulty of practical scanning. In the modeling of the source, a convenient aperture model is used. Numerical results are presented, showing that the performance of quiet zone can be evaluated by a remarkably reduced number of sampling points, which indicates that the measurement time can be efficiently decreased.

[T3D-5] 17:50 ~ 18:10

### Analytic Derivation of Mutual Impedance between Two Arbitrarily Located and Slanted Dipoles using Effective Length Vector 401

Jung-Hoon Han, Won-Young Song, Kyoung-Sub Oh, Noh-Hoon Myung, Korea Advanced Institute of Science and Technology, Korea

Antenna mutual coupling is a significant issue for the mobile communications system, near field communications system, to improve communication capacity and so on. Therefore, the accurate analysis of the mutual coupling between antennas is very important. Accordingly, calculating the mutual impedance of dipoles has been studied in cases of co- and non- planar skew. This paper proposes an exact and simple method for analyzing the mutual impedance between two arbitrarily located and slanted dipoles using the effective length vector (ELV) and derives its closed form solution as well. The proposed formula is verified by numerical tool and gives good agreement.

## [T3E] Lumped and Transmission Elements

- Date: November 7, 2013 (Thursday)
- Time: 16:30 ~ 18:10
- Room: Room E (Room 203)
- Session Chairs: Dal Ahn (Soonchunhyang University)  
Young Yun (Korea Maritime University)

[T3E-1] 16:30 ~ 16:50

### A New Comb Slow Wave CPW for on Chip Area Reduction and its RLCG Model 404

Øystein Bjørndal, Kristian Gjertsen Kjelgråd, University of Oslo, Norway

A compact low impedance transmission line in 90nm CMOS is presented. The new comb slow wave grounded coplanar waveguide (comb-S-GCPW) is modeled, simulated and fabricated. Model is a simple and analytic RLCG equivalent circuit. The model agrees well with simulation and measurements in 90nm CMOS. Measurements show a relative dielectric constant of 141 for a 12:3Ω comb slow wave line, compared to 44:7 at 23:6Ω without fingers.

[T3E-2] 16:50 ~ 17:10

### A Study on Bandwidth of Meander Line Employing Periodic Ground Structure for Application to Miniaturization of RF Components on GaAs MMIC 407

Jang-Hyeon Jeong, Sung-Jo Han, Ki-Jun Son, Jeong-Hoon Kim, Young Yun, Korea Maritime University, Korea

In this work, the meander line employing periodic ground structure (MLEPGS) was fabricated on GaAs substrate for application to a miniaturization of RF components on MMIC, and its bandwidth characteristics were thoroughly investigated for the first time. According to measured results, the MLEPGS exhibited the wavelength much shorter than conventional meander line. Concretely, the wavelength of the MLEPGS with  $T$  of 20 μm was 1.19 mm at 5 GHz, which was 16 % of the conventional meander line. We also studied the bandwidth of the passband and stopband from the  $\beta d$ -kd graph of the MLEPGS. According to the result, the MLEPGS could be employed for application to a miniaturized RF components up to Ka band. Above results indicate that the MLEPGS is a promising candidate for application to a miniaturization of RF components in microwave range.

[T3E-3] 17:10 ~ 17:30

### A Simple Millimeter-wave Transformer between Microstrip Line and Post-Wall Waveguide 411

Yusuke Uemichi<sup>1</sup>, Ryouhei Hosono<sup>1</sup>, Ning Guan<sup>1</sup>, Jiro Hirokawa<sup>2</sup>, Makoto Ando<sup>2</sup>, <sup>1</sup>Fujikura Ltd., Korea, <sup>2</sup>Tokyo Institute of Technology, Japan

We propose a new transformer between microstrip line and post-wall waveguide fabricated on liquid-crystal polymer substrates. Matching to 50 Ω impedance is accomplished by a combination of a through-hole with an anti-pad and open-ended stubs. The bandwidth of the transformer for a reflection smaller than -15 dB is 8 GHz. The estimated loss of the transformer associated with the mode conversion and the measured loss of the PWW is 0.45 dB and 0.1 dB/mm at 60 GHz, respectively.

[T3E-4] 17:30 ~ 17:50

### A Study on Basic RF Characteristics of Transmission Lines Employing Various Types of Ground Structures on Silicon Substrate for a Decision of Optimal Periodic Ground Structure 414

Sung-Jo Han, Jang-Hyeon Jeong, Ki Jun Son, Yonng Yun, Korea Maritime University, Korea

In this paper, various types of transmission lines employing the periodically arrayed ground structure (PAGS) were fabricated on silicon substrate, and their RF characteristics were thoroughly investigated for a decision of optimal structure design. According to the results, with-contact showed wavelength shorter than other types of transmission lines and insertion loss value lower than other types of transmission lines. In addition, with-contact showed effective permittivity and propagation constant value higher than other types of transmission lines. Above results indicate that the with-contact is most appropriate for application to a miniaturization of RF components on silicon substrate.

[T3E-5] 17:50 ~ 18:10

### New Approach to Electronic Band Gap Filtering Structures Combining Microstrip and Dielectric Resonators 417

Bahareh. Moradi<sup>1</sup>, Ursula. Martinez-Iranzo<sup>1</sup>, Oriol. Ymbert<sup>1</sup>, Cynthia. Martinez<sup>2</sup>, Julian Alonso<sup>1</sup>, Joan Garcia-Garcia<sup>1</sup>, <sup>1</sup>Autonomous University of Barcelona, Spain, <sup>2</sup>Institute of Integrative Nanosciences, Germany

A novel design combining standard microstrip technology with single ring resonator and high dielectric constant resonator for design of low and band pass filtering electromagnetic band gap(EBG) structures, operating in the range from 1 to 20 GHz is presented in this paper. The design is based on a high dielectric constant resonator embedded in a microstrip structure substrate. The dielectric resonator is fabricated by using commercial high dielectric constant EPOXY paste in a process compatible with serigraphy and screen printing technology.

## [T3F] Printed Antennas

- Date: November 7, 2013 (Thursday)
- Time: 16:30 ~ 18:10
- Room: Room F (Room 208)
- Session Chairs: Hisato Iwai (Doshisha University)  
Ikmo Park (Ajou University)

[T3F-1]

16:30 ~ 16:50

### Effects of Filling Factor on near Field Transmit Properties for a Dual-row Array at 300 MHz 420 Mikhail Kozlov, Robert Turner, Max Planck Institute for Human Cognitive and Brain Sciences, Germany

We evaluated the performance of purely cylindrical and conical-cylindrical non-overlapped dual-row near-field head arrays with radiative elements of axial length 70 and 80 mm. Increasing the filling factor using a conical row does not ensure an increase of the RF magnetic field averaged over the entire human brain. For the geometries, excitation conditions and volume of interest that were investigated, the conical shape resulted in an intrinsic reduction of safety excitation efficiency.

[T3F-2]

16:50 ~ 17:10

### Array of Subarrays using Adaptive Element Patterns 423 Mohammed M. Albannay, Jacob C. Coetzee, Dhammika Jayalath, Queensland University of Technology, Australia

This paper explores the use of subarrays as array elements. Benefits of such a concept include improved gain in any direction without significantly increasing the overall size of the array and enhanced pattern control. The architecture for an array of subarrays will be discussed via a systems approach. Individual system designs are explored in further details and proof of principle is illustrated through a manufactured examples.

[T3F-3]

17:10 ~ 17:30

### A Dual Planar Inverted-F Antenna with Isolation Enhancement for Wireless USB Dongle 426 Hsien Kang Tseng, Powen Hsu, National Taiwan University, Taiwan

A dual planar inverted-F antenna (PIFA) with isolation enhancement for wireless USB dongle is proposed. The antenna, which consists of two identical PIFAs, is used for multiple-input-multiple-output (MIMO) system. The two PIFAs are allocated to the top and bottom layers of the USB dongle respectively, and are merged together through two vias connected to the ground planes to enhance the antenna isolation. The antenna structure is very simple and suitable for small USB dongles. Good isolation is obtained in the frequency band of 2.5-2.69GHz for IEEE 802.16e worldwide interoperability for microwave access (WiMAX) applications. Details of the design and simulation results are presented and discussed.

[T3F-4]

17:30 ~ 17:50

### Frequency Reconfigurable Switchable Koch Fractal Dipole Employing Harmonic Traps 429 S. A. Hamzah, M. Esa, N. N. N. Abd Malik, M. K. H. Ismail, Universiti Teknologi Malaysia, Malaysia

Embedding fractal technology into an antenna provides desirable reduction of its physical size, as well as increasing its operating bandwidth and directivity. Nevertheless, the embedment of fractals is associated with proportionate increase of undesired harmonic problems associated with higher order modes of the antenna. In this paper, a microwave fractal dipole antenna that has tunable capability of a reconfigurable operation within an observed range of 400 MHz to 3.5 GHz is presented. Harmonic traps in the form of open-circuit linear short stubs are employed to eliminate each undesired harmonic of higher order mode. In addition, a small size linear tapered balun is employed at the antenna feed to improve the impedance match. This technique is suitable for developing reconfigurable antenna with harmonic suppression or for single band antennas. The antenna prototype can be tuned can be tuned from 691 MHz, 725 MHz, 743 MHz, 865 MHz, to 3010 MHz at a time. At the same time the antenna can suppress undesired harmful harmonic frequencies present from 1.8 GHz to 3.5 GHz within the observed range. Simulation and measurement results obtained are in good agreement, which have confirmed the design concept.

[T3F-5]

17:50 ~ 18:10

### Slotted Dual Band Directive Antenna with Defected Ground Plane Structure 432 M. Z. M. Nor, S. K. A. Rahim, M. I. Sabran, M. S. A. Rani, Universiti Teknologi Malaysia, Malaysia

WLAN is one of the common term that being used as many researchers where WLAN is one of the application that allows long range communication unwired. With the combination of slots in radiating element, and parabolic slotted shape at the ground plane, proposed antenna can operate at two sets of WLAN application band and their main beam can be directed at  $-62^\circ$  and  $-43^\circ$  at 2.45 GHz and 5.8 GHz respectively. Proposed antenna is suit to be used in WLAN application such in Bluetooth, Wi-Fi and access point (AP) application.

## [F1A] Power Amplifiers

- Date: November 8, 2013 (Friday)
- Time: 09:00 ~ 10:20
- Room: Room A (Room 101)
- Session Chairs: Renato Negra (Aachen University)  
Youngoo Yang (Sungkyunkwan University)

[F1A-1]

09:00 ~ 09:20

### Envelope-Tracking Power Amplifier with Enhanced Back-Off Efficiency using Average Switch Current Control of Supply Modulator 435

Jooseung Kim<sup>1</sup>, Dongsu Kim<sup>1</sup>, Yunsung Cho<sup>1</sup>, Daehyun Kang<sup>2</sup>, Bumman Kim<sup>1</sup>, <sup>1</sup>Pohang University of Science and Technology, Korea, <sup>2</sup>Broadcom Corporation, USA

This paper presents an envelope-tracking power amplifier (ET PA) for handset applications with enhanced efficiency at a back-off power region. The supply modulator consists of a linear regulator and switching converter. The supply of the linear regulator is boosted to 5 V and that of the switching converter is directly connected to a battery, forming a power management IC. Since the supply voltages of the two amplifiers are asymmetric, the average switch current level is not properly adjusted by itself according to the envelope level. For the optimum operation over the entire power region, average switch current level is adjusted by detecting the input envelope level. For a 10-MHz long term evolution signal with a 6.5 dB peak-to-average power ratio, the proposed supply modulator delivers a peak voltage of 4.5 V to a 6.5  $\Omega$  load with a measured efficiency of 76.2 %. At an average output power of 27 dBm, the proposed ET PA delivers a power-added efficiency (PAE) of 40.7 %, which is 8.6 % higher than that of a stand-alone PA. In the back-off power region, the PAE is improved by up to 2.8 % and 10.7 % compared to the conventional ET PA and stand-alone PA, respectively.

[F1A-2]

09:20 ~ 09:40

### MMICs and Front End Module Design with Selectively Anodized Aluminum Substrate 438

Kichul Kim<sup>1</sup>, Kyoungmin Kim<sup>2</sup>, Songcheol Hong<sup>1</sup>, <sup>1</sup>KAIST, Korea, <sup>2</sup>Wavenics, Inc., Korea

Highly integrated front end module (FEM) using selectively anodized aluminum substrate was proposed and designed from 2.3 GHz to 2.5 GHz for WiMAX/Wibro applications. It consists of a MMIC power amplifier (PA), a MMIC SPDT switch, and a LPF with integrated passive device (IPD) on the substrate. The PA and the SPDT switch were designed with 2  $\mu$ m GaAs HBT process and 0.5  $\mu$ m InGaAs pHEMT process, respectively. The performance of the PA is comparable with commercial WiMAX products. The FEM has the gain of 30.3 dB and EVM of 2.6 % at 23 dBm FEM linear output power with the help of aluminum substrate's good thermal dissipation, and its compact size is 4x5 mm<sup>2</sup>.

[F1A-3]

09:40 ~ 10:00

### A Triple-Band CMOS Class-E Power Amplifier for WCDMA/LTE Applications 441

Hyuk Su Son, Woo Young Kim, Joo Young Jang, Inn Yeal Oh, Chul Soon Park, KAIST, Korea

This paper presents a fully integrated triple-band CMOS class-E power amplifier (PA) for WCDMA (1.9 GHz) and LTE (1.8 GHz and 2.6 GHz) applications. The triple-band operation is achieved by activating selectively transistor cells and matching the transistor cells with low/high-band on-chip transformers for the three different frequencies. The PA is fabricated using a 0.18- $\mu$ m CMOS process and has a chip size of 1.5x1.85 mm<sup>2</sup> including matching networks and transformers. This PA obtains output powers of 27.8/28.1/27.4 dBm at 1.8/1.9/2.6GHz in continuous wave (CW) modes, respectively. The PA implemented to hybrid-EER structure satisfied the ACLR requirements up to 21 dBm for WCDMA (1.9 GHz) and up to 18 dBm and 16.3 dBm for LTE (1.8 GHz and 2.6 GHz) without any linearization technique.

[F1A-4]

10:00 ~ 10:20

### Achieving Linearity for Outphasing Amplifiers Targeting LTE Applications and Beyond 444

Thomas M. Hone, Ahmed Farouk Aref, Junqing Guan, Renato Negra, RWTH Aachen University, Germany

This paper analyses the impact of the level locations in a multi-level LINC transmitter on the obtainable linearity performance. Results show that by placing levels in the upper dynamic region of outphased signals, a linearity performance suitable for LTE applications and beyond can be achieved. A multi-level LINC transmitter with 5 levels is implemented using 10W GaN CREE devices at 1.9GHz. A 10dB PAPR 1.4MHz LTE signal is decomposed for outphasing and recombined to achieve an ACPR performance of -50dBc while delivering 2W average output power.



## [F1B] Waveguide Filters

- Date: November 8, 2013 (Friday)
- Time: 09:00 ~ 10:20
- Room: Room B (Room 102)
- Session Chairs: Zhewang Ma (Saitama University)  
Hyeong-Seok Kim (Chung-Ang University)

[F1B-1] 09:00 ~ 09:20

### A Cutoff-Waveguide Bandpass Filter using Antiresonant Elements for Sharp Passband Skirt and Wide Stopband Characteristics 447

Masataka Ohira, Takaaki Matsumoto, Zhewang Ma, Saitama University, Japan

The dual-behavior resonator used for waveguide and microstrip filters has an advantage that multiple transmission zeros (TZs) can be generated by its antiresonances, but has a problem that bandwidth of upper stopband is narrow owing to its spurious resonances. To suppress the undesired resonances, a compact cutoff-waveguide filter introducing a new resonance mechanism is proposed. The bandpass filter is simply constructed by successive arrangement of planar antiresonant elements in a cutoff waveguide. Both the resonance and the antiresonance are produced by the antiresonant elements with the help of intrinsic inductive elements of the cutoff waveguide. As an example, a bandpass filter having high skirt selectivity because of TZs, low insertion loss at the passband, high attenuation and a wide bandwidth at the stopbands is designed at X band. The effectiveness of the filter is verified by numerical and experimental demonstrations.

[F1B-2] 09:20 ~ 09:40

### Pseudo-Elliptic Substrate Integrated Waveguide Filters with Higher-Order Mode Resonances 450

Mehdi Salehi<sup>1,2</sup>, Jens Bornemann<sup>1</sup>, Esfandiar Mehrshahi<sup>2</sup>, <sup>1</sup>University of Victoria, Canada, <sup>2</sup>Shahid Beheshti University, Iran

Two substrate integrated waveguide (SIW) pseudo-elliptic bandpass filters are presented that utilize higher-order mode cavities. In the first filter, two full-wave  $TE_{102}$  resonators and two fundamental  $TE_{101}$  resonators in a compact structure are properly coupled to generate two transmission zeros in a four-pole SIW filter. The coupling matrix of the structure with a center frequency of 10 GHz and 200 MHz bandwidth is designed, and good agreement is achieved with simulations of two commercially available field solvers. In the second topology, by using symmetric inductive discontinuities and two rectangular SIW cavities,  $TE_{102}$  and  $TE_{301}$  modes are excited and generate two transmission zeros, one on each side of the passband. This dual-mode SIW filter with a center frequency of 10 GHz and bandwidth of 300 MHz has been prototypes, and the measured data are in good agreement with results obtained from the coupling matrix and CST Microwave Studio.

[F1B-3] 09:40 ~ 10:00

### Power Handling Prediction for Waveguide Harmonic Filters with Complex Geometry 453

Fabrizio De Paolis, Felice Maria Vanin, European Space Research and Technology Centre, The Netherlands

Previous work on field/voltage analysis in microwave filters is extended to cover the critical case of harmonic filters with complex geometry. It is shown here that filter power handling capability can be predicted with a fully analytical method, even for complex waveguide devices such as evanescent-mode ridged and waffle-iron filters. Very good agreement with numerical and measured data is obtained.

[F1B-4] 10:00 ~ 10:20

### Silicon-Based Substrate-Integrated Waveguide-Based Tunable Band-Pass Filter using Interdigital MEMS Capacitor 456

Hyunseong Kang, Somarith Sam, Ik-Jae Hyun, Chang-Wook Baek, Sungjoon Lim, Chung-Ang University, Korea

A novel method for designing miniaturized tunable BPF filter is proposed on the basis of the SIW technology. By loading MEMS cantilevers on the metal fingers' surface of the IDC, passband of the filter can be differently generated. The proposed structure allows relatively independent control the center frequency and the coupling coefficient. This filter is showing advantages in terms of compact size, good selectivity and stopband rejection, as well as the easy integration capability with other circuits. The proposed filter has the continuously tuning range between 23.6 GHz and 25.6 GHz with insertion between 4.59 dB to 4.13 dB.

## [F1C] Special Session: Wireless Power Transfer and Applications

- Date: November 8, 2013 (Friday)
- Time: 09:00 ~ 10:40
- Room: Room C (Room 104)
- Session Chairs: Shinohara Naoki (Kyoto University)  
Bomson Lee (Kyung Hee University)

[F1C-1]

09:00 ~ 09:25

### [Invited] Wireless Power Transfer Technology using Magnetic Field Resonance 459 Joungho Kim, Jonghoon Kim, Chiuk Song, Hongseok Kim, KAIST, Korea

This paper describes the basic principles of wireless power transfer technology based on magnetic field resonance. In addition, we introduce applications including the LED TV, OLEV, and HH-RM CCC Charger. In order to demonstrate the advantages of the coil structure with the ferrimagnetic material and metallic shielding, magnetic field distributions and the electrical performance of three different coil structures were investigated via 3D electromagnetic (EM) field solver and SPICE simulation. In addition, EMF and electromagnetic field radiation were measured and analyzed

[F1C-2]

09:25 ~ 09:50

### [Invited] WPT, RFID and Energy Harvesting: Concurrent Technologies for the Future Networked Society 462 L. Roselli, F. Alimenti, G. Orecchini, C. Mariotti, P. Mezzanotte, M. Virili, University of Perugia, Italy

The increasing attention of ICT community towards Internet of Things (IoT) is leading to the need of optimizing the management of an amount of information that grows with the addition of more objects connected to the internet. In this paper we will focus on the challenges that this scenario is inspiring and will dare suggest an holistic vision to look for solutions respectful of the environment.

[F1C-3]

09:50 ~ 10:15

### [Invited] The S-band Multi-Stage Amplifier for Single-Tone and Time-Division Microwave Communication and Power Transmission 465

Shigeo Kawasaki<sup>1</sup>, Satoshi Yoshida<sup>1</sup>, Yuta Kobayashi<sup>1</sup>, Takumasa Noji<sup>1</sup>, Makoto Ono<sup>2</sup>, Yukio Moriguchi<sup>2</sup>, Shigeki Furuta<sup>2</sup>, <sup>1</sup>Japan Aerospace Exploration Agency, Japan, <sup>2</sup>NEC Network and Sensor Systems, Ltd., Japan

The multi-stage GaN amplifier with dual output power was explained for the application of microwave communication and power transmission. For the compact transmitter, single-tone and time-division operation is adopted in this study. The maximum output power of 91.8 W and the PAE around 55.4 % were obtained at 2.1 GHz in the high power transmitter operation. In the low power transmitter operation, the 4Mbps symbol-rate QPSK signal was achieved under the 19.2 W with 35 % PAE. By combining with a multi-stage rectifier in the receiver, the compact microwave communication and power transmission system can be realized.

[F1C-4]

10:15 ~ 10:40

### [Invited] Future Wireless Power Transportation System 468 Seungyoung Ahn, Dong-Ho Cho, Korea Advanced Institute of Science and Technology, Korea

The wireless power transfer technology is a recent hot issue for microwave engineers and power electronics engineers. The application expands from the portable mobile devices in the market to the solar power satellite in the future. The transportation system is one of the promising markets for wireless power transfer technology because people want safer, cheaper, and more convenience transportation which matches to the target of wireless power transfer technology. In this paper, we review electric characteristics of the wireless charging electric vehicle and evaluate the cost effectiveness of the small-battery system. The application of wireless power transfer technology to railway system is analyzed in the view of energy cost and stability.

## [F1D] Antennas for Vehicle, Satellite, Military Applications I

- Date: November 8, 2013 (Friday)
- Time: 09:00 ~ 10:50
- Room: Room D (Room 105)
- Session Chairs: Arokiaswami Alphones (Nanyang Technological University)  
Se-Yun Kim (Korea Institute of Science and Technology)

[F1D-1] 09:00 ~ 09:30

### [Invited] Substrate Integrated Waveguide and its applications to Leaky Wave Antennas 470

A. Alphones<sup>1</sup>, Manisha Mujumdar<sup>1</sup>, Cheng Jin<sup>2</sup>, <sup>1</sup>Nanyang Technological University, Singapore, <sup>2</sup>Institute of Microelectronics, Singapore

Substrate Integrated Waveguide has been an emerging technology for the realization of microwave and millimeter wave regions. It is the planar form of the conventional rectangular waveguide. It has profound applications at higher frequencies, since prevalent platforms like microstrip and coplanar waveguide have loss related issues. This paper discusses basic concepts of SIW, design aspects and their applications to leaky wave antennas. A brief overview of recent works on Substrate integrated Waveguide based Leaky Wave Antennas has been provided.

[F1D-2] 09:30 ~ 09:50

### Analysis of Cross-Borehole Pulse Radar Signatures on a Half Water-Filled Tunnel 473

Ji-Hyun Jung, Se-Yun Kim, Korea Institute of Science and Technology, Korea

The effect of the water collected in the bottom of an empty tunnel on cross-borehole radar signatures is analyzed using the finite-difference time-domain (FDTD) method. The cross-borehole pulse radar is represented by 3-dimensional model and B-scan images are calculated in two cases of fully air-filled and half water-filled tunnels. The first positive peak in the B-scan image appears in a later time and moves upward direction than the tunnel center as the water is collected in tunnel. To estimate the central position of the half water-filled tunnel, the first negative peak is adopted here and its utility is described clearly.

[F1D-3] 09:50 ~ 10:10

### Analysis of a Carbon Fibre Reinforced Polymer Slotted Waveguide Array Fed by a Loop Type End Launcher 476

A. Bojovschi, N. Shariati, K. Ghorbani, RMIT University, Australia

The investigations of an end-launcher transition in Carbon Fibre Reinforced Plastic (CFRP) WR90 waveguides is presented. The applicability of the feed for CFRP slotted waveguide antenna is addressed. Some of the aspects pertaining to the efficiency of CFRP slotted waveguide antenna and its use for radar applications are discussed. The results are presented in comparison with those obtained from the same concepts implemented in aluminium waveguides. A recently implemented anisotropic model for CFRP laminates, which describes the electrical anisotropy of the composite material, was used. The data obtained provide promising indicators for the potential use of slotted waveguide antennas made of CFRP for radar applications.

[F1D-4] 10:10 ~ 10:30

### Design of 2-axis Gimbal Spaceborne X-band Antenna for High Data Rate Payload Transmission 479

Sae-Han-Sol Cheong<sup>1</sup>, Tae-Hong Kim<sup>1</sup>, Jin-Mi Jung<sup>2</sup>, Sang-Gyu Lee<sup>3</sup>, Yong-Hoon Kim<sup>1,2</sup>, <sup>1</sup>Gwangju Institute of Science and Technology, Korea, <sup>2</sup>Millisys Inc., Korea, <sup>3</sup>Korea Aerospace Research Institute, Korea

The space borne X-band 2-axis gimbal antenna needs frequency re-uses techniques by dual circular polarization for the very high data transmission. The gimbal antenna consists of 2-axis driving mechanism, high efficient horn antenna, very low loss non-contact type RF transmission line of coaxial type rotary joint. This paper designed high efficient horn antenna and very low loss non-contact type RF transmission line of coaxial type rotary joint and 2-axis driving mechanism.

[F1D-5] 10:30 ~ 10:50

### Ferrite Loaded Tunable SIW Slot Antenna 482

Li-rong Tan<sup>1,2</sup>, Rui-xin Wu<sup>1</sup>, Cong-yi Wang<sup>1</sup>, <sup>1</sup>Nanjing University, China, <sup>2</sup>Nanjing College of Information Technology, China

This work proposes a design of novel magnetically tunable substrate integrated waveguide (SIW) slot antenna with one ferrite slab loaded in the antenna. The operation frequency of the antenna can be tuned more than 380 MHz in the X-band from 9.32 to 9.70 GHz when the bias magnetic field changes from 0 to 0.12 tesla. Within the tunable frequency range, antenna gain is more than 6 dBi. The radiation patterns and the gain are almost not affected by the changing of applied magnetic field, showing a good high gain antenna with frequency tunable feature.

## [F1E] Band Pass Filters

- Date: November 8, 2013 (Friday)
- Time: 09:00 ~ 10:00
- Room: Room E (Room 203)
- Session Chairs: Atsushi Sanada (Yamaguchi University)  
Dal Ahn (Soonchunhyang University)

[F1E-1]

09:00 ~ 09:20

### Wideband Bandpass Filters with High Passband Selectivity using SAW-like Resonators 485 Xiaoming Lu, Koen Mouthaan, Yeo Tat Soon, National University of Singapore, Singapore

A wideband bandpass filter (BPF) using two cascaded sections, each consisting of a SAW-like resonator and one or two transmission lines, is proposed. The lower and higher transitions of the passband are separately defined by the SAW-like resonators. The roll-off at the band edges can be controlled by properly designing the SAW-like resonators to achieve a highly selective passband. As an example, a prototype BPF centered at 0.42 GHz is implemented on PCB, in which the SAW-like resonators are realized by lumped elements. The measured filter has a 3-dB bandwidth of 47% and high passband selectivity is observed. To obtain a wideband rejection, one transmission line in the filter is loaded with an open stub and a low pass filter is added. Experimental results show good high out-of-band rejection up to more than 20 GHz.

[F1E-2]

09:20 ~ 09:40

### A Ka-Band Lumped Element Dual-Behavior Resonator (DBR) Filter in Standard 0.13- $\mu\text{m}$ CMOS Technology 488 Xiaoming Lu, Koen Mouthaan, Yeo Tat Soon, National University of Singapore, Singapore

A  $K_a$ -band lumped element Dual-Behavior Resonator (DBR) filter in 0.13- $\mu\text{m}$  CMOS is presented. The DBR filter consists of Dual-Behavior Resonators (DBRs) and inverters connecting the DBRs. The inverters and the DBRs, which define the stopband transmission zeros, are realized by CMOS spiral inductors and metal-insulator-metal (MIM) capacitors. A second order DBR filter with two transmission zeros is designed and fabricated in standard 0.13- $\mu\text{m}$  CMOS technology. The measured filter has a 3-dB bandwidth of 15% at the center frequency of 27.8 GHz. High rejections larger than 48 dB are realized at the two transmission zero frequencies of 20.2 GHz and 37 GHz.

[F1E-3]

09:40 ~ 10:00

### Ultra Sharp Roll-off Bandpass Filter Design for near Pass-band RFI Mitigation 491 Yoon S. Chung, Alex Dunning, Mark A. Bowen, CSIRO Astronomy and Space Science, Australia

This paper presents the design of a compact, suspended microstrip line, bandpass filter with precision Radio-Frequency Interference (RFI) mitigation capability. The presence of strong RFI adjacent to the lower-end of the operating band of the recently upgraded Australia Telescope Compact Array (ATCA) 1-3 GHz cryogenic receiver systems necessitated the development of a band defining filter with a very sharp roll-off characteristic. A bandpass filter with a null for RFI mitigation has been developed and deployed in the newly upgraded 1-3 GHz band receivers. We adopt the image parameter method with  $m$ -derived filter section for filter design to obtain very sharp roll-off characteristics for near pass-band RFI mitigation.

## [F1F] Digital RF

- Date: November 8, 2013 (Friday)
- Time: 09:00 ~ 10:40
- Room: Room F (Room 208)
- Session Chairs: Noriharu Suematsu (Tohoku University)  
Byung-Sung Kim (Sungkyunkwan University)

[F1F-1] 09:00 ~ 09:20

### Transconductance-tunable Radio-Frequency Digital-to-Analog Converter for Dual-Mode Frequency Translating $\Delta$ Ms 494 Dongmin Kang<sup>1</sup>, So Young Kang<sup>2</sup>, Hi Yuen Song<sup>1</sup>, Hyunseok Choi<sup>1</sup>, Inn Yeal Oh<sup>1</sup>, Chul Soon Park<sup>1</sup>, <sup>1</sup>KAIST, Korea, <sup>2</sup>Samsung Electronics, Korea

In this paper, a Transconductance(gm)-tunable Radio-Frequency Digital-to-Analog converter (RFDAC) that used in Frequency Translating Delta-Sigma Modulator (FTDSM) is presented. The proposed RFDAC can support dual-mode operation for FTDSM. To guarantee the linear gm control, constant current density technique is used. To verify the RFDAC, the prototype of 4th order FTDSM is fabricated using a 90 nm CMOS process and measured in the laboratory. The measured SNDR for 800 MHz/1.6 GHz dual mode operation was 43 dB and 44 dB for each.

[F1F-2] 09:20 ~ 09:40

### A Current-Mode FIR-Filter-Based Receiver Front-End For Blocker Filtering 497 Duksoo Kim, Byungjoon Kim, Junhyuk Choi, Sangwook Nam, Seoul National University, Korea

A digital RF receiver front-end employing a FIR(Finite Impulse Response) filter is proposed for SAW-less receiver architecture, where the large out-of-band interferer can be rejected selectively by using a scalable frequency response property of FIR filter. The FIR filter, followed by the transconductor stage and current-commutating passive mixer, operates in current domain to improve the linearity. Also, the clock generator circuit can be simplified by making the FIR filter operate with 8-phase clock signal. The designed receiver front-end is fabricated using UMC 0.13  $\mu$ m CMOS process. The chip shows unwanted blocker rejection over 80 dB, with good linearity of +3.94 dB  $IP_3$ .

[F1F-3] 09:40 ~ 10:00

### Direct RF Under Sampling Reception Method with Lower Sampling Frequency 500 Daliso Banda, Osamu Wada, Tuan Thanh Ta, Suguru Kameda, Noriharu Suematsu, Kazuo Tsubouchi, Tohoku University, Japan

In conventional RF under sampling front ends the sampling frequency is greater than the anti-aliasing filter's bandwidth, which is usually larger than the desired signals bandwidth. In this paper a technique for lowering the sampling frequency required for an RF under sampling receiver is presented. Mathematical expressions to ensure that signal integrity is preserved have been derived. Using these expressions the minimum sampling frequency required is halved. To validate the technique, simulation and measurement of a front-end using the conventional and the proposed techniques has been performed. In the simulation conventional and proposed techniques both achieved an SNR of 33.5dB. The measured SNR for the conventional technique was 19.8dB and 20.3dB for the proposed. Using QPSK modulation the EVM was measured to be -19.8dB for the conventional and -19.5dB for the proposed techniques.

[F1F-4] 10:00 ~ 10:20

### Design of a Capacitive DAC Mismatch Calibrator for Split SAR ADC in 65 nm CMOS 503 Anh Trong Huynh<sup>1</sup>, Hoa Thai Duong<sup>2</sup>, Hoang Viet Le<sup>1</sup>, Efstratios Skafidas<sup>1,2</sup>, <sup>1</sup>National ICT Australia, Australia, <sup>2</sup>University of Melbourne, Australia

This paper presents the design and implementation of a capacitive digital to analog converter (CDAC) mismatch calibrator used in split successive approximation resistor (SAR) analog to digital converter (ADC) in a 65 nm complementary metal oxide semiconductor (CMOS) process. The calibrator adopts a compensation capacitor connected to the least significant bit (LSB) capacitor array to calibrate the mismatch between the lowest-bit capacitor of the most significant bit (MSB) array and the LSB array. An 11-bit 50-MS/s split SAR ADC using this calibrator was developed. The measurement results show that the calibration process improves the differential nonlinearity (DNL) value from -1.2/+1.9 LSBs to -0.55/+0.75 LSBs and the integral nonlinearity (INL) value from -1.9/+2.12 LSBs to -0.95/+0.99 LSBs. The calibrated ADC achieves a signal to noise and distortion ratio (SNDR) of 58.95 dB near the Nyquist frequency and an effective number of bits (ENOB) of 9.5 bits.

[F1F-5] 10:20 ~ 10:40

### A Design Technique for a High-speed SAR ADC using Non-binary Search Algorithm and Redundancy 506 Toru Okazaki, Daisuke Kanemoto, Ramesh Pokharel, Keiji Yoshida, Haruichi Kanaya, Kyushu University, Japan

This paper presents a design technique of minimizing time for each bit decision and adding appropriate redundancy bits. The technique helps the design of a SAR ADC. We show that the conversion time of proposed SAR ADCs can get faster than that of conventional ones by using the technique.

## [F2A] Special Session: Sub-mm-wave and Terahertz Technologies

- Date: November 8, 2013 (Friday)
- Time: 11:10 ~ 12:50
- Room: Room A (Room 101)
- Session Chairs: Tadao Nagatsuma (Osaka University)  
Jae-Sung Rieh (Korea University)

[F2A-1]

11:10 ~ 11:35

### [Invited] Sub-mm-wave Technologies: Systems, ICs, THz Transistors 509

M. J. W. Rodwell, University of California, USA

mm-wave and sub-mm-wave outdoor communications links have high available bandwidth and can support multiple independent spatial transmission channels but suffer from extremely high worst-case foul-weather attenuation. Link analysis suggests that several useful systems can be realized using power amplifiers with ~50-200 mW output power, low-noise amplifiers with ~4-7 dB noise figure, and arrays of ~64-128 elements. Such systems can be realized with Si VLSI beamformers, InP HEMT LNAs, and InP HBT or GaN HEMT power amplifiers

[F2A-2]

11:35 ~ 12:00

### [Invited] CMOS Sources and Detectors for Sub-Millimeter Wave Applications 512

Dongha Shim<sup>1</sup>, Yaming Zhang<sup>2,3</sup>, Ruonan Han<sup>4</sup>, Dae Yeon Kim<sup>2</sup>, Youngwan Kim<sup>2</sup>, Shinwoong Park<sup>2</sup>, Zeshan Ahmad<sup>2</sup>, Eun-Young Seok<sup>5</sup>, Kenneth K. O.<sup>2</sup>, <sup>1</sup>Seoul National University of Science & Technology, Korea, <sup>2</sup>The University of Texas, USA, <sup>3</sup>Samsung Electronics, USA, <sup>4</sup>Cornell University, USA, <sup>5</sup>Texas Instruments Inc., USA

An integrated chain composed of an 195-GHz oscillator with frequency doubled output at ~390 GHz followed by two cascaded  $\pm 2$  injection locked frequency dividers with output frequency of ~49 GHz is demonstrated in 45-nm CMOS. The peak power radiated at ~390 GHz by an on-chip antenna is ~2  $\mu$ W. This work indicates it is possible to phase-lock sub-millimeter wave signals in CMOS. Polysilicon Gate separated Schottky diodes that can be fabricated without any process modifications in a foundry 130-nm CMOS process are utilized to implement 280-GHz and 860-GHz detectors for imaging. A fully-integrated 280-GHz 4x4 imager array exhibits measured NEP of 29pW/Hz<sup>1/2</sup> and responsivity of 5.1kV/W (323V/W without the amplifier). The 860-GHz detector without an amplifier achieves responsivity of 273V/W and NEP of 42pW/Hz<sup>1/2</sup>.

[F2A-3]

12:00 ~ 12:25

### [Invited] Graphene Materials and Devices for Terahertz Science and Technology 515

Taiichi Otsuji, Maki Suemitsu, Victor Ryzhii, Tohoku University, Japan

This article reviews recent advances in graphene-based materials and devices for terahertz science and technology. The fundamental basis of the optoelectronic properties of graphene is first introduced. Then the synthesis and crystallographic characterization of graphene materials, particularly focused on the authors' original heteroepitaxial graphene-on-silicon technology, are briefly described. Then nonequilibrium carrier relaxation and recombination dynamics in optically or electrically pumped graphene is discussed to introduce the possibility of negative dynamic conductivity toward the creation of graphene terahertz lasers. Unique terahertz dynamics of the two-dimensional plasmons in graphene are also addressed.

[F2A-4]

12:25 ~ 12:50

### [Invited] Technology Demonstrators for Low-cost Terahertz Engineering 518

Stepan Lucyszyn, Fangjing Hu, William J. Otter, Imperial College London, UK

There is no doubt that terahertz (THz) technology is rapidly growing in interest. Its frequency range lies in a commercially unexploited part of the electromagnetic spectrum. Front-end systems operating in the THz gap, i.e. frequency range between where the performance of conventional electronics falls off and that of photonics increases, have generally existed for expensive scientific applications and have relied on precision free-space (quasi-)optics and often cryogenic cooling. However, in order to move away from less profitable high-end applications, engineering solutions are needed to create a positive spiral of technological growth with more profitable ubiquitous applications. This review paper introduces recent examples of THz technologies that may have the potential for future commercial exploitation.

## [F2B] Multi-Mode Band-Pass Filters

- Date: November 8, 2013 (Friday)
- Time: 11:10 ~ 12:50
- Room: Room B (Room 102)
- Session Chairs: Hung-Wei Wu (Kun Shan University)  
Sungtek Kahng (Incheon National University)

[F2B-1]

11:10 ~ 11:30

### Design of Planar Dual-Band Bandpass Filters With Stepped-Impedance Resonators 521

Liang-Ying Chen<sup>1</sup>, Ching-Wen Tang<sup>1</sup>, Chien-Tai Tseng<sup>1</sup>, Yuan-Chih Lin<sup>2</sup>, <sup>1</sup>National Chung Cheng University, Taiwan, <sup>2</sup>Metal Industries Research & Development Centre, Taiwan

Novel planar dual-band bandpass filters with stepped-impedance resonators have been proposed. The central frequency of dual passbands can be easily controlled by the stepped-impedance resonators. Moreover, two stepped-impedance open stubs can generate transmission zero between two passbands, therefore the isolation can be increased. With the proposed structure, additional transmission zeros will appear around two passbands. In addition, the match between measurement and the theoretical simulation validates the proposed structure.

[F2B-2]

11:30 ~ 11:50

### Compact Microstrip Dual-Mode Dual-Wideband Bandpass Filter For GPS/WiMAX Application 524

Jin Xu, Wen Wu, Nanjing University of Science and Technology, China

This paper presents a novel dual-mode dual-wideband bandpass filter (BPF) structure. The proposed structure exhibits two resonant modes in each passband and two transmission zeros located at the lower side of the first passband and the upper side of the second passband. There is a transmission zero between two passbands, which can improve the band-to-band isolation. As an example, a dual-mode dual-wideband BPF centered at 1.59/3.51 GHz with 3 dB fractional bandwidth of 32%/16% is designed and fabricated. The fabricated filter has the compact size of  $0.07\lambda_g \times 0.17\lambda_g$ . Good agreement can be observed between the simulation and the measurement.

[F2B-3]

11:50 ~ 12:10

### Design of Compact Tri-Band Bandpass Filter using Multilayer Substrate Technique 527

Yu-Fu Chen<sup>1</sup>, Shih-Hua Huang<sup>2</sup>, Hung-Wei Wu<sup>2</sup>, Hsin-Ying Lee<sup>1</sup>, <sup>1</sup>National Cheng Kung University, Taiwan, <sup>2</sup>Kun Shan University, Taiwan

In this paper, the compact tri-band bandpass filter (BPF) using multilayer substrate technique is presented. The filter is designed at 2.4 GHz, 3.5 GHz and 5.2 GHz. The multilayered filter consists of the cross-shaped stepped-impedance resonator (CS-SIR) on the top layer for generating the 1st passband and two T-shaped stepped-impedance resonators (TS-SIR) on the bottom layer for generating the 2nd and 3rd passband, respectively. The transmission zeros at each passband skirts can be controlled by tuning the proposed resonators. The measured results are in good agreement with the full-wave electromagnetic (EM) simulation results.

[F2B-4]

12:10 ~ 12:30

### Triple-Passband Bandpass Filter with Wide Stopband Based on Microstrip-to-Defected Stepped Impedance Resonator (SIR) Structure 530

Yung-Wei Chen<sup>1</sup>, Guan-Syun Chen<sup>2</sup>, Hung-Wei Wu<sup>2</sup>, Yan-Kuin Su<sup>1,2</sup>, <sup>1</sup>National Cheng Kung University, Taiwan, <sup>2</sup>Kun Shan University, Taiwan

In this paper, we proposed the new triple-passband bandpass filter (BPF) with wide stopband based on the microstrip-to-defected stepped impedance resonator (SIR) structure. The proposed filter is composed of the coupled stub-loaded stepped impedance resonators (SL-SIR) on the top layer and the defected SIR structures etched off on the ground plane. By using the proposed structure, the center frequencies of the filter are designed to 1.575 / 1.8 / 2.45 GHz and the wide stopband range can be obtained around -30 dB from 3 to 11 GHz. The improved passbands selectivity is obtained since the transmission zeros are located at each passband edges. The simulated and measured results have a good agreement with the proposed design concept.

[F2B-5]

12:30 ~ 12:50

### Miniaturized Dual Wideband Bandpass Filter with Coupled Ladder Structure 533

Tai-Yi Chen, Yi-Hsin Pang, National University of Kaohsiung, Taiwan

A dual wideband filter utilizing a coupled ladder structure has been proposed in this paper. With the ladder structure which exhibits a slow-wave property, the size of the filter could be reduced. In addition, two additional transmission zeros were obtained due to the coupled ladder structure. Good frequency selectivity was achieved. The proposed circuit has been fabricated on a RO4003C substrate and could be operated at 1.82 GHz and 4.0 GHz. The measured fractional bandwidth are around 70.8% and 20.4% for return loss larger than 10 dB. The circuit occupied a small area which is around  $0.08 \lambda \times 0.314 \lambda$  at 1.86 GHz. Both the simulated and measured data are displayed and validate the operation of the filter.

## [F2C] Microwave Sensing

- Date: November 8, 2013 (Friday)
- Time: 11:10 ~ 12:50
- Room: Room C (Room 104)
- Session Chairs: Xiuping Li (University of Posts and Telecommunications Beijing)  
Ikuo Awai (Ryutech Corporation)

[F2C-1]

11:10 ~ 11:30

### Proximity Coupled Vital Sign Sensor Based on Phase Locked Loop Under Injection 536

Byung-Hyun Kim<sup>1</sup>, Yunseog Hong<sup>1,2</sup>, Yong-Jun An<sup>1</sup>, Sang-Gyu Kim<sup>1</sup>, Gi-Ho Yun<sup>3</sup>, Jong-Gwan Yook<sup>1</sup>, <sup>1</sup>Yonsei University, Korea, <sup>2</sup>Samsung Thales, Korea, <sup>3</sup>Sungkyul University, Korea

In this paper, a phase locked oscillator under injection is designed with proximity vital sign sensor at 2.4 GHz. The proposed system is composed of a sensor oscillator with a planar resonator, a phase locked loop (PLL) synthesizer, and a voltage controlled oscillator (VCO). The planar resonator functions not only as a series feedback component to an oscillator but also as a detector which measures respiration and heartbeat signal. The input impedance of the planar resonator varies according to a distance between the human body and the planar resonator. This impedance variation changes the oscillation frequency of the sensor oscillator. The sensor oscillator injects its output into the VCO so that the VCO is locked to the sensor oscillator's frequency. At last, the PLL puts out control voltage to the VCO to prevent frequency from shifting by vital signs. Therefore, the VCO control voltage mirrors vital signs. Measurement results prove that this sensor can detect vital sign up to 40 mm away from a subject.

[F2C-2]

11:30 ~ 11:50

### Specific Absorption Rate in Human Fetus with Fetal Growth for RF Far-Field Exposure 539

Tomoaki Nagaoka<sup>1</sup>, Tetsu Niwa<sup>2</sup>, Soichi Watanabe<sup>1</sup>, <sup>1</sup>National Institute of Information and Communications Technology, Japan, <sup>2</sup>Tokai University School of Medicine, Japan

The adverse health effects of radio-frequency electromagnetic fields have become of increasing concern. We conducted a specific absorption rate (SAR) dosimetry study of pregnant females and their fetuses at various gestational ages. We developed novel pregnant female models with anatomically realistic fetal and gestational tissues at 20, 26, and 29 weeks of pregnancy. In this paper, we present the modeled SAR characteristics of pregnant females and their fetuses exposed to vertically and horizontally polarized EM waves from 30 MHz to 3 GHz at the three gestational ages.

[F2C-3]

11:50 ~ 12:10

### Saw-Tooth Shaped Legs Birdcage RF Coil for Small Animal NMR Imaging at 1.5T MRI System 542

Jung-Min Kim, Sheikh Faisal Ahmad, Ick Chang Choi, Young Cheol Kim, Hyun Deok Kim, Kyungpook National University, Korea

In this paper we are demonstrating a novel method of designing and implementing a modified birdcage type Radio Frequency (RF) coil for small animal Nuclear Magnetic Resonance (NMR) imaging. This RF coil is basically a band pass type birdcage coil which is specifically designed to perform the whole body NMR imaging of small animal at 1.5T MRI systems. The designed RF coil contains the saw tooth shaped pattern as the leg conductors. The magnetic field produced at 63.85 MHz resonance frequency by this designed saw toothed shaped leg pattern RF coil is significantly stronger than the magnetic field produced by a conventional straight leg band pass type birdcage coil designed with the same dimension. A full wave 3D electromagnetic simulation is carried out to optimize the RF coil dimensions, capacitor values and to study the RF coil electromagnetic characteristics.

[F2C-4]

12:10 ~ 12:30

### Study of Earthquake Location using Electromagnetic Precursors 545

Yi Wang, Xiao Yuan, Qunsheng Cao, Nanjing University of Aeronautics and Astronautics, China

A technique to locate earthquake hypocenters using extremely low frequency (ELF) electromagnetic (EM) precursors is proposed. This technique relies on recording EM eruptions caused by underground physical mechanisms during the earthquake preparing process. Using the triangulation algorithm and the attenuation rate of EM waves in the Earth-ionosphere system, the source (usually the earthquake hypocenter) can be located. During the locating process, the attenuation rate of EM waves in local regions is modified in order to improve accuracy of result. Based on this technique, simulations are carried out using the geodesic finite difference time-domain (G-FDTD) method. Results show that the locating error is within one cell of the FDTD method.

[F2C-5]

12:30 ~ 12:50

### Reactive Near-Field to Near-/Far-Field Transformation in Semi-Anechoic Chamber 548

Soon-Soo Oh, Young Seung Lee, Sang-Bong Jeon, Seun-Keun Park, Woo-Jin Byun, Hyung-Do Choi, ETRI, Korea

In this paper, the technique of the reactive near-field to near-/far-field transformation has been proposed. The different thing compared with the previous work is that the semi-anechoic chamber with the ground plane was assumed during the transformation. The sources of electronic device are reconstructed from the detected reactive near-field. And then, the composite array source using the image theory is built, and then the transformation from the composite source to the near-/far-field are performed. For the verification, the simulated results have been utilized, and their results show small errors. Therefore, the proposed technique in this paper could be applied to predict the radiated field at 3 m or 10 m without the expensive large semi-anechoic chamber.



## [F2D] Antennas for Vehicle, Satellite, Military Applications II

- Date: November 8, 2013 (Friday)
- Time: 11:10 ~ 12:50
- Room: Room D (Room 105)
- Session Chairs: Toshikazu Hori (University of Fukui)  
Jaehoon Choi (Hanyang University)

[F2D-1] 11:10 ~ 11:30

### RF Transmit Robustness of Dual-row MRI Array at 300 MHz 551

Mikhail Kozlov, Robert Turner, Max Planck Institute for Human Cognitive and Brain Sciences, Germany

We evaluated the performance of overlapped 8 and 16 channel dual-row near-field arrays with radiative elements of axial length 90 mm, after optimization of both array circuit and near-field behavior at 297.2 MHz. For each number of channels, an array performance measure was evaluated for four human head-and-torso model positions and three circuit level optimization strategies. For both channel numbers, this measure was very similar when "mode" or power reflected by the entire array based optimizations were applied. Reducing the array channel simplified array construction, at the cost of an intrinsic reduction of safety excitation efficiency and complexity of circuit level optimization.

[F2D-2] 11:30 ~ 11:50

### Miniaturization of Bow-Tie Slot Antenna for Mounting on Human Arm 554

Masahiro Asano, Toshikazu Hori, Mitoshi Fujimoto, University of Fukui, Japan

In Wireless Body Area Network (WBAN) which is the network around a human body, Ultra Wide Band (UWB) communication is one of the candidate for a realizing a high transmission rate. However, characteristics of antennas are degraded due to the influence of the human body. Also, in general broadband antennas which cover the bandwidth of UWB are too large for WBAN's antennas. In this paper, an antenna with a slot of a bow-tie shape is focused and downsizing technique is discussed. In comparison with the basic shape, it is downsized by approximately 10% in the y-direction, 68% in the z-direction. And, average Front to Back ratio of 1.95dB is obtained in band from 4.7 to 10.6GHz.

[F2D-3] 11:50 ~ 12:10

### Design of a Circular-ring Patch on-body Antenna with Shorting vias for WBAN Application 557

Jinpil Tak, Kyeol Kwon, Jaehoon Choi, Hanyang University, Korea

A circular-ring patch on-body antenna with a shorting via for WBAN application is proposed. The proposed circular-ring patch antenna has the maximum radiation direction along the body surface for on-body communication in the industrial, scientific, and medical (ISM) 2.45 GHz band. In order to achieve low profile, the proposed antenna used shorting vias to excite TM<sub>31</sub> mode at ISM 2.45 GHz. To enhance bandwidth performance, an annular ring with shorting via is closely located around a circular patch. Proposed antenna is fed by a via connected with a microstrip line. The overall dimension of proposed antenna is 50 mm×55 mm×3.15 mm.

[F2D-4] 12:10 ~ 12:30

### Design and Simulation of a Reflectarray Antenna using A New Hexagon Element N/A

Iman Arianyan, Abdolali Abdipour, Gholamreza Moradi, Amirkabir Univ. of Tech., Iran

In this paper we design a reflectarray antenna to have a high gain using phase synthesis in a frequency band of 11 GHz up to 11.7 GHz. First, a new loop element is proposed to design reflectarray antenna. Then, by this element a reflectarray antenna is designed using phase-only algorithm and the amplitude of the field on the reflectarray surface is forced by the feed. Our method is applied to design a 1.2 m reflectarray for different beam directions. Focal length is 1.5 m which is set for maximum efficiency. The resulted radiation patterns show that the maximum gain is 42 dB for the required bandwidth and the maximum efficiency is 73%.

[F2D-5] 12:30 ~ 12:50

### Optimal Snapshot Number of Power Inversion Adaptive Array in ITS Communication Environment 563

Takuya Ukawa, Mitoshi Fujimoto, Toshikazu Hori, University of Fukui, Japan

It is worried that the ITS may suffer interference from broadcast system or mobile communication system. Thus, we proposed a power inversion adaptive array which can suppress an interference wave in ITS propagation environment. However, the interference suppression performance is reduced due to multipath fading. As a countermeasure, we devised a continue control method for power inversion to follow the change of propagation environment. In this paper, the optimal snapshot number for properly estimating a correlation matrix is examined. As the result of examination, it is clarified that the optimal number of snapshots is about 30 times.

## [F2E] Radar Systems and Applications

- Date: November 8, 2013 (Friday)
- Time: 11:10 ~ 13:00
- Room: Room E (Room 203)
- Session Chairs: T. S. Jason Horng (National Sun Yat-sen University)  
Moon-Que Lee (University of Seoul)

[F2E-1]

11:10 ~ 11:40

### [Invited] Self-Injection-Locked Radar: an Advance in Continuous-Wave Technology for Emerging Radar Systems 566 Tzzy-Sheng Horng, National Sun Yat-Sen University, Taiwan

This paper introduces an innovative continuouswave (CW) radar technology, called the self-injection-locked (SIL) radar. It can compete with pulse radar technology in resisting clutter and interference, but maintains the advantage of low complexity that is associated with the CW radar. Accordingly, an SIL radar can be implemented at low cost, providing high performance and low power consumption. It therefore has great potential to accelerate the killer application development of portable radars for wireless health and safety services, especially when installed in personal mobile devices.

[F2E-2]

11:40 ~ 12:00

### Low Power Monostatic Pulse Borehole Radar with an Active Circulator and an Absorptive Switch 570 Jae-Hyoung Cho<sup>1,2</sup>, Jong-Gwan Yook<sup>2</sup>, Se-Yun Kim<sup>1</sup>, <sup>1</sup>Korea Institute of Science and Technology, Korea, <sup>2</sup>Yonsei University, Korea

A low power monostatic pulse borehole radar system is designed and tested for detecting a subversive intrusion tunnel with about 2 m diameter. According to our calculated budget under the condition that the transmitting signal is over 1 V peak with 10 ns full width half maximum, its switching speed becomes faster than 100 ns for detecting an air-filled tunnel nearby the employed borehole. To satisfy the above requirement, the monostatic pulse radar is fabricated with an active circulator using operational amplifiers and a switch for guaranteeing isolation and cutting off the direct signal. Then, the system performance is evaluated in a well suited tunnel test site. The measured data illustrate that the monostatic pulse radar provides the parabolic pattern of a typical tunnel signature comparable to that of a conventional bistatic pulse radar.

[F2E-3]

12:00 ~ 12:20

### Evaluative Comparison of Clutter Canceller Beamformer and Amplitude Comparison Monopulse Estimation Scheme in HF SWR 573 Anshu Gupta, Thomas Fickenscher, Helmut Schmidt University, Germany

Clutter Canceller Beamformer (CCB) and Amplitude Comparison Monopulse Estimation Scheme (ACMES) are two schemes for resolving targets in noise dominated scenarios which have been presented in the literature. These two schemes are compared on the basis of minimum required value of Signal to Clutter Ratio (SCR) value needed to achieve a given probability of false alarm (PFA) value. For this comparison the probability density function of both the received signal for both the schemes is determined. Assuming that the input noise has additive white Gaussian distribution it is reported that the required SCR for CCB is 2 dB less than ACMES to achieve  $P_{FA}$  of  $10^{-6}$ .

[F2E-4]

12:20 ~ 12:40

### 79GHz-band Radar Cross Section Measurement for Pedestrian Detection 576 Makoto Yasugi, Yunyun Cao, Kiyotaka Kobayashi, Tadashi Morita, Takaaki Kishigami, Yoichi Nakagawa, Panasonic Corporation, Japan

This paper presents radar cross section (RCS) measurement for pedestrian detection in 79GHz-band radar system. For a human standing at 6.2 meters, the RCS distribution's median value is -11.1 dBsm and the 90 % of RCS fluctuation is between -20.7 dBsm and -4.8 dBsm. Other measurement results (human body poses beside front) are shown. And we calculated the coefficient values of the Weibull distribution fitting to the human body RCS distribution.

[F2E-5]

12:40 ~ 13:00

### Soil Density Prediction Tool using Microwave Ground Penetrating Radar 579 Mardeni R., K. S. Subari, I. S. Shahdan, Multimedia University, Malaysia

In this paper, a microwave surface reflection method is proposed to analyze the effect of soil density with its electrical properties using ground penetrating radar (GPR) principal. Three types of soil samples are chosen for the analysis of this project, namely sandy, loamy and clay. The work is based on measurement, simulation and model development. In the analysis, it is found that the average error percentages from the three developed models are 0.04%, 0.21% and 0.74% for sandy, loamy and clay soil, respectively. The effect of soil density with its electrical characteristics in terms of permittivity, propagation velocity and two-way wave travel time are also discussed. At the end of this paper, a soil density prediction tool is developed using the empirical models introduced consisting the density and attenuation for each soil sample at frequency range of 1.7 GHz to 2.6 GHz.

## [F2F] EM Analysis

- Date: November 8, 2013 (Friday)
- Time: 11:10 ~ 13:00
- Room: Room F (Room 208)
- Session Chairs: Yury Yukhanov (Southern Federal University)  
Taek-Kyung Lee (Korea Aerospace University)

[F2F-1]

11:10 ~ 11:40

### [Invited] Synthesis of Impedance of Axisymmetric Body 582

Yury V. Yukhanov, Tatiana Y. Privalova, Southern Federal University, Russia

Formulas for coefficients of reflection of a plane wave from a inhomogeneous impedance plane that refracts incident wave in a given direction were obtained. We have solved the problem of synthesis of inhomogeneous impedance rotation body of arbitrary shape of generatrix for a given scatterplot for co- and cross polarizations. Impedance distribution was obtained in explicit form. Formulated restrictions on the class of implementable scatterplots.

[F2F-2]

11:40 ~ 12:00

### Analytical Expression of Linear Antenna's Characteristics using Multipole Expansion and Chu's Equivalent Circuit 585

Akira Saitou, Ryo Ishikawa, Kazuhiko Honjo, The University of Electro-Communications, Japan

Analytical expression including higher-order modes for a linear dipole antenna is derived with the multipole expansion and Chu's equivalent circuits. Current distribution on the antenna's conductor and loss caused by the radiation are consistently combined. Input power at the port is approximated to be guided totally on the conductor up to an effective antenna's radius, and to propagate in free space beyond the radius. The circuit for the power to propagate in the free space is expressed by Chu's equivalent circuits for all the TM modes. With the derived formulae, numerical estimations of the current distributions and input impedances are shown up to 3<sup>rd</sup>-order-mode's resonant frequency. The numerical data are compared with measured data for the antennas with different line widths, and the data are shown to agree well.

[F2F-3]

12:00 ~ 12:20

### Use of Load Modulation for Interference Control Between Primary and Secondary Systems 588

Takuma Ito<sup>1</sup>, Naoki Honma<sup>1</sup>, Keisuke Terasaki<sup>1</sup>, Kentaro Nishimori<sup>2</sup>, Yoshitaka Tsunekawa<sup>1</sup>, <sup>1</sup>Iwate University, Japan, <sup>2</sup>Niigata University, Japan

Controlling interference from the secondary system to the receiver of the primary system is important issues when the secondary system uses the same frequency band in the area of television broadcast system. The reason includes that the secondary system cannot know the interference channel to the primary receiver, which does not have a transmitter. In this paper, we propose the interference control method between primary receiver and secondary system, where a load modulation scheme is introduced to the primary receiver. In this method, the signal from the transmitter station is scattered by switching load impedance at the primary receiver. Also, the secondary system estimates the reflected wave from receiver and estimates the interference suppression weights. Based on the simulation, it is shown that the proposed method is effective in controlling interference between primary receiver and secondary system.

[F2F-4]

12:20 ~ 12:40

### Equivalent Circuit Analysis for Double Layer Patch Type AMC in Consideration of Mutual Coupling between Layers 591

Ryuji Kuse<sup>1</sup>, Toshikazu Hori<sup>1</sup>, Mitoshi Fujimoto<sup>1</sup>, Takuya Seki<sup>2</sup>, Keisuke Sato<sup>2</sup>, Ichiro Oshima<sup>2</sup>, <sup>1</sup>University of Fukui, Japan, <sup>2</sup>Denki Kogyo Co., Ltd., Japan

This paper describes the equivalent circuit analysis of a double layer AMC (Artificial Magnetic Conductor) in consideration of mutual coupling between layers. The AMC with double layer patch type FSS (Frequency selective surface) is focused. This paper treats two type double layer structures. The one is stacked structure, and the other is alternated structure. It was shown that the calculated results by using the equivalent circuit well agreed with the results of the FDTD analysis. In addition, it was clarified that the stacked and alternated structures cause the common mode and the differential mode coupling, respectively. Moreover, it was shown that the miniaturization of the AMC is designed by setting the distance between the layers of double layer FSS as thin as possible.

[F2F-5]

12:40 ~ 13:00

### Optimum Area of Arranged Unit Cell of Artificial Magnetic Conductor Reflector for Dipole Antenna 594

Y. Murakami, T. Hori, M. Fujimoto, University of Fukui, Japan

A high gain and low-profile antenna can be realized by using an AMC (Artificial Magnetic Conductor) reflector that has PMC (Perfect Magnetic Conductor) characteristics. Since a configuration of the AMC reflector must be adjusted for each antenna, studies on the configuration of the optimum AMC reflector are not enough yet. This paper describes the optimum AMC reflector configuration for high directive gain and low-profile dipole antenna with the AMC reflector. Here, the arranged unit cell area and the thickness of the AMC reflector are considered. The AMC treated in this paper are composed of the patch or loop type FSS (Frequency Selective Surface) and the ground plane. It is shown that the area of the arranged unit cell is one of the important factors to obtain the high directive gain. Moreover, it is shown that the high directive gain dipole antenna with the AMC reflector can be realized by the optimum area of the arranged unit cell.

## Special Tutorial

- Date: November 8, 2013 (Friday)
- Time: 15:00 ~ 15:50
- Room: Room A (Room 101)

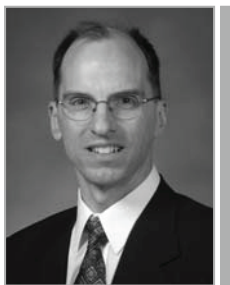
### How to Write a Paper for IEEE MTT-S Journals and Navigate the Review Process

**Speaker: George E. Ponchak (Editor-in-Chief, IEEE Transactions on Microwave Theory and Techniques)**

The careers of many people depends on their success in writing and getting their papers published. More important, the scientific process requires that scientific findings be published so that other researchers may build on your ideas or refute your findings. If authors are not able to publish their papers, then their careers are hurt and scientific progress slows and stops. Therefore, it is critical that researchers and engineers understand the process of writing and getting published their papers in reputable and cited journals and scientific conferences. However, often, authors' papers are rejected because they did not understand what reviewers, Associate Editors, and Editors are looking for in a paper, even if the technical results are good.

This presentation will cover the steps that an author should take to increase the acceptance rate of their papers in journals and conference. It will cover the reasons most papers are rejected and how an author should organize their paper to avoid those reasons. Lastly, it will present what steps you should take if your paper is rejected to get it published in the same journal or in a different journal.

#### About the Instructor:



**George E. Ponchak** received the B. E. E. degree from Cleveland State University, Cleveland, OH in 1983, the M.S.E.E. degree from Case Western Reserve University, Cleveland, OH in 1987, and the Ph.D. in electrical engineering from the University of Michigan, Ann Arbor, MI in 1997.

He joined the staff of the Communications, Instrumentation, and Controls Division at NASA Glenn Research Center, Cleveland, OH in 1983 where he is now a senior research engineer. In 1997-1998 and in 2000-2001, he was a visiting professor at Case Western Reserve University in Cleveland, OH. He has authored and co-authored over 150 papers in refereed journals and symposia proceedings. His research interests include the development and characterization of microwave and millimeter-wave printed transmission lines and passive circuits, multilayer interconnects, uniplanar circuits, Si and SiC Radio Frequency Integrated Circuits, and microwave packaging.

Dr. Ponchak is a Fellow of the IEEE and an Associate Member of the European Microwave Association.

Dr. Ponchak is Editor-in-Chief of the *IEEE Transactions Microwave Theory and Techniques*, he was the Editor-in-Chief of the *IEEE Microwave and Wireless Components Letters* from 2006-2009, and he was Editor of a special issue of *IEEE Trans. on Microwave Theory and Techniques* on Si MMICs. He founded the *IEEE Topical Meeting on Silicon Monolithic Integrated Circuits in RF Systems* and served as its Chair in 1998, 2001, and 2006. He was the General Chair of the *2011 IEEE Radio and Wireless Symposium* and he was the Technical Program Chair of the *2010 IEEE Radio and Wireless Symposium*. He served as Chair of the Cleveland MTT-S/AP-S Chapter (2004-2006), and he has chaired many symposium workshops and special sessions. He is a member of the IEEE International Microwave Symposium Technical Program Committee on Transmission Line Elements and served as its Chair in 2003-2005 and a member of the IEEE MTT-S Technical Committee 12 on Microwave and Millimeter-Wave Packaging and Manufacturing. He served on the IEEE MTT-S AdCom Membership Services Committee (2003-2005) and was elected to the MTT-S AdCom in 2010. He received the Best Paper of the ISHM'97 30<sup>th</sup> International Symposium on Microelectronics Award.

## Poster Session III: Antennas and Propagation & Emerging Technologies

- Date: November 8, 2013 (Friday)
- Time: 14:20 ~ 16:00
- Room: Room 103

[P3-1] 14:20 ~ 16:00

### A K-Band Gm-Boosting Differential Colpitts VCO in 0.18- $\mu\text{m}$ CMOS 1042 Sen Wang, Wen-Jie Lin, National Taipei University of Technology, Taiwan

A modified K-band differential Colpitts voltage-controlled oscillator (VCO) which uses gm-boosting and capacitive filtering techniques to improve the performance of phase noise is proposed. The VCO achieves a good phase noise of -108.19 dBc/Hz at 1-MHz offset frequency, and the chip size is merely 0.27 mm<sup>2</sup>. The dc power consumption is 32.34 mW from a 2.2-V power supply. Compared with the previously published K-band VCOs, the proposed Colpitts VCO exhibits a superior phase noise characteristic and a highest FOM.

[P3-2] 14:20 ~ 16:00

### Novel High Gain Dual-band Dipole Antenna 1046 Junzhi Yu, Tsinghua University, China

Using 50-Ohm differential microstrip and limited reflection board, the conversion from unbalance to balance is subtly achieved and a high-qualified sheet-shaped resonator half-wave dipole antenna is designed. Such antenna has measured gains 6.6dBi@890MHz, 6.7dBi@960MHz, 7.1dBi@1700MHz and 8.3dBi@1880MHz. Besides, the radiation direction meets the proposed goal.

[P3-3] 14:20 ~ 16:00

### Design Monopole Antenna with Fluorescent Tube at 4.9GHz 1049 H. Jaafar<sup>1</sup>, M. T. Ali<sup>1</sup>, A. N. Dagang<sup>2</sup>, H. M. Zali<sup>1</sup>, N.A. Halili<sup>1</sup>, <sup>1</sup>Universiti Teknologi MARA, Malaysia, <sup>2</sup>Universiti Malaysia Terengganu, Malaysia

This paper presents of analysis the performance monopole antenna with fluorescent tubes. The antenna was designed at the operating frequency which is 4.9GHz. The fluorescent tubes consist of a glass tube filled with mixture mercury vapor and argon gas. After get sufficient voltage the gas inside the tube will ionize to plasma and formed plasma column. The plasma frequency is equal to 5.634e11. The plasma is highly conducting and acts as a reflector. When all of the tubes surrounding the antenna are electrified, the radiation is trapped inside when the plasma frequency is greater than radio frequency. An accomplishment of the design has been carried out using CST microwave studio software. The developed antenna has potential in military application. To conclude, antenna's performance was analyzed in terms of return loss, radiation pattern and gain.

[P3-4] 14:20 ~ 16:00

### PIN Diode Switches for Frequency-Reconfigurable Stacked Patch Microstrip Array Antenna using Aperture-Coupled Technique 1052 N. Ramli<sup>1</sup>, M. T. Ali<sup>1</sup>, A. L. Yusof<sup>1</sup>, S. Muhamud - Kayat<sup>1</sup>, A. A. A. Aziz<sup>2</sup>, <sup>1</sup>Universiti Teknologi Mara, Malaysia, <sup>2</sup>Politeknik Sultan Salahuddin Abdul Aziz, Malaysia

This paper presents a novel design of frequency- reconfigurable antenna by using an aperture coupled as feeding technique and stacked patch technology. The proposed antenna is generally constructed of three substrate layers (RT-Rogers 5880) and air gap filled between feedline substrate and layer 2 substrates. Four PIN diode (BAP51-02) switches are implemented to configure the length of the feedline by configuring the switches to ON or OFF mode. A new approach of coupling methods is presented. During all the switches are in ON mode, the signal will be passed through to selective aperture slot and activate the particular radiating patch layer to achieve the frequency reconfigurability either at 2.6 GHz or 3.5 GHz. The prototype of the proposed antenna is tested/ fabricated with the biasing circuit to validate the antenna's performance. A good agreement between the simulated and measured results are achieved to confirm the performance of the antenna.

[P3-5] 14:20 ~ 16:00

### A MIMO Antenna with Built-In Isolation for WLAN USB Dongle Applications 1055 Cho-Jung Lee, Lih-Tyng Hwang, T.-S. Jason Horng, Shun-Min Wang, Yi-Chieh Lin, Kun-Hui Lin, National Sun Yat-Sen University, Taiwan

A novel couple-fed dual-bands MIMO antenna is proposed for WLAN 2.4/5.2/5.8 GHz bands. The MIMO antenna system consists of two parallel folded branch monopoles with an edge-to-edge separation of 0.2 mm. The antenna elements are printed on an FR4 substrate and are located at the top edge of the ground plane. Size of the antenna is 20 mm (W)×11 mm (L). The isolation is achieved by introducing a round off-set structure at the end of the coupled feeding-line. Measured results show that antennas have good impedance matching and port isolation. Since we have not introduced any isolation enhancing structure, the MIMO antenna appeared to have a built-in decoupling mechanism. When one end was fed, the current distributions on the other feed line was reduced in magnitude by a self generated counter current occur at the round off-set structure area. That is, the self generated counter current has contributed the needed isolation between the two antennas. The results suggest that the proposed novel simple, compact antenna structure has indeed attained good isolation characteristics required for MIMO operations. Moreover, the antenna is easy to fabricate and suitable for applications at the 2.4/5.2/5.8-GHz bands.

## Poster Session III: Antennas and Propagation & Emerging Technologies

- Date: November 8, 2013 (Friday)
- Time: 14:20 ~ 16:00
- Room: Room 103

[P3-6] 14:20 ~ 16:00

### Three-Dimensional Numerical Simulation of Multipactor in Open Antenna Structures 1058

Yun Li, Na Zhang, Rui Wang, Wanzhao Cui, China Academy of Space Technology, China

A three-dimensional numerical simulation method of multipactor in open-structured high-power microwave systems is presented in this work. This method considering the perfect absorption of electrons at open boundaries, the commonly used absorption method with perfect-matched layers in electro-magnetic simulations has been modified and an improved absorbing boundary has been established which avoids the instability of computation. Together with the electromagnetic Particle-In-Cell technologies and the secondary electron emission models, the high-diffusion effect and the nonlinear dynamics of electrons in multipactor phenomena are intuitively investigated for the first time in open structures. As an illustration, the simulation results of a spiral antenna are provided, which reveals the transient evolution of electron accumulation in this typical open structure. By analyzing the tendency of the evolution, the multipactor threshold of the antenna has been successfully estimated.

[P3-7] 14:20 ~ 16:00

### Compact Polarization Diversity Antenna using a Pair of Parallel Dipoles for Mobile RFID 1061

Dong-Jin Lee, Soo-Ji Lee, Kwang-Suk Kim, Jong-Won Yu, Korea Advanced Institute of Science and Technology, Korea

A novel compact polarization diversity antenna using a pair of parallel dipoles for mobile UHF radio frequency identification (RFID) is presented. The antenna is composed of a pair of parallel dipoles orthogonally placed on the feeding network. Compare to half wavelength conventional dipole antenna, the overall size of this antenna is less than quarter wavelength. With the compact and simple feeding network below the parallel dipoles, the proposed antenna can generate vertical linear polarization and horizontal linear polarization. The use of the proposed polarization diversity antenna may lead to the higher detection of capability of RFID tags, thus providing the stable and reliable RFID services. Antenna gain is 2.05 dBi and isolation between the two input ports is less than -18dB. Details of the antenna design are shown, and the measurement and simulation results are also provided to validate the proposed idea.

[P3-8] 14:20 ~ 16:00

### Analysis of the BDF using Caustics of Parabolic Reflector Antennas 1064

N. Abd Rahman<sup>1,2</sup>, M. Islam<sup>3</sup>, N. Misran<sup>1</sup>, Y. Yamada<sup>4</sup>, N. Michishita<sup>4</sup>, <sup>1</sup>Universiti Kebangsaan Malaysia, Malaysia, <sup>2</sup>Universiti Teknologi MARA, Malaysia, <sup>3</sup>Universiti Kebangsaan Malaysia, Malaysia, <sup>4</sup>National Defense Academy, Japan

When designing contour beams by combining multiple beams, the antenna beam direction and feed position become very important. This relation between the beam direction and feed position is known as the beam deviation factor (BDF). Previously, an equation for the BDF was derived from an aperture phase distribution of a parabolic reflector antenna. In this paper, the BDF relation is estimated from the calculated results of caustics in the focal region of a reflector antenna. To obtain the caustics, focal region ray tracings are obtained for incident plane waves at various antenna parameters and incident angles. In particular, the differences between the caustics in the scanning and transverse planes are investigated. The obtained feed positions are compared with the previous BDF and electromagnetic simulation characteristics. Finally, the accuracy of the focal region ray tracings is ensured by comparing the BDF values obtained from both methods.

[P3-9] 14:20 ~ 16:00

### Substrate-Integrated Fabry-Pérot Cavity Antenna Fed by Slot-Coupled Patch Array for Directivity Enhancement 1067

Ling Ji, JiaDi Wang, WeiDong Chen, Chang Chen, University of Science and Technology of China, China

This paper presents a substrate-integrated Fabry-Pérot cavity (FPC) antenna fed by a slot-coupled patch array. The patch array contributes to a homogeneous excitation on antenna aperture and achieves further improvement on directivity. The effects of array's interelement distance on antenna's radiation characteristics are investigated to show a different trend with that of arrays in air-filled FPC antennas. Besides, the slot-coupled structure is introduced to feed the patch array to prevent the feeding network from radiating in the cavity. For verification, substrate-integrated FPC antennas fed with 1 and 4 patches operating in X-band are manufactured. The measurement shows that the antenna fed by 4 patches presents a maximum gain of 15.5 dBi at 10.0 GHz, which is 1.5 dB more than antenna fed by 1 patch.

[P3-10] 14:20 ~ 16:00

### Full-wave Simulation of Frequency Diverse Array Antenna using the FDTD Method 1070

Jinwoo Shin<sup>1</sup>, Jun-Ho Choi<sup>1</sup>, Junyeon Kim<sup>1</sup>, Jongwon Yang<sup>1</sup>, Woosang Lee<sup>1</sup>, Joonho So<sup>1</sup>, Changyul Cheon<sup>2</sup>, <sup>1</sup>Agency for Defense Development, Korea, <sup>2</sup>University of Seoul, Korea

This paper describes 2-D analysis of a frequency diverse transmit array antenna with a periodic modulated pattern in range using the finite difference time domain methods. The elements of applied linear array are equally spaced and have same phase but operated at different frequencies. The result pattern of frequency diverse array forms range-dependent beam patterns whereas conventional array pattern forms same beam patterns in far field range. This range-dependent beam pattern provides more flexible beam scan options and lessens undesirable interferences such as multipath. The simulation results for radiation patterns of open-ended waveguide (OEG) antenna array are presented. The characteristics of radiation pattern were investigated by the each different simulation for frequency offset change, radiation element space change and array number change.

## Poster Session III: Antennas and Propagation & Emerging Technologies

- Date: November 8, 2013 (Friday)
- Time: 14:20 ~ 16:00
- Room: Room 103

[P3-11] 14:20 ~ 16:00

### Broadband CPW-Fed Circularly Polarized Square Slot Antenna with Combining C-Shaped Strip and Asymmetry Ground Plane 1073

Te-Hsing Chen, Deng-Yin Wang, Wen-Hua Tu, National Central University, Taiwan

A new broadband circularly polarized (CP) square slot antenna with coplanar waveguide (CPW) fed is designed in this paper. An asymmetry ground plane makes the adjacent resonant mode to merge into a wide operation bandwidth, and the C-shaped structure can offer the current path, two orthogonal electric fields with a 90° phase difference for exciting a circular polarization radiation wave. The measured impedance bandwidth ( $VSWR \leq 2$ ) is 0.92 GHz (46% relative to the center frequency at 2 GHz). The 3-dB axial ratio bandwidth (ARBW) is 0.65 GHz (32.5% relative to the center frequency at 2 GHz), and antenna peak gain is 3.31 dBi with gain variations of less than 1 dB.

[P3-12] 14:20 ~ 16:00

### Quadruple Linear and Circular Polarized Diversity Antenna with Reconfigurable Coupler 1076

Hyun-Sung Tae<sup>1</sup>, Wang-Sang Lee<sup>1</sup>, Kyoung-Sub Oh<sup>1</sup>, Dong-Hoon Park<sup>2</sup>, Moon-Que Lee<sup>2</sup>, Jong-Won Yu<sup>1</sup>, <sup>1</sup>Korea Advanced Institute of Science and Technology, Korea, <sup>2</sup>University of Seoul, Korea

In this paper, a quadruple linear polarization (LP) and circular polarization (CP) diversity antenna with a reconfigurable coupler is presented. The proposed antenna has two linear (vertical and horizontal) and two circular (right-handed and left-handed) polarizations. In order to implement real-time polarization diversity antenna, the electrical switches are used in the proposed antenna feeding network which is four mode reconfigurable coupler. The measured gains and the axial ratios of the proposed antenna are 5.6 ~ 6 dBi and 0.5 ~ 1.5 dB in four operation modes and two CP modes.

[P3-13] 14:20 ~ 16:00

### Development of Circularly Polarized Planar Slot Antenna for 5.8 GHz-DSRC Application 1079

Tomoya Ijiguchi<sup>1</sup>, Daisuke Kanemoto<sup>2</sup>, Kuniaki Yoshitomi<sup>1</sup>, Keiji Yoshida, Akira Ishikawa<sup>3</sup>, Shugo Fukagawa<sup>3</sup>, Noriyuki Kodama<sup>3</sup>, Akihiro Tahira<sup>3</sup>, Haruichi Kanaya<sup>1</sup>, <sup>1</sup>Kyushu University, Japan, <sup>2</sup>University of Yamanashi, Japan, <sup>3</sup>Kyushu Ten Ltd., Japan

A novel design method of circularly polarized planar slot antenna for 5.8 GHz Dedicated Short Range Communications (DSRC) applications is proposed. For realized circularly polarized wave, we use planar slot antenna. By optimizing the lengths and widths of antenna slot, resonances can be obtained at 5.8 GHz frequency. The antenna generates a circularly polarized wave providing a slot in the two orthogonal directions. Improving the gain by providing a slot in the same direction, arrayed structure is adopted. The final antenna size is 17 mm × 15 mm × 1.6 mm. Our antenna was fabricated on the FR4 substrate and impedance bandwidth is 310 MHz from 5.62 to 5.93 GHz. Moreover circularly polarized wave can be obtained.

[P3-14] 14:20 ~ 16:00

### Design of Ka band Reconfigurable Beam Antenna using Genetic Algorithm 1082

Manseok Uhm, Sohyeon Yun, Hongyeal Lee, Changsoo Kwak, Donghwan Shin, Inbok Yom, ETRI, Korea

This paper presents an efficient design method based on genetic algorithm and design results for Ka band reconfigurable beam antenna composed of an array-fed reflector. The effective cost functions for the contoured beam and the boosted beams were used to find the best solution. During the optimization, it was confirmed that the average cost and the best cost were converged. The contoured beam antenna is designed with the gain ripple less than 3 dB over the coverage. The boost level greater than 7 dB for Seoul area is obtained.

[P3-15] 14:20 ~ 16:00

### Wide-Beam Circularly Polarized Composite Cavity-Backed Crossed Scythe-Shaped Dipole 1085

Son Xuat Ta<sup>1</sup>, Jea Jin Han<sup>1,2</sup>, Richard W. Ziolkowski<sup>3</sup>, Ikmo Park<sup>1</sup>, <sup>1</sup>Ajou University, Korea, <sup>2</sup>Danam Systems, Korea, <sup>3</sup>University of Arizona, USA

In this paper, a wide-beam circularly polarized (CP) composite cavity-backed crossed scythe-shaped dipole is proposed. Each dipole arm contains a meander line whose end is shaped like a scythe chine to accomplish a significant reduction in the radiator size. The scythe-shaped dipoles are crossed through a 90° phase delay line of a vacant-quarter printed ring in order to generate CP radiation and broadband impedance matching. The crossed scythe-shaped dipole is incorporated with a cavity-backed reflector to improve the radiation pattern in terms of the CP radiation beamwidth and front-to-back ratio. The proposed antenna yields broad impedance-matching and 3-dB axial-ratio bandwidths, a high front-to-back ratio, and a wide beamwidth.

## Poster Session III: Antennas and Propagation & Emerging Technologies

- Date: November 8, 2013 (Friday)
- Time: 14:20 ~ 16:00
- Room: Room 103

[P3-16] 14:20 ~ 16:00

### A Compact Multiband Planar Monopole Antenna with Proximity-Coupling Radiator 1088

Ching-Song Chuang<sup>1</sup>, Hung-Chih Liu<sup>2</sup>, <sup>1</sup>Electronic Engineering, Lunghwa University, Taiwan, <sup>2</sup>Lunghwa University, Taiwan

A compact multiband planar monopole antenna is presented in this paper. The operating frequency bands of the proposed antenna cover the multiple wireless access protocols of GSM (880-960MHz), DCS (1710-1880MHz), WiMAX (3.2-3.6GHz), WLAN and Bluetooth (2.4GHz), and WLAN (5.1-5.35GHz). The antenna is constructed by two distinct monopoles which are individually located at the opposite side of the substrate; a broadband meander-line monopole is structured to create the triple lower frequency bands, on the other hand, a tree-type monopole is built not only to produce the dual higher frequency bands, but also to act as a proximity-coupled feed for the meander-line resonator. The antenna together with several attractive characteristics, such as small in size, broad in operating frequency band and omni-directional in radiation pattern, makes itself particularly suitable to the integrated mobile wireless access applications. The measurement results demonstrate the success of the antenna design approach.

[P3-17] 14:20 ~ 16:00

### A Separated Cross-Shaped Isolation Element for WLAN MIMO Applications 1091

Wen-Shan Chen<sup>1</sup>, Ke-Ming Lin<sup>1</sup>, Bau-Yi Lee<sup>2</sup>, Chun-Lin Ciou<sup>1</sup>, <sup>1</sup>Southern Taiwan University of Science Technology, Taiwan, <sup>2</sup>Tung Fang Design University, Korea

In the article, two PIFA antennas fabricated on both ends of an FR4 substrate are introduced for MIMO application. The two identical PIFAs excite resonant bands ( $S_{11}$  and  $S_{22}$ ) both at 2.45 GHz for WLAN application. The isolation mechanism is accomplished through a separated cross-shaped isolation element, which is extended from the ground plane and located between the PIFAs. By adding the isolation element, the radiating emission between the PIFAs and the conducting current through the ground plane are decreased. The measured  $S_{21}$  in WLAN band is below -15 dB. The overall dimensions (20x45 mm<sup>2</sup>) of the proposed MIMO antenna including an antenna portion (10x20 mm<sup>2</sup>) and a system ground (35x20 mm<sup>2</sup>) are suitable for applying in a wireless device. Beside, the radiation patterns, ECC (Envelope Correlation Coefficient) and radiation efficiency will be presented.

[P3-18] 14:20 ~ 16:00

### X-Band Image Reconstruction by Modified Range Migration Algorithm 1094

Yong-Sun Cho, Hyun-Kyo Jung, Seoul National University, Korea

The radar imaging algorithms can be divided into three general groups as range migration algorithm (RMA), polar format algorithm (PFA) and chirp scaling algorithm (CSA). In this letter, we explore the RMA technique in X-band suitable for the strip-map mode of a synthetic aperture radar (SAR) system, and then propose a modified RMA to obtain better image resolution than is normally obtained using a conventional RMA. Finally, the reconstructed images generated using the modified RMA demonstrates that the proposed algorithm shows the better performance than a conventional RMA.

[P3-19] 14:20 ~ 16:00

### Phase Error Minimization by Refocusing Rotman Lens 1097

Joo-Rae Park<sup>1</sup>, Dong-Chul Park<sup>2</sup>, <sup>1</sup>Agency for Defense Development, Korea, <sup>2</sup>Chungnam National University, Korea

In this paper, we propose a refocusing method for minimizing phase errors of Rotman lenses. The method is based on finding the optimal  $\alpha$  and  $F$  minimizing the phase errors by moving off-axis focal points along a feed curve. It ensures additional phase error reduction without significant changes of feed and array curve shapes. Simulation results show considerably improved phase performance when this method is applied to Rotman lenses with the conventional circular, elliptical, and optimized feed curves.

[P3-20] 14:20 ~ 16:00

### Investigations of Compact Tri-Band Antenna For CNSS Application 1100

Pingping Zhang<sup>1</sup>, Hao Wang<sup>1</sup>, Yan Wang<sup>1</sup>, Yong Huang<sup>2</sup>, Jie Wang<sup>2</sup>, Xiaolong Shao<sup>1</sup>, <sup>1</sup>Nanjing University of Science and Technology, China, <sup>2</sup>Suzhou Bohai Microsystem Co., Ltd., China

In this paper, a new tri-band antenna with characteristic of miniaturization and low profile is proposed. The size is less than 45mmx45mmx9mm. This compact antenna is working at B<sub>3</sub>, L and S frequencies of Compass Navigation Satellite System (CNSS). The tri-band antenna is obtained with two microstrip patch antennas and a quadruple inverted-F antenna (QIFA) which is inserted in the two layers of substrates to reduce the height and achieve low profile. The simulated and measured results of this antenna are presented. Furthermore, the isolation performances of this antenna are investigated. This results are served as a guideline, therefore, another improved tri-band antenna which is less than 35mmx35mmx15mm is achieved. This 35mm antenna provides good isolation performances than the 45mm one. Meanwhile, the 35mm antenna has the stable performances.



## Poster Session III: Antennas and Propagation & Emerging Technologies

- Date: November 8, 2013 (Friday)
- Time: 14:20 ~ 16:00
- Room: Room 103

[P3-21] 14:20 ~ 16:00

### Investigation on W-band LTCC Helical Antenna With Substrate Integrated Horn 1103

Changfu Sun<sup>1</sup>, Baolin Cao<sup>1</sup>, Hao Wang<sup>1</sup>, Yong Huang<sup>2</sup>, Jie Wang<sup>2</sup>, Weixing Sheng<sup>1</sup>, <sup>1</sup>Nanjing University of Science & Technology, China, <sup>2</sup>Suzhou Bohai Microsystem Co., Ltd., China

A W-band helical antenna element with substrate integrated horn (SIH) using low temperature cofired ceramic (LTCC) technology is proposed in this paper. Using the multilayer process of the LTCC technology, the planar helical antenna is achieved. Furthermore, to calibrate the errors of planar LTCC helical antenna's axial direction mode, which is caused by the fabrication limitations of LTCC technology, the SIH structure has been designed. To verify the theory, the investigations of two LTCC antennas with and without SIH have been given. From the simulated results, the proposed antenna shows a wide impedance bandwidth from 85 to 110 GHz for  $|S_{11}| < -10\text{dB}$ , and a wideband axial ratio (AR) bandwidth from 91 to 106 GHz for  $\text{AR} < 3\text{ dB}$  respectively. The peak gain is greater than 4.5dBi in the AR bandwidth.

[P3-22] 14:20 ~ 16:00

### Characterization of 4x4 Planar Antenna Arrays for the Frequencies 77 GHz and 94 GHz using an Antenna Scanning System 1106

Mohammed Salhi, Carolin Peiss, Michael Botschka, Thomas Kleine-Ostmann, Thorsten Schrader, Physikalisch-Technische Bundesanstalt, Germany

Due to the excessive need for bandwidth, a tendency has been noticed towards using higher frequencies up to the millimeter and sub-millimeter wave range. Antennas are essential components in any communication system. Therefore, we present the design and characterization of two 4x4-phasedarray patch antennas which work at 77 and 94 GHz. We also present a transition block from the rectangular waveguide source to the planar structure to forward the radiation to the antenna patches. The radiation pattern of the antennas was measured with a new high-precision antenna scanning system. The antennas are designed for applications in communications and for the development of antenna measuring techniques.

[P3-23] 14:20 ~ 16:00

### Broadband Channel Propagation Measurements on Millimeter and Sub-Millimeter Waves in a Desktop Download Scenario 1109

M. Salhi<sup>1</sup>, T. Kleine-Ostmann<sup>1</sup>, M. Kannicht<sup>1,2</sup>, S. Priebe<sup>2</sup>, T. Kürner<sup>2</sup>, T. Schrader<sup>1</sup>, <sup>1</sup>Physikalisch-Technische Bundesanstalt, Germany, <sup>2</sup>Institut für Nachrichtentechnik, Germany

Along with the steady increase of data rates in communication applications, the utilized bandwidths are growing accordingly, thus requiring higher carrier frequencies in face of the almost entirely occupied spectrum in the mm wave range and below. Therefore, channel measurements up to the lower THz frequency range are necessary for the development of modern and future communication systems. In this paper we present a comprehensive channel characterization covering the complete five waveguide frequency bands from 50 GHz up to 325 GHz. The measurements are performed in conditions which simulate a short-range indoor download environment. For spatially resolved measurements, a motorized setup was designed and employed.

[P3-24] 14:20 ~ 16:00

### A Dual-Band Azimuth Pattern Reconfigurable Antenna N/A

Guoming Ma, Mingchun Tang, Shaoqiu Xiao, University of Electronic Science and Technology of China, China

A novel pattern reconfigurable microstrip antenna was demonstrated in this paper. The proposed antenna, which could operate in both lower and upper bands of WLAN simultaneously, possesses excellent radiation pattern reconfigurability. According to our simulation investigation, by changing the state of the switches, the main beam in azimuth plane of proposed antenna can be easily adjusted in different four directions in both frequency bands with relative stable radiation patterns and little peak gain variations (less than 3dB). Moreover, compared to conventional antennas, this antenna has good impedance bandwidth and front-to-back ratios.

[P3-25] 14:20 ~ 16:00

### A Novel Low-cost, Low-profile, Wideband, Millimeter-Wave Dipole-Loop Antenna and Array 1115

Mingjian Li, Kwai-Man Luk, City University of Hong Kong, Hong Kong

A printed reflector-backed dipole antenna with printed loops connecting the two arms of the dipole is proposed. This antenna with a very low profile of  $0.05\lambda_0$  exhibits wide impedance bandwidth and high antenna gain. It is attractive to be used in an array environment. Experimentally, a 50-element antenna array is fabricated and measured. It achieves a wide impedance bandwidth of 12.5% covering the 57-64GHz frequency band. Over this band, the measured antenna gain is ranged from 22.5-25.2dBi. The measured radiation pattern has low cross-polarization of less than -30dB and back lobe of smaller than -31dB. This design is very low cost in fabrication as it is only made from a single-layer printed circuit board.

## Poster Session III: Antennas and Propagation & Emerging Technologies

- Date: November 8, 2013 (Friday)
- Time: 14:20 ~ 16:00
- Room: Room 103

[P3-26] 14:20 ~ 16:00

### Interlayer Tuning of X-Band Frequency-Selective Surface using Liquid Crystal 1118

Amir Ebrahimi, Pouriya Yaghmaee, Withawat Withayachumnankul, Christophe Fumeaux, Said Al-Sarawi, Derek Abbott, The University of Adelaide, Australia

In this paper, a new concept of a voltage-controlled tunable frequency-selective surface (FSS) is introduced based on liquid crystal technology. The designed FSS consists of two periodically patterned metallic layers, separated by a thin dielectric substrate. Tunability is achieved by integrating liquid crystal cells within the substrate for each unit cell, producing interlayer capacitors. By applying a bias voltage between the front and back metallic arrays, the anisotropy axis of the liquid crystal molecules can be re-oriented, and thus the effective relative permittivity of the liquid crystals can be modified to cause a frequency shift in transmission response. Electromagnetic simulations predict 5.6% of continuous frequency tuning for this multi-layer FSS.

[P3-27] 14:20 ~ 16:00

### Feasibility Evaluation of Near-Field Communication in Clay with 1-mm<sup>3</sup> Antenna 1121

Jin Kono, Masanori Hashimoto, Takao Onoye, Osaka University, Japan

We are working toward actualizing a real-time 3D modeling system that uses a sensor network that distributes many 1mm<sup>3</sup>-class sensor nodes in plastic clay. This paper focuses on 1mm<sup>3</sup>-class small antenna and discusses the feasibility of near-field communication with such small antennas. In order to clarify the communication characteristic for evaluating the feasibility, we designed 1mm<sup>3</sup>-class spiral antennas having three different resonant frequencies and carried out 3D full-wave electromagnetic simulations. When two antennas are embedded in the clay model with 10mm distance, the maximum  $|S_{21}|$  values at 30MHz, 340MHz, and 1.3GHz are -81.1dB, -69.6dB, and -64.7dB, respectively. This simulation result suggests that the near-field communication with 1mm<sup>3</sup>-class antennas is feasible.

[P3-28] 14:20 ~ 16:00

### Efficient Uplink Time Difference of Arrival Mobile Device Localization in Cellular Networks 1124

Mardeni R., K. Anuar, Paria Shahabi, Mohsen Riahi Manesh, Multimedia University, Malaysia

In this work, mobile station (MS) localization in cellular systems is considered based on uplink time difference of arrival (UTDOA) of MS signal at spatially separated base stations with known locations is presented. The UTDOA estimation is conducted using normalized least mean square (NLMS) based adaptive line enhancer (ALE) followed by a cross correlation. More precisely, the use of ALE-pre-filtered cross correlation is proposed in hyperbolic localization to improve the accuracy of UTDOA estimation for reducing the uncertainty in localizing the mobile station. Computer simulation results indicate that proposed ALE-UTDOA technique can achieve superior positioning accuracy than conventional cross correlation (CC) based method with range of 67%-75%.

[P3-29] 14:20 ~ 16:00

### A Compact UWB Band-Notched Monopole Antenna with Modified CSRR N/A

Di. Jiang, Yuehang. Xu, Ruimin. Xu, University of Electronic Science and Technology of China, China

A compact CPW fed dual-band-notched ultra wideband (UWB) antenna using modified complementary split ring resonators is proposed and investigated. The proposed antenna can reject dual frequency band by etching two modified complementary split ring resonators (CSRRs) in the radiating patch. The proposed antenna occupies a compact area of 25x28 mm<sup>2</sup> only. The measurement result shows that the proposed antenna can guarantee a wide bandwidth from 2.48 GHz to 10.78 GHz (VSWR < 2) with dual unwanted band-notches successfully. The antenna demonstrates omnidirectional radiation patterns across almost whole operating bandwidth, which is useful for UWB application.

[P3-30] 14:20 ~ 16:00

### On-Body UWB MIMO Antenna for UWB Application 1130

Enman Joo, Kyeol Kwon, Joonggi Park, Jaehoon Choi, Hanyang University, Korea

In this paper, a UWB MIMO antenna for an on-body application is proposed and antenna performance with body effect and the impact on the human body are investigated. The proposed MIMO antenna is composed of an UWB antenna above ground plane and an additional isolator located between the two antennas to enhance the isolation characteristic. A Simulation is performed to analyze the effect of the human body on the antenna performance when the human body is located near the antenna. According to the simulated result, the diversity performance of the proposed antenna is good since the Envelope Correlation Coefficient(ECC) remains below 0.1 over the UWB lower band. The simulated SAR value of antenna is 0.92 W/kg, when 1 mW input power is engaged. This value satisfies the FCC guideline which states that the 1-g average SAR should be lower than 1.6 W/kg.

## Poster Session III: Antennas and Propagation & Emerging Technologies

- Date: November 8, 2013 (Friday)
- Time: 14:20 ~ 16:00
- Room: Room 103

[P3-31]

14:20 ~ 16:00

### Z-Shaped Monopole Antenna for Wideband Circularly Polarized Radiation 1133

Benyang Hu<sup>1</sup>, Nasimuddin<sup>2</sup>, Zhongxiang Shen<sup>1</sup>, <sup>1</sup>Nanyang Technological University, Singapore, <sup>2</sup>Institute for Infocomm Research, Singapore

This paper presents a Z-shaped printed monopole antenna for wideband circularly polarized radiation. The antenna consists of a Z-shaped strip radiator fed by a microstrip line attached the Z-shaped strip. The antenna is fabricated on a thin FR4 dielectric substrate. The measured performances of the antenna are 1.28 GHz (2.53-3.81 GHz) for 10-dB return loss bandwidth, 1.75 GHz (2.25-4.0 GHz) for 3-dB axial ratio bandwidth, and gain around 1.7 dBic over the 3-dB axial ratio bandwidth. The volume of the proposed antenna is 50 mm×40 mm×0.8 mm.

[P3-32]

14:20 ~ 16:00

### Compact UHF Wide Slot Antenna for Microwave Stethoscope Designed for Heart Failure Detection 1136

S. Ahdi Rezaeieh, A. Abbosh, University of Queensland, Australia

A wide-slot antenna to be used in a compact microwave stethoscope for heart failure detection system is presented. The proposed antenna is based on the conventional slot antenna. However, changing the slot's shape and modifying the surface current path and consequently changing the electric field distribution inside the slot, provides the antenna with a broadband operation and a compact structure. To accomplish the unidirectional radiation pattern necessary for the heart failure detection system, a series of copper posts connected at certain positions to the reflector is employed to both suppress the back radiation and keep the antenna's profile low. The proposed antenna has a wide operating bandwidth of 16 % (822-966 MHz), maximum gain of 3.1 dBi and efficiency of over 90 %. The overall size of the antenna is  $0.27 \lambda \times 0.19 \lambda \times 0.05 \lambda$ , where  $\lambda$  is the wavelength at the first resonance of the antenna.

[P3-33]

14:20 ~ 16:00

### Low-Sidelobe Conformal Antenna Array Based on Substrate Integrated Waveguide Technology 1139

Yu Jian Cheng<sup>1,2</sup>, Wei Na Huang<sup>1</sup>, Jie Wu<sup>1</sup>, Yong Fan<sup>1</sup>, <sup>1</sup>University of Electronic Science and Technology of China, China, <sup>2</sup>Southeast University, China

A millimeter-wave low-sidelobe substrate integrated conformal array antenna is demonstrated in this paper. An array mounted on a cylindrical surface with a radius of 20 mm, i.e.  $2.3\lambda$ , is synthesized at the center frequency of 35 GHz. All components, including a 1-to-4 divider, a phase compensated network and a 4×8 slot array antenna are fabricated in a single dielectric substrate together. In simulation, it has a -30 dB sidelobe level (SLL) beam in H-plane and a -25 dB SLL in E-plane at 35 GHz. The cross-polar is lower than -40 dB at the beam direction. This type of antenna is a good choice in the development of millimeter-wave conformal applications.

[P3-34]

14:20 ~ 16:00

### A Modified Three-Circular-Ring Monopole Antenna for WLAN/WiMAX Triple-Band Operations 1142

Joong Han Yoon<sup>1</sup>, Young Chul Rhee<sup>2</sup>, <sup>1</sup>Silla University, Korea, <sup>2</sup>Kyungnam University, Korea

In this paper, a novel triple-band modified three-circular-ring monopole antenna with a rectangular slot in the ground plane for WLAN/WiMAX applications is proposed. The proposed antenna consists of two circular rings and one open-ended circular ring. The numerical and experiment results demonstrated that the proposed antenna satisfied the -10 dB impedance bandwidth requirement while simultaneously covering the WLAN and WiMAX bands. Furthermore, this paper presents and discusses the 2D radiation patterns and 3D gains according to the results of the experiment.

[P3-35]

14:20 ~ 16:00

### An Axial Ratio Beamwidth Enhancement of S-band Satellite Antenna with Parasitic Elements 1145

Eun-Cheol Choi, Jae W. Lee, Taek-Kyung Lee, Korea Aerospace University, Korea

In this article, a structural modification of S-band turnstile antenna to enhance the axial ratio beamwidth by attaching parasitic elements is suggested and investigated. Through the parametric studies and optimization, the positions, shapes and values of the final optimized elements have been obtained with two crossed Bow-tie dipole antennas. The overall structure is composed of main radiator and feeding part using Wilkinson power divider with two stubs for generating phase difference. The electrical performances have been verified in terms of the return loss, radiation pattern, and axial ratio beamwidth by using commercially available full EM simulator.

## Poster Session III: Antennas and Propagation & Emerging Technologies

- Date: November 8, 2013 (Friday)
- Time: 14:20 ~ 16:00
- Room: Room 103

[P3-36] 14:20 ~ 16:00

### Reflection Phase Characteristics of Active EBG Structures using Varactor Diodes on a Single Layer 1148

Jungmi Hong, Youngsub Kim, and YoungJoong Yoon, Yonsei University, Korea

A proposed active Electromagnetic Band-gap (EBG) can control the reflection phase using a varactor diode instead of by changing structure physically. This structure uses only one diode per four unit cells. It can operate as a group cell changing the reflection phase by simply varying varactor capacitances through an appropriate biasing voltage. The conventional loading of a single varactor for each of the unit cells of the EBG is overcome by connecting the unit cells to a feeding network directly without via. Moreover, this structure does not need via and uses single layer so it is simple to fabricate and can decrease cost. The proposed EBG structure can cover the reflection phase range of the group cell from  $-132^\circ$  to  $122^\circ$  at 10 GHz.

[P3-37] 14:20 ~ 16:00

### Dual Band Metamaterial Antenna with Loaded Resonators 1151

Bashir D. Bala, Mohamad Kamal A. Rahim, Noor Asniza Murad, Sharul Kamal A. Rahim, Universiti Teknologi Malaysia, Malaysia

This paper, a dual band metamaterial antenna is presented. The antenna consists of complementary split ring resonator (CSRR), slotted capacitor loaded strip (SCLS) and avia. The CSRR and SCLS enable the resonance frequency at 5.33 GHz and 2.39 GHz respectively for the dual band operation. The overall size of the antenna is  $0.53\lambda_0 \times 0.52\lambda_0 \times 0.023\lambda_0$  ( $36\text{mm} \times 35\text{mm} \times 1.52\text{mm}$ ) at 2.39 GHz. The peak realized gains of 4.17 dBi and 2.2 dBi are obtained at 5.33 GHz and 2.39 GHz respectively. Simulated and measured reflection coefficient are presented and discussed.

[P3-38] 14:20 ~ 16:00

### The Effective Directivity of Resonator Antenna using Curved Strip Dipole 1154

Nuchanart Fhafhien, P. Krachodnok, Rangsang Wongsan, Suranaree University of Technology, Thailand

This paper presents the optimum shape of a curved strip dipole antenna for maximum directive gain, which is used for excitation source of the circularly polarized resonator antenna. The proposed antenna consists of three main components, a curved strip dipole, conductor plane, and electromagnetic band gap (EBG). A curved strip dipole is constructed of a metallic sheet and bended to be a half of annular with feed point at the center for yielding wider beamwidth. Furthermore, EBG and conductor plane are used for cavity wall which is made practical use for high gain antenna. In this study, two difference shape of a curved strip dipole antenna located on conductor plane at  $45^\circ$  angle are appropriated, they are begotten the circularly polarized antenna. Finally, a well shape optimization case is presented together with axial ratio, directivity, and radiation patterns.

[P3-39] 14:20 ~ 16:00

### Millimeter-wave Metallic-Rectangular-Grooves based Reflectarray Antenna and Its Applications to E-band Multi-Gbps System 1157

Woo-Jin Byun<sup>1</sup>, Yong-Heui Cho<sup>2</sup>, Min-Soo Kang<sup>1</sup>, Kwang-Seon Kim<sup>1</sup>, Bong-Su Kim<sup>1</sup>, Myung-Sun Song<sup>1</sup>, <sup>1</sup>Electronics and Telecommunications Research Institute, <sup>2</sup>Mokwon University, Korea

A novel metallic-rectangular-groove based Cassegrain-type reflectarray antenna is proposed. This antenna is design using overlapping T-block method based on modematching method, virtual current cancellation, and superposition principle, thereby obtaining analytic scattering equations in rapidly convergent and numerically efficient integrals. Cassegrain-type antenna has low loss feeding structure connecting between a transceiver and an antenna.

[P3-40] 14:20 ~ 16:00

### Radiation Characteristics of an E-plane Linear Inductive Loaded Patch Phased Array Antenna 1160

Eun-Hyuk Kwak, Young-Min Yoon, Jae-Hyun Kim, Boo-Gyoun Kim, Soongsil University, Korea

Radiation characteristics of linear 5-element phased array antennas (PAAs) equidistantly positioned along the E-plane composed of  $5 \times 2$  inductive loaded patch antennas (ILPAs) are measured and compared to those of a linear PAA composed of conventional patch antennas. The radiation characteristics of linear PAAs composed of ILPAs are significantly improved compared to those of a linear PAA composed of conventional patch antennas such as low variations of the main beam gain and side-lobe level over wide scan angle range.

## Poster Session III: Antennas and Propagation & Emerging Technologies

- Date: November 8, 2013 (Friday)
- Time: 14:20 ~ 16:00
- Room: Room 103

[P3-41] 14:20 ~ 16:00

### Modified Low-Frequency Compensated TEM (LFCTEM) Horn Antenna to Improve the Radiation Performance 1163 HyeongSoon Park<sup>1</sup>, JaeSik Kim<sup>1</sup>, JiHeon Ryu<sup>2</sup>, JinSoo Choi<sup>2</sup>, YoungJoong Yoon<sup>1</sup>, <sup>1</sup>Yonsei University, Korea, <sup>2</sup>Agency for Defense Development, Korea

A Low Frequency Compensated TEM (LFCTEM) horn antenna realizes a poor gain in the lower part of operating bandwidth. This paper presents the Modified LFCTEM (MLFCTEM) antenna which has elliptical cutting shapes on LFCTEM to improve performance at the low frequency. To verify the improvement of the proposed antenna performance, MLFCTEM is compared with the LFCTEM antenna. Simulated results show that the MLFCTEM has return loss less than -10 dB in the frequencies from 2 to 18 GHz. In the case of being compared to the LFCTEM, it also has had an improved gain value at the low frequency which increases up to about 2.5 dB and has more directive radiation pattern.

[P3-42] 14:20 ~ 16:00

### Sidelobe Level Suppression using Unequal Four-Way Power Divider for Proximity Coupled Microstrip Antenna 1166 Fitri Yuli Zulkifli, Taufal Hidayat, Basari, Eko Tjipto Rahardjo, Universitas Indonesia, Indonesia

A four-way unequal power divider is developed to feed a linear array proximity coupled microstrip antenna. The unequal power divider excitation coefficients follow the chebyshev polynomial. The simulation result shows that the four element proximity coupled microstrip antenna array with unequal power divider has achieved a sidelobe level suppression of 18.7 dB with backlobe level suppression of 16.5 dB. Furthermore the antenna gain of 8.81 dB was also achieved. Measurement results of the antenna with unequal power divider show similar result with the simulation. Measurement results show sidelobe level suppression of 18.1 dB with backlobe level suppression of 19.4 dB.

[P3-43] 14:20 ~ 16:00

### A Compact Dual Band Tree-Type MIMO Antenna for Mobile Wireless Access Network Application 1169 Ching-Song Chuang, Wu-Tung Hsu, Lin Ming Chun, Lунghwa University, Taiwan

In order to obtain the full advantages of modern mobile MIMO wireless communication system, a compact and low mutual coupling antenna array is essential. Hence, this paper presents a compact dual band two element MIMO antenna operating in the 2.4GHz and 5.2GHz bands for mobile wireless LAN application. The dual band antenna element is structured with a planar two-branch inverted-L tree-type monopole, where, the two collinear inverted-L radiators have been purposely organized such that a squeezed element radiation pattern is obtainable. The MIMO antenna is then incorporated with two tree-type monopoles and a simple narrow band isolator to achieve an excellent mutual coupling performance. Besides, the characteristics of small size and nearly omnidirectional coverage in array radiation pattern make the proposed MIMO antenna entirely compatible with the mobile wireless network applications. The measurement results of the fabricated antenna array demonstrate the success of the suggested design topology.

[P3-44] 14:20 ~ 16:00

### Design of Planar Rectangular Spiral Antennas for the Wireless Vehicle Battery Charging System 1172 K. Phaebua<sup>1</sup>, D. Torrungrueng<sup>2</sup>, C. Phongcharoenphanich<sup>3</sup>, <sup>1</sup>King Mongkut's University of Technology North Bangkok, Thailand, <sup>2</sup>Asian University, Thailand, <sup>3</sup>King Mongkut's Institute of Technology Ladkrabang, Thailand

A design of planar rectangular spiral antennas for the wireless vehicle battery charging system operating at 13.56 MHz is presented in this paper. The proposed antennas are designed with low-cost, low-complexity and low-profile constraints. The study is performed by analyzing the power transmission efficiency of the spiral antennas via scattering parameters and associated reflection coefficients. Moreover, the misalignment between the transmitting and receiving antennas and effects of a car structure on the power transmission efficiency are investigated. It is found that the misalignment and the car structure strongly affect the power transmission efficiency.

[P3-45] 14:20 ~ 16:00

### Shorted Helix Antenna for Ingestible Medical Device Applications 1175 Hyungang Park, Jaehoon Choi, Hanyang University, Korea

In this article, a shorted helix antenna for an ingestible medical device applications is proposed. To investigate the performance of the antenna in an in-body environment, the antenna in the human-equivalent flat phantom is analyzed through simulation and measurement. The antenna is characteristic of wideband (386~409 MHz) covering MICS band. Radiation patterns have quasi-omnidirectional characteristic. In various organs, the antenna is characteristic not only of the return loss covering MICS band but also of quasi-omnidirectional radiation patterns.

## Poster Session III: Antennas and Propagation & Emerging Technologies

- Date: November 8, 2013 (Friday)
- Time: 14:20 ~ 16:00
- Room: Room 103

[P3-46] 14:20 ~ 16:00

### Secant Pattern Radiator for X-band Data Transmission 1178

Jung Min Lim<sup>1</sup>, Jae Ki Son<sup>2</sup>, Taek-Kyung Lee<sup>1</sup>, Jae W. Lee<sup>1</sup>, Woo Kyung Lee<sup>1</sup>, <sup>1</sup>Korea Aerospace University, Korea, <sup>2</sup>Avago Technologies Korea, Korea

In this paper, a design scheme for secant pattern radiator is presented. By combining a CP (Circular Polarization) generating adapter and a secant pattern radiator, a secant pattern antenna is designed. A secant pattern antenna is suitable for the data transmission in LEO satellite requiring wide angle coverage of the earth for the longer time visibility. In addition, secant pattern antenna is smaller and lighter compared to the ISOFLUX pattern antenna used in larger satellite. It is shown that the desired electrical performances including radiation pattern mask and return loss are satisfied through properly optimized parameters.

[P3-47] 14:20 ~ 16:00

### Microfluidic Channel on Organic Substrates as Size Reducing Technique for 915 MHz Antenna Designs 1181

Aida L. Vera López<sup>1</sup>, David B. Giles<sup>1</sup>, Wasif T. Khan<sup>1</sup>, Outmane Chlieh<sup>1</sup>, George E. Ponchak<sup>2</sup>, John Papapolymerou<sup>1</sup>, <sup>1</sup>Georgia Institute of Technology, USA, <sup>2</sup>NASA Glenn Research Center, USA

This paper presents for the first time, the use of a microfluidic channel with organic substrates to reduce the size of different antenna designs at 915 MHz (dipole and loop). The channel was created by drilling a cavity on a 50 mil RO3003™ substrate and bonding it to two 5 mil substrates in order to seal the structure. Compared to designs fabricated on an unperturbed substrate, the overall size reduction in length for the dipole with water-filled channel was ~44% (60 mm), while a 54% reduction in area was observed for loop counterpart. Broad bandwidths of 22% and 11% were achieved for the water loaded dipole and loop, respectively. The results obtained for both designs agreed well with simulations.

[P3-48] 14:20 ~ 16:00

### Planar Array Antenna Design with Beam Shaping for ETCS-RSE 1185

Jae-Su Jang, Nyung-Hak Kang, YeongWoo Koo, Jae-Kwon Ha, BlueWaveTel Co., Ltd., Korea

Abstract — A new planar array antenna with special beam shaping for ETCS-RSE (Electronic Toll Collection System-Road Side Equipment) is presented. The proposed 10×10 array antenna was obtained flat-topped radiation pattern by using Woodward and Lawson pattern synthesis. The measured electrical performances of the fabricated antenna in an operating band of 5.79~5.85 GHz showed VSWR of less than 1.72, antenna gain of more than 14.3dBi, and 3dB beam width of about 33°, low side lobe level of more than 26dB outside of ±34°.

[P3-49] 14:20 ~ 16:00

### Antenna Configurations of Microwave Breast Imaging 1188

Hoi-Shun Lui<sup>1</sup>, Andreas Fhager<sup>2</sup>, Mikael Persson<sup>2</sup>, <sup>1</sup>The University of Queensland, Australia, <sup>2</sup>Chalmers University of Technology, Sweden

The quality of the forward scattering data is crucial for the microwave breast imaging. Early study showed that the quality of the forward data varies in different polarization basis. In the actual imaging scenarios where antenna arrays are usually required, mutual coupling effects between the antenna elements would affect the quality of the forward data and thus the resultant images. Here, we aim to determine how the array size and thus the mutual coupling could impact on the forward data. The forward problems of different array configurations are studied and evaluated via full-wave numerical simulations, and found that small arrays with stronger coupling are preferred.

[P3-50] 14:20 ~ 16:00

### Dual-Band Metamaterial Absorbers at Terahertz Frequency Based on Gold/Parylene-C/Silicide Structure 1191

Yongzheng Wen<sup>1</sup>, Wei Ma<sup>1</sup>, Joe Bailey<sup>1,2</sup>, Guy Matmon<sup>2</sup>, Xiaomei Yu<sup>1</sup>, Gabriel Aeppli<sup>2</sup>, <sup>1</sup>Peking University, China, <sup>2</sup>University College London, UK

We design, fabricate and characterize dual-band terahertz (THz) metamaterial absorbers with high absorption based on a structures consisting of a cobalt silicide (Co-Si) ground plane, a parylene-C dielectric spacer and a metal top layer. By combining two periodic metal resonators that couple separately within a single unit cell, a polarization-independent absorber with two distinct absorption peaks was obtained. By varying the thickness of the dielectric layer, we obtain absorptivity of 0.76 at 0.76THz and 0.97 at 2.30THz, which indicates the Co-Si ground plane absorbers present good performance.

## Poster Session III: Antennas and Propagation & Emerging Technologies

- Date: November 8, 2013 (Friday)
- Time: 14:20 ~ 16:00
- Room: Room 103

[P3-51] 14:20 ~ 16:00

### Influence of Transistor Packages and Circuit Dimensions For Accurate Design of Negative Impedance Converters 1194 Takuya Kaneko, Yasushi Horii, Kansai University, Japan

Negative impedance converters (NICs), which can produce negative capacitances or negative inductances, are quite attractive for their potential for developing a new type of circuits we have never designed so far. However, those circuits, composed of active devices such as transistors or operational amplifiers, can easily become unstable due to their non-linearity, undesired couplings and excessive loop gains. Therefore, accurate circuit design is strongly requested. This paper theoretically studies the influence of transistor packages and circuit dimensions on NIC circuits, in collaboration with a circuit simulator Ansys Designer and a full-wave EM simulator Ansys HFSS.

[P3-52] 14:20 ~ 16:00

### Design of a Photoconductive Antenna with an Angled DC Bias Connection on an Extended Hemispherical Lens Substrate 1197 Truong Khang Nguyen, Ikmo Park, Ajou University, Korea

The input impedance and radiation characteristics of photoconductive antennas with different DC bias connection angles printed on an extended hemispherical lens made of high-dielectric-constant substrate was presented. Antennas with different bias connection angles exhibited different gain and radiation efficiency spectra for a specific lens geometry. The antennas with larger DC bias connection angles provided stable input impedance and improved antenna gain levels, particularly in the low-frequency region. This indicates that the DC bias connection angle has specific effects on the overall performance of the photoconductive antenna design.

[P3-53] 14:20 ~ 16:00

### 5.8-GHz Stacked Differential Mode Rectenna Suitable for Large-Scale Rectenna Arrays 1200 Tatsuki Matsunaga, Eisuke Nishiyama, Ichihiko Toyoda, Saga University, Japan

In this paper, a novel stacked differential mode rectenna is proposed and its characteristics are experimentally evaluated. The proposed rectenna operates in a differential mode. Therefore, the proposed rectenna can effectively rectify microwave power even under low power environments. The conversion efficiency of 37.1% was obtained when the received power density was as low as  $0.04 \text{ W/m}^2$ . The proposed rectenna can easily achieve large-scale rectenna arrays by simply stacking the rectifying diodes and microstrip antennas because the stacking structure does not degrade the conversion efficiency.

[P3-54] 14:20 ~ 16:00

### Accurate Analysis Method of Wireless Power Transfer System with Multiple Relays 1203 Ju-Hui Kim, Byung-Chul Park, Jeong-Hae Lee, Hongik University, Korea

In this paper, two methods for calculating the maximum efficiency of the wireless power transfer system with multiple relays are presented. One method utilizes the ABCD matrix of two-port network by ignoring the non-adjacent couplings. To improve the accuracy of the analysis, the other method takes into account the non-adjacent couplings between the resonators. The program based on circuit equations is coded by MATLAB. As expected, the method including the nonadjacent couplings gives rise to more accurate result. From the parametric study regarding the number of couplings, at least one non-adjacent coupling should be considered to predict the maximum efficiency and the shifted frequency of the WPT system with relays adequately.

[P3-55] 14:20 ~ 16:00

### Analytical Study of mm-Wave and THz Beams, Application to RF Metrology 1206 Alireza Kazemipour, Thomas Kleine-Ostmann, Thorsten Schrader, Physikalisch-Technische Bundesanstalt, Germany

Using mm-wave and THz radiation as a reliable measurement tool in spectroscopy and remote-sensing requires accurate beam characterization. Gaussian approximation is a practical model to describe the radiated beam of Laser sources and high-directivity THz/mm-wave horn antennas. The radiated beam is analytically studied in this paper and a simple closedform formula is presented for the wave-front phase distribution. Analytical results are compared with measurements and good agreement is observed for mm-wave horns. The closed-form formula is used for a parametric error-analysis and uncertainty evaluation as needed in RF metrology. Therefore, the contribution of all the source characteristics and its geometrical parameters to the phase deviation can be shown.

## Poster Session III: Antennas and Propagation & Emerging Technologies

- Date: November 8, 2013 (Friday)
- Time: 14:20 ~ 16:00
- Room: Room 103

[P3-56] 14:20 ~ 16:00

### Specular Reflection from a Sinusoidal Periodic Boundary by a Carpet Cloak of Invisibility 1209 Tsutomu Nagayama, Atsushi Sanada, Yamaguchi University, Japan

A carpet cloak of invisibility for sinusoidal periodic boundaries to mimic a specular flat floor is introduced. The material parameters are derived based on a non-conformal coordinate transformation, and a carpet cloak is designed and implemented with an equivalent circuit model based on the transmission line metamaterials concept. Wideband specular reflection operations are confirmed by circuit simulations.

[P3-57] 14:20 ~ 16:00

### Investigation of Metamaterial with Extended Constitutive Relationships by using Transmission Line Circuit Theory 1212 Toshikazu Sekine, Yasuhiro Takahashi, Gifu University, Japan

An equivalent circuit representation of the metamaterials with extended constitutive relationships which are coupling between the electric field and the magnetic field are derived. Those are analogized in coupled transmission lines. And reciprocity, passivity, and reactivity are investigated by using this equivalent circuit. We obtain analytically that these metamaterial are non-reciprocal in general, but are reciprocal when there are opposite coupling coefficients between the electric field and the magnetic field. And they are lossless when the coupling coefficients are imaginary. To confirm the validity of our results, the frequency response  $S_{21} = -S_{12}$  is calculated using the proposed equivalent circuit.

[P3-58] 14:20 ~ 16:00

### A Consideration of Designing Coil Array in Wireless Power Transfer with Magnetically Coupled Resonance 1215 Keishi Miwa, Hisamichi Mori, Nobuyoshi Kikuma, Hiroshi Hirayama, Kunio Sakakibara, Nagoya Institute of Technology, Japan

A two-dimensional transmitting coil array is used to expand receiving area in wireless power transfer with magnetically coupled resonance and the effect of the array is discussed in this paper. The transmitting coil array has more than one resonant frequency due to mutual couplings between transmitting coils. Therefore, we propose a method of designing the transmitting coil array and the receiving coil to keep high transmission efficiency in wider receiving area. The computer analysis and the experiment show the improvement of transmission efficiency of the proposed method.

[P3-59] 14:20 ~ 16:00

### Simplified Modeling of RR(Ring Resonator) Using Magnetization with Broader Negative Permeability Bandwidth 1218 Dongho Jeon, Bomson Lee, Kyung Hee University, Korea

In this work, the ring resonator (RR), the original form of the split ring resonator (SRR), is simply modeled using the concept of magnetization and one convenient expression for its effective permeability is presented. An equivalent circuit for the ring resonator is also provided with closed-form expressions for all circuit elements. A method of achieving a wider negative permeability by decreasing the Q value is provided. The ring resonator with its resonant frequency of 13.56 MHz was designed and its characteristics were examined in terms of S-parameters, effective permeability, loss rate, bandwidth, etc. The theoretical, circuit-, and EM-simulated results are shown to be in an excellent agreement.

[P3-60] 14:20 ~ 16:00

### Design of Adaptive Optimal Load Circuit for Maximum Wireless Power Transfer Efficiency 1221 Youn-Kwon Jung, Bomson Lee, Kyung Hee University, Korea

An adaptive optimal load circuit (ALC) for the maximum wireless power transfer (WPT) efficiency is presented for a magnetically coupled resonant WPT system at 13.56 MHz. The ALC is based on the lumped-element matching circuit. The series part is composed of a series capacitor block and an inductor. The shunt part is composed of a varactor and a capacitor block with switches. The tunable range of the optimal load impedance is from 0.2 to 50 Ohms. The provided examples demonstrate the usefulness and effectiveness of the ALC to achieve the maximum efficiency.



## Poster Session III: Antennas and Propagation & Emerging Technologies

- Date: November 8, 2013 (Friday)
- Time: 14:20 ~ 16:00
- Room: Room 103

[P3-61]

14:20 ~ 16:00

### A Low-Profile Third-Order Frequency Selective-Surface with Ultra-Wideband Response 1224

Yuehe Ge<sup>1,2</sup>, Hai Zhang<sup>1</sup>, <sup>1</sup>Huaqiao University, China, <sup>2</sup>Southeast University, China

By combining the non-resonant element and the resonant element, a low-profile, third-order FSS is proposed for ultra-wideband operations. The FSS is composed of three periodic metallic arrays, separated by two identical electrically thin dielectric layers. The design principle is discussed and an example is designed to demonstrate the validity of the principle. Simulation results show that a third-order frequency response with a bandwidth of 82.5% can be obtained. The FSS example has a thickness of  $\lambda/12$  and a small size of  $\lambda/8$  for the unit cell, without any polarization limitation, both for TE and TM incidence.

[P3-62]

14:20 ~ 16:00

### Wideband Metamaterial Absorber using an RC Layer 1227

Minyeong Yoo, Sungjoon Lim, Chung-Ang University, Korea

In this paper, a novel wideband metamaterial (MM) absorber is proposed. The proposed absorber is composed of a hexagonal MM structure and a resistor-capacitor (RC) layer, with an air gap between the two layers. The additional RC layer comprises a series resistor and capacitor; this layer and an air gap have an important effect on the wider bandwidth. The proposed absorber shows absorbing properties over a very wide bandwidth. The performance of the proposed absorber is demonstrated by simulation and measurement results.

## [F3A] High Power Devices and Amplifiers

- Date: November 8, 2013 (Friday)
- Time: 16:30 ~ 18:10
- Room: Room A (Room 101)
- Session Chairs: Renato Negra (Aachen University)  
Hyunchul Ku (Konkuk University)

[F3A-1]

16:30 ~ 16:50

### A K-band Compact Fully Integrated Transformer Power Amplifier in 0.18- $\mu\text{m}$ CMOS 597 Che-Chung Kuo, Yu-Hsuan Lin, Hsin-Chia Lu, Hwei Wang, National Taiwan University, Taiwan

A K-band, 24 GHz, fully integrated transformer power amplifier (PA) is designed and fabricated in the standard 0.18- $\mu\text{m}$  deep N-well (DNW) CMOS technology. This power amplifier is a 2-stage design using cascode RF NMOS configuration. The on-chip transformers are adopted for the power combining and impedance transformation for the matching network with a small size. The measurement results of this PA are linear gain of 15 dB,  $OP_{1\text{dB}}$  of 18 dBm and  $P_{\text{SAT}}$  of 23.5 dBm with power added efficiency (PAE) of 12%. Due to the small size of transformer, the size of the chip is only  $0.86 \times 0.56 \text{ mm}^2$ . To the author's knowledge, this PA not only demonstrates the highest output power among the CMOS PA in a 0.18- $\mu\text{m}$  CMOS process, but also achieves the highest ratio of output power to chip size among the all reported K-band CMOS PAs.

[F3A-2]

16:50 ~ 17:10

### Measurement of a Planar 9-Way Metamaterial Power Combined Amplifier 600 Wei-Chiang Lee, Tah-Hsiung Chu, National Taiwan University, Taiwan

In this paper, a planar 9-way metamaterial power combined amplifier is presented. The power divider/combiner structure is a metamaterial lens composed of positive refractive index (PRI) material with right-handed unit cells and zero refractive index (ZRI) material with left-handed unit cells. A semi-circular interface is between PRI and ZRI materials. Due to its uniform isolation characteristics of the power divider/combiner, the graceful degradation performance of this power combined amplifier is shown to be independent of the amplifier failure sequence. The power combining of nine 1 W amplifiers gives an output power of 7.64 W with a combining efficiency of 85% at 1.008 GHz, and the graceful degradation characteristic of this power combined amplifier is experimentally demonstrated.

[F3A-3]

17:10 ~ 17:30

### GaN MMIC Broadband Doherty Power Amplifier 603 Seunghoon Jee<sup>1</sup>, Juyeon Lee<sup>1</sup>, Bonghyuk Park<sup>2</sup>, Cheol Ho Kim<sup>2</sup>, Bumman Kim<sup>1</sup>, <sup>1</sup>Pohang University of Science and Technology, Korea, <sup>2</sup>Electronics and Telecommunications Research Institute, Korea

A quarter-wavelength transformer, phase compensation network, offset line are the bandwidth limiting factors of Doherty PAs. In this paper, we expand the bandwidth of the Doherty PA by employing a new structure. The conventional phase compensation network is merged into an input matching circuit and the offset line is resonated-out by an inductor. The quarter wavelength transformer has a low-Q characteristic compared to that of conventional one. With the proposed topology, a broadband Doherty PA is implemented using TriQuint 3MI 0.25 $\mu\text{m}$  GaN-HEMT MMIC process. Across 2.1-2.7 GHz, the implemented PA delivered a DE of over 40.5%, a gain of over 11.8 dB and ACPR of below -45dBc at an average power of over 33.2 dBm for LTE signal with a 6.5 dB peak-to-average power ratio. This fully integrated circuit has a chip-size of 3.5mm by 1.9mm.

[F3A-4]

17:30 ~ 17:50

### GaN MMIC Broadband Saturated Power Amplifier 606 Juyeon Lee<sup>1</sup>, Seunghoon Jee<sup>1</sup>, Bonghyuk Park<sup>2</sup>, Cheol Ho Kim<sup>2</sup>, Bumman Kim<sup>1</sup>, <sup>1</sup>Pohang University of Science and Technology, Korea, <sup>2</sup>Electronics and Telecommunications Research Institute, Korea

We design a broadband power amplifier (PA) for a base-station in a wireless communication system. This PA covers ultra-wide band including most of the mobile operation frequencies. To achieve the broadband operation, we adopt a saturated PA topology. The saturated PA has simple input and output matching networks because only the fundamental impedance needs to be controlled actually. The internal output nonlinear capacitance generates appropriate amounts of the 2nd and 3rd harmonic voltage components and does not need any complicated matching networks for the harmonic impedance matching. We simulate the optimum load and source impedances for the target frequency bands and match the fundamental impedances in the target impedance area. For operating frequency from 0.9 GHz to 3.6 GHz, output power is varied from 39.5 dBm to 43.4 dBm, drain efficiency from 48% to 66.7% and the gain is 9.5~13.4 dB. Although this PA covers a very wide range of frequencies, it can provide high efficiency using simple matching networks.

[F3A-5]

17:50 ~ 18:10

### Shielding Cover Effects on the RF Performance of LDMOSFET Power Amplifier for WCDMA Application 609 Liang Lin<sup>1,2</sup>, Gang Cheng<sup>2</sup>, Wen-Yan Yin<sup>1</sup>, Liang Zhou<sup>1</sup>, <sup>1</sup>Shanghai Jiao Tong University, China, <sup>2</sup>NXP Semiconductors(Shanghai) Co., Ltd., China

Shielding cover effects on the RF performance of LDMOSFET power amplifier(PA) is investigated. In our measurement, the PA cover is made of aluminum, with its height adjusted from 8.4 to 14.4mm. The input-output responses of several PA samples with cover are measured and compared for different cover heights. Both experiment and simulation show that as the cover height is reduced, the PA performance is degraded, but its power efficiency and linearity are not varied approximately. Further, it is found that, even the cover height is decreased, but through careful optimizing of its internal impedance matching networks consisting of multiple bonding wires, the PA performance can be improved effectively. This research can provide some useful design guidance for the development of compact and miniaturized PA module with high performance.

## [F3B] Band-Stop Filters and Diplexers

- Date: November 8, 2013 (Friday)
- Time: 16:30 ~ 17:50
- Room: Room B (Room 102)
- Session Chairs: Nam-Young Kim (Kwangwoon University)  
Changsoo Kwak (ETRI)

[F3B-1]

16:30 ~ 16:50

### A Compact Microstrip Triple-Band Bandstop Filter with Rectangular Meandered SIR for WiMAX Applications 612 Rajendra Dhakal, Nam-Young Kim, Kwangwoon University, Korea

This paper presents a microstrip triple-band bandstop filter realized using tri-section meandered-lines stepped impedance resonator with a length equal to quarter wavelength ( $\lambda/4$ ) to operate at stop bands of 2.42 GHz, 6.47 GHz, and 10.30 GHz. A drastic reduction in size of the filter was achieved by taking advantage of a simplified architecture based on meandered-line stepped impedance resonator. To increase bandwidth of each stop band, the two shunt connected structures are employed with a microstrip transmission line. Furthermore, an equivalent circuit model of the proposed filter is developed to match well by the electromagnetic simulations. The return losses of the fabricated filters are measured to be -26.34, -23.52, and -18.58 dB while the insertion losses are -0.41, -0.55, and -1.87 dB at the respective stop bands.

[F3B-2]

16:50 ~ 17:10

### Compact Diplexer Design using Spiral-Oriented Resonator N/A Xun Luo<sup>1</sup>, Guoan Wang<sup>2</sup>, <sup>1</sup>Huawei Technologies Co., Ltd., China, <sup>2</sup>University of South Carolina, USA

In this letter, a miniaturized diplexer is presented based on one spiral-oriented resonator (SOR) and two quarterwave-length ( $\lambda/4$ ) spiral resonators with a spiral-coupled scheme. The SOR consists of a  $\lambda/2$  spiral-resonator and a loaded openstub. It allocates the dual-resonance for the proposed diplexer: 1) the first-resonance for the first-channel is achieved by the fundamental resonance  $f_1$  of the  $\lambda/2$  spiral-resonator in the SOR; 2) the loaded open-stub shifts the first-spurious  $f_2$  of the  $\lambda/2$  spiral-resonator downward with a large tuning range, which leads to a finely adjusted second-channel. Meanwhile, two  $\lambda/4$  spiral resonators operated at  $f_1$  and  $f_2$ , respectively, are integrated to form the spiral-coupled scheme with the SOR for implementing the diplexer. To verify the mechanism of the structures mentioned above, a compact diplexer operated at 1.015 and 1.615 GHz is proposed and fabricated. The diplexer exhibits the following high merits: insertion loss less than 0.61 dB in both channels, common port return loss greater than 19.3 dB, and typical inband isolation about 40 dB.

[F3B-3]

17:10 ~ 17:30

### Development of LC EMI Filter Arrays for 4G-LTE Applications 618 Li-Ju Chen, Ken-Huang Lin, National Sun Yat-Sen University, Taiwan

In this investigation, a 4 channel EMI filter array for 4G-LTE application is proposed with multilayer structure and formed by low-temperature co-fired technique. In order to miniaturize the size of the component and improve its performance, a mixed powder material is employed to design and fabricate the filter. The overall dimension of EMI Filter Array is 1.6 mm (L)×0.8 mm (W)×0.5 mm (H), the smallest one reported so far. The measured results of the developed filter are in a good agreement with the simulated results by full-wave electromagnetic simulator.

[F3B-4]

17:30 ~ 17:50

### A Novel Compact Triple-Mode Microstrip Bandstop Filter with Adjustable Reflection Zeros 621 Ali Kursad Gorur, Ceyhan Karpuz, Pinar Ozturk Ozdemir, Zuhra Karaca, Pamukkale University, Turkey

In this letter, the effect of open-circuited stubs on the frequency response of a microstrip square loop resonator shaped as a meander form is investigated with a full-wave electromagnetic (EM) simulator and a triple-mode microstrip bandstop filter is designed by using this effect. Proposed filter configuration is consisted of a microstrip square loop resonator shaped meander and four open-circuited stubs vertically and horizontally located inside the resonator. These stubs not only can be used to adjust the reflection poles in the stopband, but also used to obtain the miniaturisation. Central reflection pole is related with the horizontally located stubs, whereas the other two reflection poles are obtained from the vertically located stubs. In addition, the proposed configuration allows the controlling of the reflection zeros by changing the lengths of the stubs. Designed filter is simulated, fabricated and tested. Measured results show a good agreement with the simulated results.

## [F3C] RF Measurement Techniques

- Date: November 8, 2013 (Friday)
- Time: 16:30 ~ 18:10
- Room: Room C (Room 104)
- Session Chairs: Qunsheng Cao (Nanjing University of Aeronautics and Astronautics)  
Jinsup Kang (KRISS)

[F3C-1] 16:30 ~ 16:50

### Study on Noninvasive Measurement of Temperature Distribution in Carbonized Moxa-Needle Treatment 624

Suguru Nakamura<sup>1</sup>, Masamichi Nakamura<sup>2</sup>, Eiichi Maeda<sup>3</sup>, Yoshio Nikawa<sup>1</sup>, <sup>1</sup>Kokushikan University, Japan, <sup>2</sup>Tokyo Therapeutic Institute, Japan, <sup>3</sup>Okinawa College of Integrative Medicine, Japan

Various heating treatments are performed in the medical field through the world. To monitor the temperature distribution in the treatment area, it is strongly demanded to develop a noninvasive temperature measuring technique. In order to measure the temperature change for the deep target noninvasively, it becomes very difficult because the temperature change can generate very slight difference in the physical parameter in tissues. Recent development of electromagnetic wave technique enables noninvasive temperature measurement inside material using Magnetic Resonance Imaging (MRI). In this paper, under carbonized moxa-needle treatment which is one of the methods of acupuncture and moxibustion therapy, the temperature distribution is measured using MRI by measuring the phase of longitudinal relaxation time of proton. The result of temperature analysis during carbonized moxa-needle treatment is also reported.

[F3C-2] 16:50 ~ 17:10

### Spherical Scanned Radiation Pattern Measurement by Phase Retrieval Method 627

Eriko Ohashi, Hiroyuki Arai, Yokohama National University, Japan

This paper presents spherical scanned radiation pattern measurement by phase retrieval method. We firstly derive near-field to far-field transformation formulas for magnetic near-field distributions measurement, and discuss correct far-field extrapolation using phase retrieval method. A key parameter in this method is to select appropriate probe scanning radius. This paper clarifies optimal distance between two measurement planes by the simulation with a half-wavelength ( $\lambda/2$ ) dipole, a  $3/2 \lambda$  dipole and a handset antenna consisting a folded F-shaped antenna on rectangular ground plane. We also verify the simulation results by measurements.

[F3C-3] 17:10 ~ 17:30

### Impact of Terahertz Radiation on Cells 630

Tsurkan M.V., Smolyanskaya O. A., St. Petersburg National Research University of IT, Russia

Knowledge of the biological effects induced by THz radiation can have a crucial impact in future developments in fields of medicine, biology or chemistry. The lack of THz radiation sources with sufficient power as well as the missing knowledge of the specifics of their use led to the fact that the impact of microwave radiation on different organisms, including microorganisms has not yet been investigated. The aim of our study was to assess the impact of broadband pulsed THz radiation in the frequency range of 0.05 to 1.2 THz on cell systems. Studies conducted in vitro.

[F3C-4] 17:30 ~ 17:50

### Bandwidth Broadening of Shielding Effectiveness Measurement by KEC Method 633

Hongliang Gu<sup>1</sup>, Hiroyuki Arai<sup>2</sup>, Seiichi Izumi<sup>2</sup>, Toshiyasu Tanaka<sup>3</sup>, <sup>1</sup>Yokohama National University, Japan, <sup>2</sup>KEC Kansai Electric Industry Development Center, Japan, <sup>3</sup>Microwave Factory Co., Ltd, Japan

This paper presents a bandwidth broadening of KEC method. Proposed instrument is made up of double ridge horn antenna surrounded by absorber wall and test sample. It increases bandwidth in KEC method to 1 ~ 13GHz. In order to discuss the feasibility of proposed instrument, we simulated two kinds of materials and compared simulation value with theoretical value.

[F3C-5] 17:50 ~ 18:10

### Multiport Network Measurement using a Three-Port VNA 636

Chih-Jung Chen<sup>1</sup>, Tah-Hsiung Chu<sup>2</sup>, <sup>1</sup>National Taiwan Ocean University, Taiwan, <sup>2</sup>National Taiwan University, Taiwan

S-matrix reconstruction transforms are widely used in measurements of multiport devices using a two-port vector network analyzer, especially for noncoaxial applications because high-quality matched loads are hardly accessible. For noncoaxial measurements, strongly reflecting termination, such as a short-circuited or an open-circuited transmission line is more repeatable, reliable and economical than terminations with loss like resistors. Accordingly, the numerical instability associated with strongly reflecting auxiliary terminations is of concern to noncoaxial applications. In this paper, a technique that allows a three-port vector network analyzer to measure multiport devices using strongly reflecting auxiliary terminations is developed to ease the noncoaxial measurements. As demonstrated in Section III, the technique eradicates the numerical instability associated with strongly reflecting auxiliary terminations, and results in an accurate reconstruction of the multiport S-matrix.

## [F3D] MIMO and Handset Antennas

- Date: November 8, 2013 (Friday)
- Time: 16:30 ~ 18:10
- Room: Room D (Room 105)
- Session Chairs: Chuwong Phongcharoenpanich (King Mongkut's Inst. of Tech. Ladkrabang)  
Bomson Lee (Kyung Hee University)

[F3D-1] 16:30 ~ 16:50

### A Compact Printed MIMO Antenna Integrated into A 2.4 GHz WLAN Access Point Applications 639

Shun-Min Wang<sup>1</sup>, Lih-Tyng Hwang<sup>1</sup>, Fa-Shian Chang<sup>2</sup>, Chih-Feng Liu<sup>2</sup>, Sheng-Ting Yen<sup>2</sup>, <sup>1</sup>National Sun Yat-Sen University, Taiwan, <sup>2</sup>Cheng Shiu University, Taiwan

A low-cost, printed single-plate two-antenna system suitable for multiple-input multiple-output (MIMO) applications operating at the 2.4 GHz WLAN bands is presented. It is best embedded inside the wireless access point (AP) from the size consideration. The antenna consists of two folded monopoles orthogonally located at the edges of a rhombic ground plane. The feed points drive the monopoles from the edges. The two monopoles are joined together near the intercept of the edges. This configuration provides diverged patterns with a good isolation characteristic through the 90° polarization. Impedance matching for the 2.4 GHz bands can easily be achieved by tuning the feeding positions. Measured envelope correlation is less than 0.06 within the band of interest.

[F3D-2] 16:50 ~ 17:10

### Detection Performance Evaluation of MIMO Sensor for Outdoor Surveillance Application 642

Keita Konno<sup>1</sup>, Naoki Honma<sup>1</sup>, Kentaro Nishimori<sup>2</sup>, Yoshitaka Tsunekawa<sup>1</sup>, <sup>1</sup>Iwate University, Japan, <sup>2</sup>Niigata University, Japan

We investigated the antenna arrangement suitable for outdoor MIMO (Multiple-Input Multiple-Output) sensor which is used for intruder surveillance application. Detection rate characteristics are evaluated as functions of the height of antenna array in several environments. A channel correlation that compares the MIMO channels with and without a person is used in the intrusion detection algorithm. The experimental results indicated the intruder detection performance is improved by lowering the height of antenna than the height of targets in outdoor environment.

[F3D-3] 17:10 ~ 17:30

### Planar Shorted Monopole Antenna with Coupled feed and Parasitic Strip for LTE/WWAN Mobile Handset Applications 645

Do-Gu Kang, Jaehoon Choi, Hanyang University, Korea

In this paper, a shorted monopole antenna with coupled feed and parasitic strip for LTE/WWAN mobile handset applications is presented. A basic resonance of the shorted monopole along with the resonance formed by the coupled feed provides the enough bandwidth to cover the LTE700, GSM850, and GSM900 bands. By adding the parasitic strip, a matching characteristic of a harmonic of the monopole antenna and a loop resonance is improved to cover the GSM1800, GSM1900, UMTS, and LTE2300 bands. Consequently, the proposed antenna covers the LTE700, GSM850, GSM900, GSM1800, GSM1900, and UMTS bands. Stable and omni-directional radiation patterns are observed over the operating bands.

[F3D-4] 17:30 ~ 17:50

### A Compact GPS and WLAN PIFA for Full Metal-Rimmed Mobile Handset using the Ground Bridges 648

SungHyun Kim, HyunWook Moon, WooJoong Kim, JaeSik Kim, YoungJoong Yoon, Yonsei University, Korea

This paper proposes a compact dual band PIFA (Planar Inverted F Antenna) covering GPS (Global Positioning System) and WLAN (Wireless Local Area Network) bands for the full metal rimmed mobile handset. The proposed antenna is positioned on the full metal rim which is connected to ground plane via several ground bridges as a ground contact. This ground bridge can be used to obtain the additional resonant frequency with the proposed antenna. The bandwidth has improved by adjusting the position of the ground bridge. The simulation is executed by CST simulator and the simulation result shows a good performance on return loss, efficiency, and radiation pattern.

[F3D-5] 17:50 ~ 18:10

### Design of A Novel Dual-band Circularly Polarized Handset Antenna 651

Youbo Zhang<sup>1</sup>, Yuan Yao<sup>1</sup>, Junsheng Yu<sup>1</sup>, Xiaodong Chen<sup>2</sup>, <sup>1</sup>Beijing University of Posts and Telecommunications, China, <sup>2</sup>University of London, UK

A novel circularly polarized handset antenna which is compatible with multiple Global Navigation Satellite Systems is proposed. The antenna comprises a palm-size slab as the handset test bench, a small antenna chip mounted at the corner of the slab, a meander line, three branches, and a ground plane with rectangle clearance region. The antenna is featured with several characteristics such as dual frequency band operation, circularly polarized reception, low fabrication cost, compact size. Both of the simulated and measured results are shown to illustrate the good performance of the proposed antenna.

## [F3E] Future Wireless Communications and Radars

- Date: November 8, 2013 (Friday)
- Time: 16:30 ~ 18:10
- Room: Room E (Room 203)
- Session Chairs: Chen Qiang (Tohoku University)  
ChoonSik Cho (Korea Aerospace University)

[F3E-1]

16:30 ~ 17:00

### [Invited] Reflectarray Development for Improving NLOS Radio Channel 654

Qiang Chen, Tohoku University, Japan

In urban areas where there are many high buildings, the radio wave from base stations of cellular mobile communications may be blocked by these buildings, particularly in narrow streets right under these buildings. In order to improve the radio channel in these blocked areas, we have carried out researches to develop reflectarray as a passive reflector mounted on the wall of these buildings to scatter the incident wave from the base station antennas to these areas. This report gives a brief review of our previous researches on reflectarray development for improving wireless propagation channel, including development of reflectarray with band-pass filter, dual-band reflectarray, and so on. An outdoor measurement is demonstrated to show the effectiveness of the reflectarray approach in improving the NLOS radio channel in urban areas.

[F3E-2]

17:00 ~ 17:30

### [Invited] Integration of RF Transmission Lines in Carbon Fiber Reinforced Polymer (CFRP) Structures 657

Kamran Ghorbani, Ali Daliri, RMIT University, Australia

Multifunctional structures are essential parts of future air vehicles to reduce the weight and add extra capabilities. Recently, integration of various elements in carbon fiber reinforced polymer (CFRP) panels has been the center of attention among RF and structural engineers. This paper investigates the feasibility of integrating RF transmission lines in CFRP skins. The effect of CFRP conductivity on the performance of common RF transmission lines has been studied. The results of this study suggest coaxial line with CFRP as the outer conductor is the most suitable type of transmission line for this purpose and its insertion loss is about 0.7 dB/m, which is reasonable for UHF-Satcom.

[F3E-3]

17:30 ~ 17:50

### Error-free 30-50 Gbps Wireless Transmission at 300 GHz 660

Shogo Horiguchi, Kazuki Arakawa, Yusuke Minamikata, Tadao Nagatsuma, Osaka University, Japan

This paper presents a 300-GHz band wireless link using a photonics-based transmitter. We improve the bandwidth of components such as photodiodes and Schottky-barrier-diodes, and introduce a polarization multiplexed scheme using two wiregrid polarizers. Error-free transmission experiments with bit error rates of less than  $10^{-11}$  are successfully demonstrated at a bit rate of 33 Gbps and 48 Gbps by a single polarization link and a polarization multiplexed link, respectively.

[F3E-4]

17:50 ~ 18:10

### Target Detection for UWB Radars using the Standard Deviation 663

Moon Kwang Jang, Choon Sik Cho, Korea Aerospace University, Korea

UWB radars operating at 3.1 GHz-10.6 GHz are used for detecting the targets under clutter environment. Since UWB radars deal with various clutters, it is somewhat difficult to discriminate the target accurately. By reflecting the standard deviation of power spectrum, and the improvement factor using moving speed of the radar and antenna angle, target detection is performed by removing multiple clutters. In this paper, we apply digital signal processing to analyze performance of the proposed detection method based on standard deviation. The proposed algorithm shows successful detection of car and person.

## [F3F] Beam Steering Applications

- Date: November 8, 2013 (Friday)
- Time: 16:30 ~ 18:10
- Room: Room F (Room 208)
- Session Chairs: Takuji Arima (Tokyo University of Agriculture and Technology)  
Hosung Choo (Hongik University)

[F3F-1]

16:30 ~ 16:50

### Array Configuration Optimization using an Objective Function for Accurate DOA Estimation 666

Gangil Byun<sup>1</sup>, Jeungmin Joo<sup>2</sup>, Kichul Kim<sup>2</sup>, Seungmo Seo<sup>2</sup>, Sunwoo Kim<sup>1</sup>, Hosung Choo<sup>3</sup>, <sup>1</sup>Hanyang University, Korea, <sup>2</sup>Agency for Defense Development, Korea, <sup>3</sup>Hongik University, Korea

This paper proposes a deterministic method of array configurations using an objective function for accurate DOA estimation in a wide frequency range. The objective function is defined to describe appropriate baseline distributions of an 8-element circular array for the max-min frequency ratio of 6:1 and used to find the most similar distributions among a number of random array configurations. The resulting array configuration obtained from the proposed method is evaluated by root mean square error (RMSE) and ambiguity in comparison with a uniform circular array (UCA). The results demonstrate that the proposed method is efficient for achieving accurate DOA estimation in a wide frequency range.

[F3F-2]

16:50 ~ 17:10

### Studies on the Equivalent Circuit of the Excitation to a Cavity-Backed Slot Antenna 669

Kenta Sato, Masashi Komeya, Hitoshi Shimasaki, Kyoto Institute of Technology, Japan

In this paper, an equivalent circuit is newly described for a cavity-backed slot antenna considering the feeder and the slot element. The slot antenna has employed an electromagnetic coupling, so no solder or conductive adhesive is used. The slot is treated as a distributed constant line with a short-circuited termination, a tuning stub is treated as distributed constant line with an open termination, and then the mutual inductances between the feeder microstrip line and the slot are derived into the equivalent circuit. The calculated reflection characteristics by the circuit simulation are compared with the measured ones for a fabricated antenna.

[F3F-3]

17:10 ~ 17:30

### Design and Implementation of An Active Antenna Array for TD-LTE System Based on DDS Phase Shifter 672

Linsheng Li, Wei Hong, Peng Chen, Southeast University, China

In this paper, a novel active antenna array is proposed for TD-LTE base station system. This array includes two parallel eight-element uniform linear sub-arrays for the dual polarization operation and provides a usable bandwidth of 100 MHz. Beamforming in the vertical dimension is achieved which improves the performance of cellular mobile communication systems. Each radiation antenna element is integrated with a complete transceiver to reduce the cable loss. Each transmitter is capable of generating up to 21 dBm of output power. Each receiver signal path achieves a gain of 37 dB and a noise figure below 3.5 dB. The eight-path sub-array improves the signal-to-noise ratio at the output by 9 dB in receiving mode compared with a conventional single receiver. Direct digital synthesizer (DDS) chips generate the local oscillator (LO) signal and work as active phase shifters in each path. This active phase shifting infrastructure provides a 360° phase shifting range and accurate tuning step which leads to a beam-steering resolution of 0.1°.

[F3F-4]

17:30 ~ 17:50

### Doppler Spread Spectrum of Antenna Configurations in a Reverberation Chamber 675

Myung-Hun Jeong<sup>1</sup>, Byeong-Yong Park<sup>1</sup>, Jung-Hwan Choi<sup>2</sup>, Seong-Ook Park<sup>1</sup>, <sup>1</sup>KAIST, Korea, <sup>2</sup>Samsung Electronics, Korea

In this letter, we describe the Doppler phenomenon according to some antenna configuration in a reverberation chamber. The Doppler spread spectrums with some rotational velocities of RX antenna using platform stirring are described. The Doppler effects of single and multiple antennas at 2.6GHz are characterized by polarization and spatial parameters.

[F3F-5]

17:50 ~ 18:10

### Evaluation of Propagation Loss Difference between 5.8GHz and 700MHz Bands in V2V Communication Environments 678

Ryoji Yoshida, Hisato Iwai, Hideichi Sasaoka, Doshisha University, Japan

The 700MHz band is newly allocated as the radio spectrum to ITS (Intelligent Transport System) in Japan. In the 700MHz band, which is the lower frequency than the existing ITS band at 5.8GHz, service area can be ensured owing to the decrease of the diffraction loss, particularly in NLOS (Non Line-of-Sight) environments. In this paper, assuming a V2V (Vehicle to vehicle) communication environment over intersections where the situation is a typical NLOS environment, the propagation loss difference between the 5.8GHz and 700MHz bands is evaluated. We first analyze the difference theoretically using the ray tracing method. In addition, the experimental results obtained in the field experiments are shown. A comparative evaluation of these results is also discussed.